Density Model for Risso's Dolphin (*Grampus griseus*) for the U.S. Gulf of Mexico: Supplementary Report

Duke University Marine Geospatial Ecology Lab*

Model Version 2.3 - 2015-09-29

Citation

When referencing our methodology or results generally, please cite our open-access article:

Roberts JJ, Best BD, Mannocci L, Fujioka E, Halpin PN, Palka DL, Garrison LP, Mullin KD, Cole TVN, Khan CB, McLellan WM, Pabst DA, Lockhart GG (2016) Habitat-based cetacean density models for the U.S. Atlantic and Gulf of Mexico. Scientific Reports 6: 22615. doi: 10.1038/srep22615

To reference this specific model or Supplementary Report, please cite:

Roberts JJ, Best BD, Mannocci L, Fujioka E, Halpin PN, Palka DL, Garrison LP, Mullin KD, Cole TVN, Khan CB, McLellan WM, Pabst DA, Lockhart GG (2015) Density Model for Risso's Dolphin (*Grampus griseus*) for the U.S. Gulf of Mexico Version 2.3, 2015-09-29, and Supplementary Report. Marine Geospatial Ecology Lab, Duke University, Durham, North Carolina.

Copyright and License

Revision History

Version	Date	Description of changes
1	2014-10-19	Initial version.
2	2015-01-09	Added three missing sightings and refitted models.
2.1	2015-02-02	Updated the documentation. No changes to the model.
2.2	2015-05-14	Updated calculation of CVs. Switched density rasters to logarithmic breaks. No changes to the model.
2.3	2015-09-29	Updated the documentation. No changes to the model.

*For questions, or to offer feedback about this model or report, please contact Jason Roberts (jason.roberts@duke.edu)

Survey Data

Survey	Period	Length (1000 km)	Hours	Sightings
SEFSC GOMEX92-96 Aerial Surveys	1992-1996	27	152	4
SEFSC Gulf of Mexico Shipboard Surveys, 2003-2009	2003-2009	19	1156	39
SEFSC GulfCet I Aerial Surveys	1992-1994	50	257	38
SEFSC GulfCet II Aerial Surveys	1996-1998	22	124	33
SEFSC GulfSCAT 2007 Aerial Surveys	2007-2007	18	95	0
SEFSC Oceanic CetShip Surveys	1992-2001	49	3102	158
SEFSC Shelf CetShip Surveys	1994-2001	10	707	10
Total		195	5593	282

Table 2: Survey effort and sightings used in this model. Effort is tallied as the cumulative length of on-effort transects and hours the survey team was on effort. Sightings are the number of on-effort encounters of the modeled species for which a perpendicular sighting distance (PSD) was available. Off effort sightings and those without PSDs were omitted from the analysis.

Period	Length (1000 km)	Hours	Sightings
1992-2009	195	5592	282
1998-2009	62	2679	79
% Lost	68	52	72

Table 3: Survey effort and on-effort sightings having perpendicular sighting distances. % Lost shows the percentage of effort or sightings lost by restricting the analysis to surveys performed in 1998 and later, the era in which remotely-sensed chlorophyll and derived productivity estimates are available. See Figure 1 for more information.

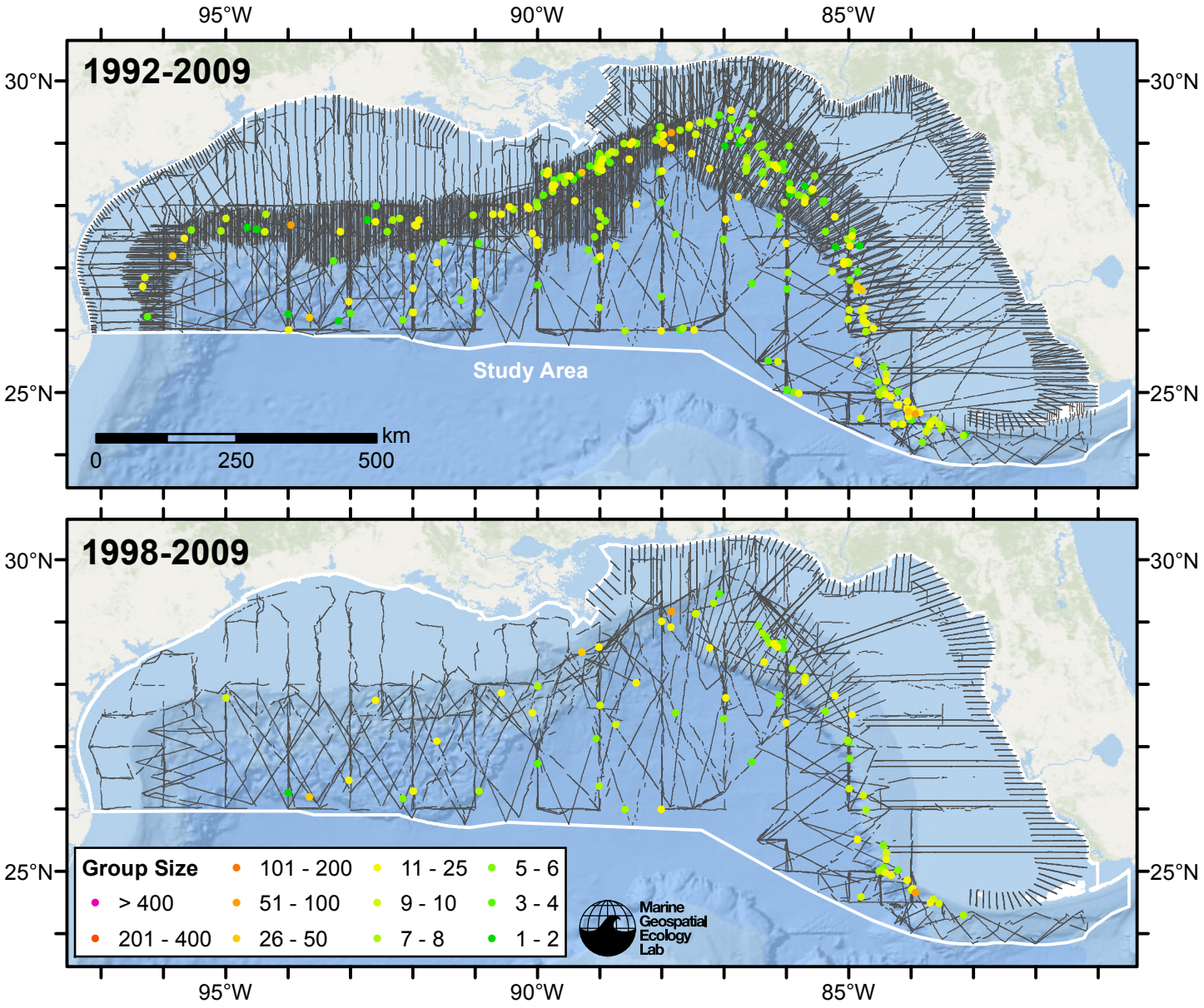

Figure 1: Risso's dolphin sightings and survey tracklines. The top map shows all surveys. The bottom map shows surveys performed in 1998 or later. the era in which remotely-sensed chlorophyll and derived productivity estimates are available. Models fitted to contemporaneous (day-of-sighting) estimates of those predictors only utilize these surveys. These maps illustrate the survey data lost in order to utilize those predictors. Models fitted to climatogical estimates of those predictors do not suffer this data loss.

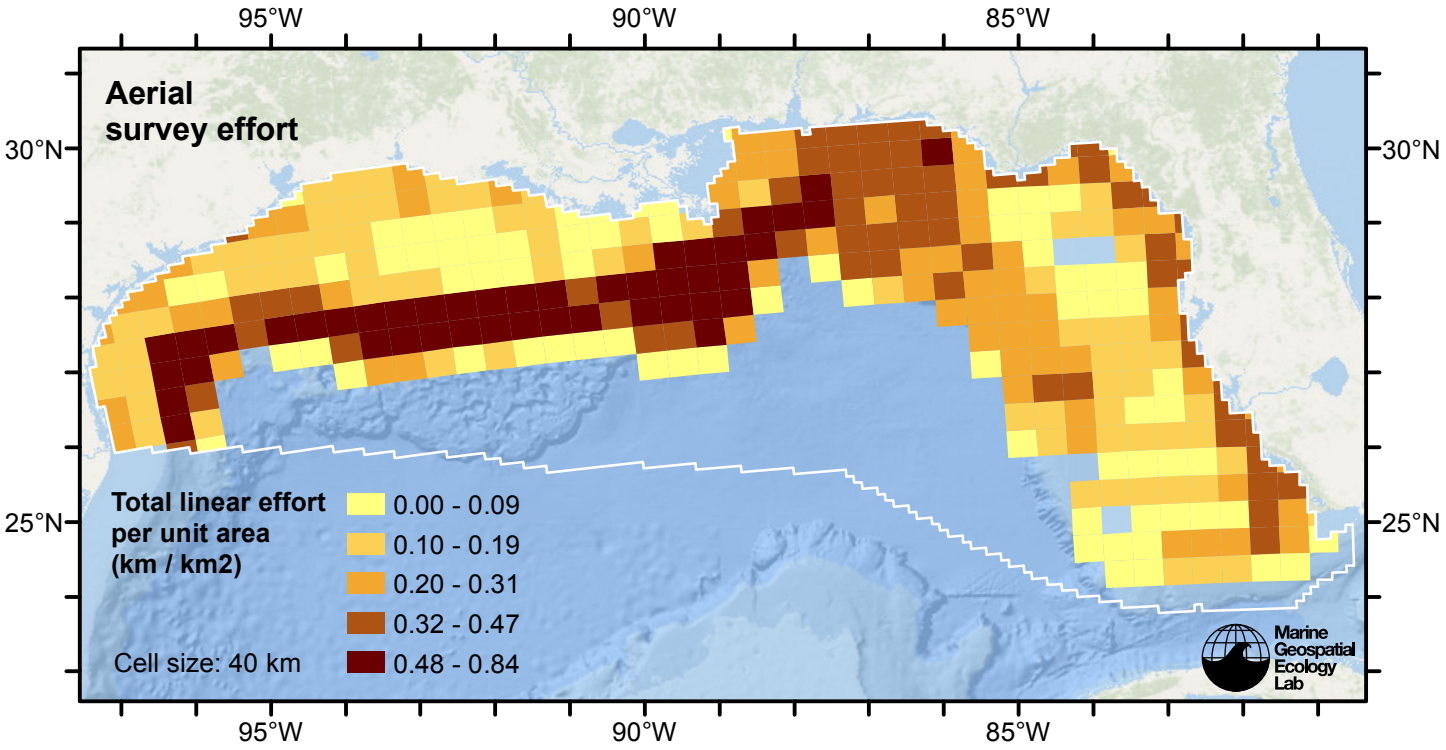

Figure 2: Aerial linear survey effort per unit area.

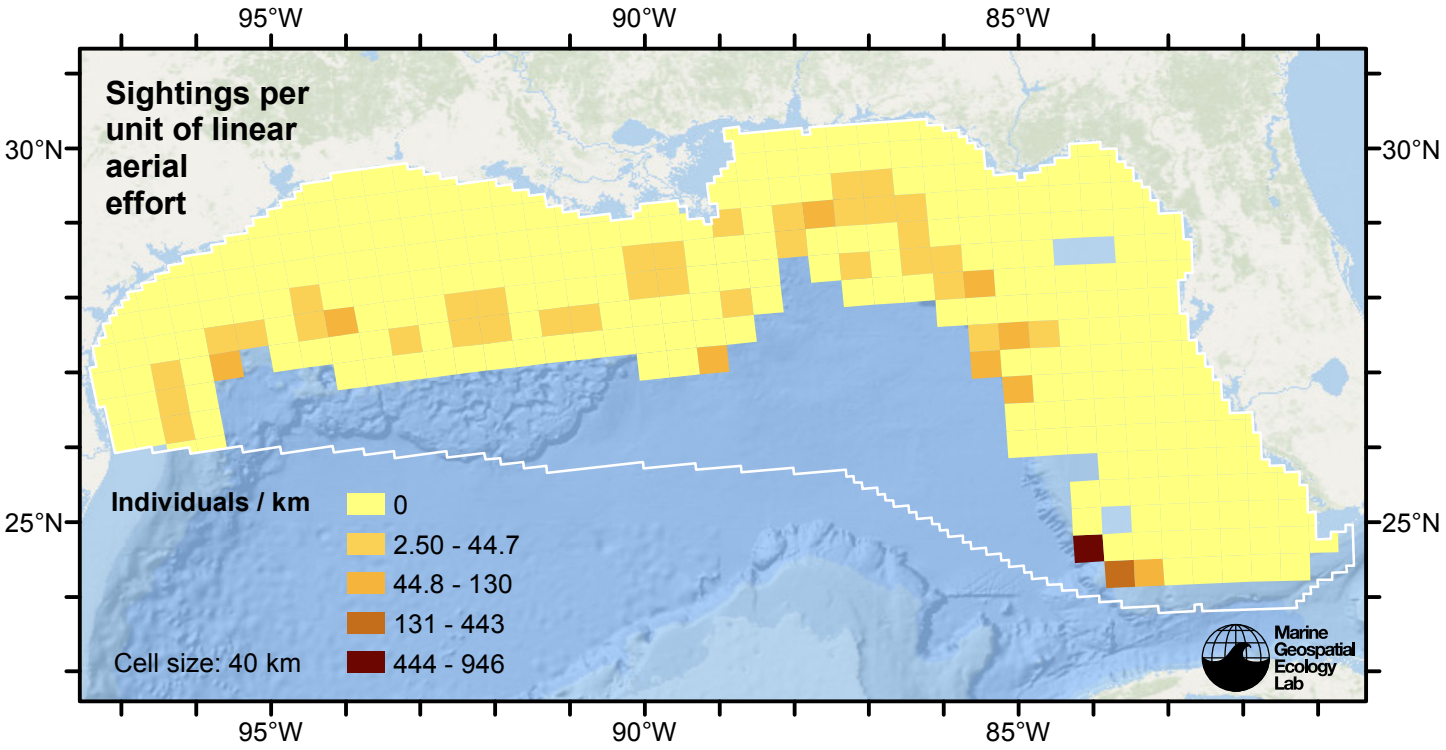

Figure 3: Risso's dolphin sightings per unit aerial linear survey effort.

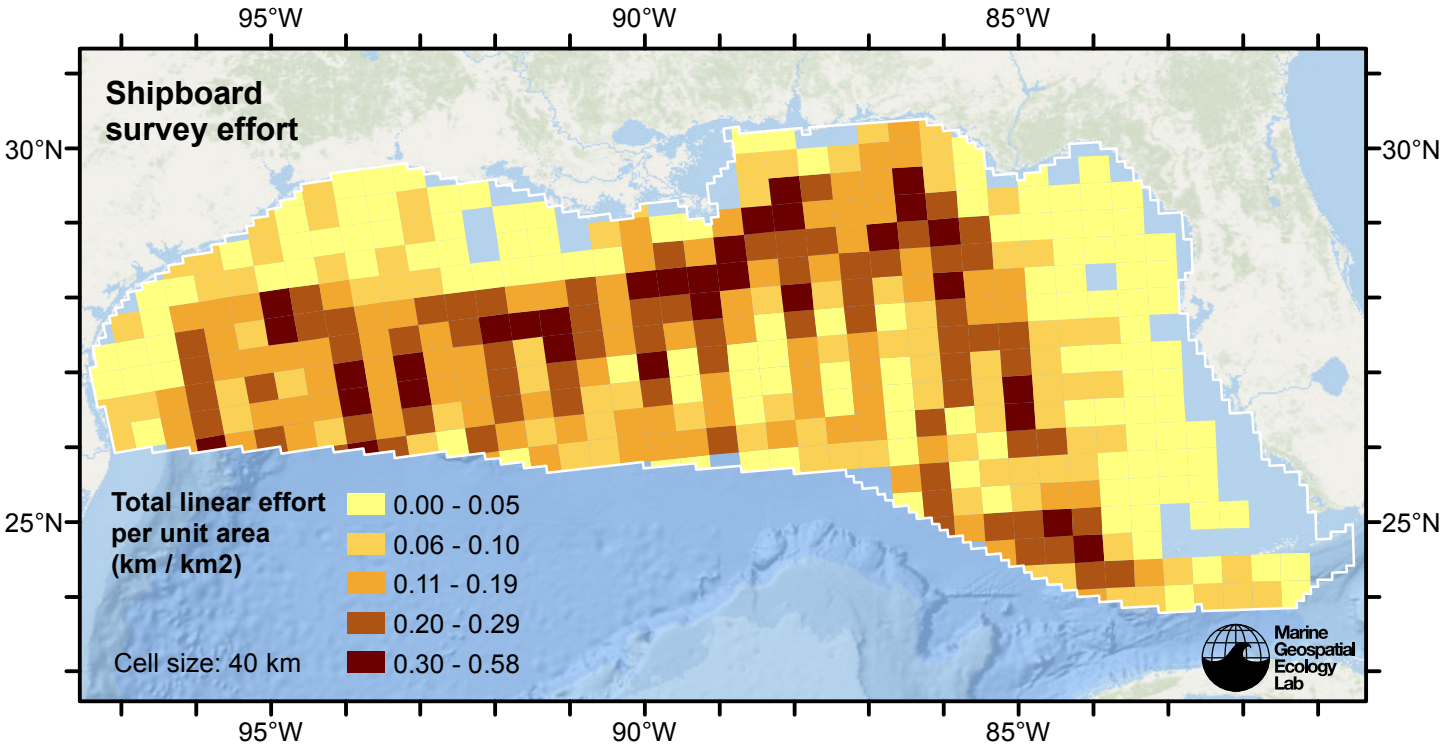

Figure 4: Shipboard linear survey effort per unit area.

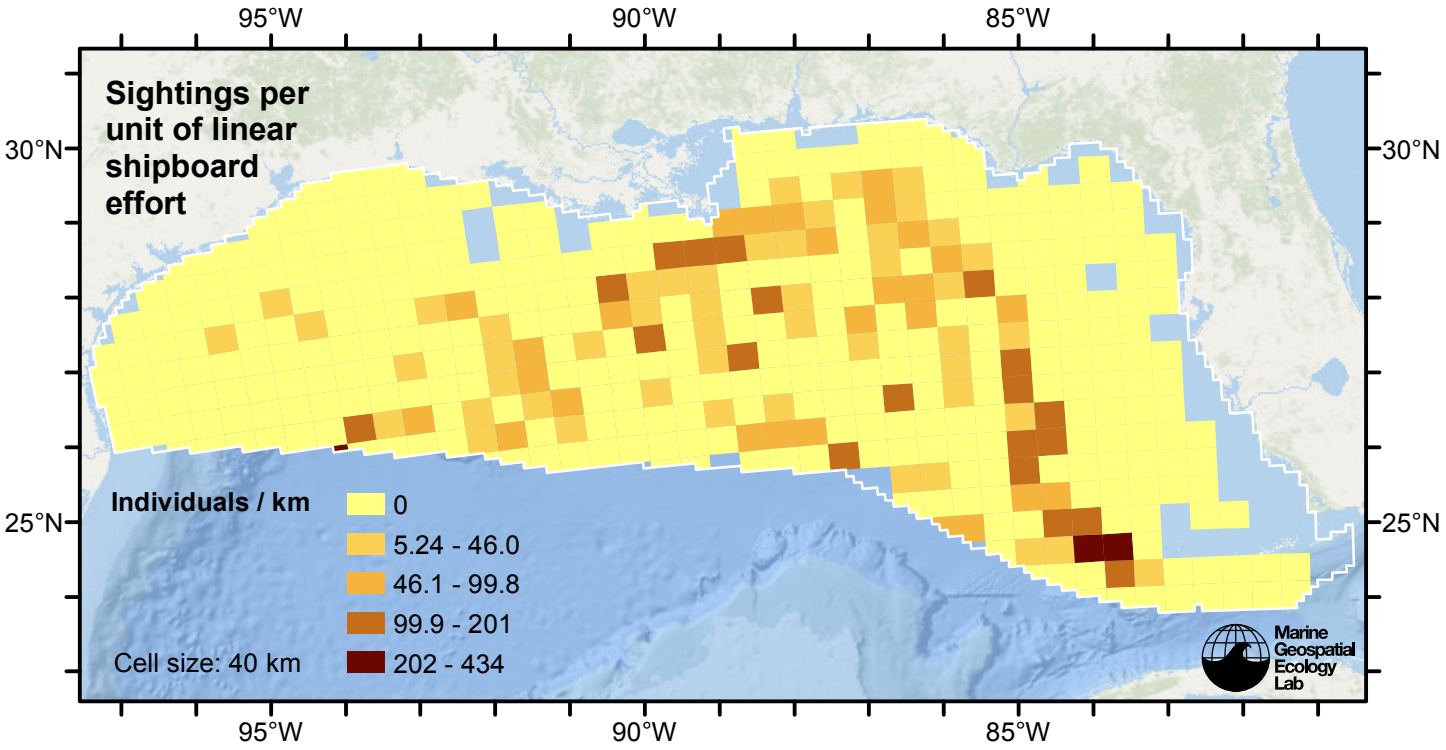

Figure 5: Risso's dolphin sightings per unit shipboard linear survey effort.

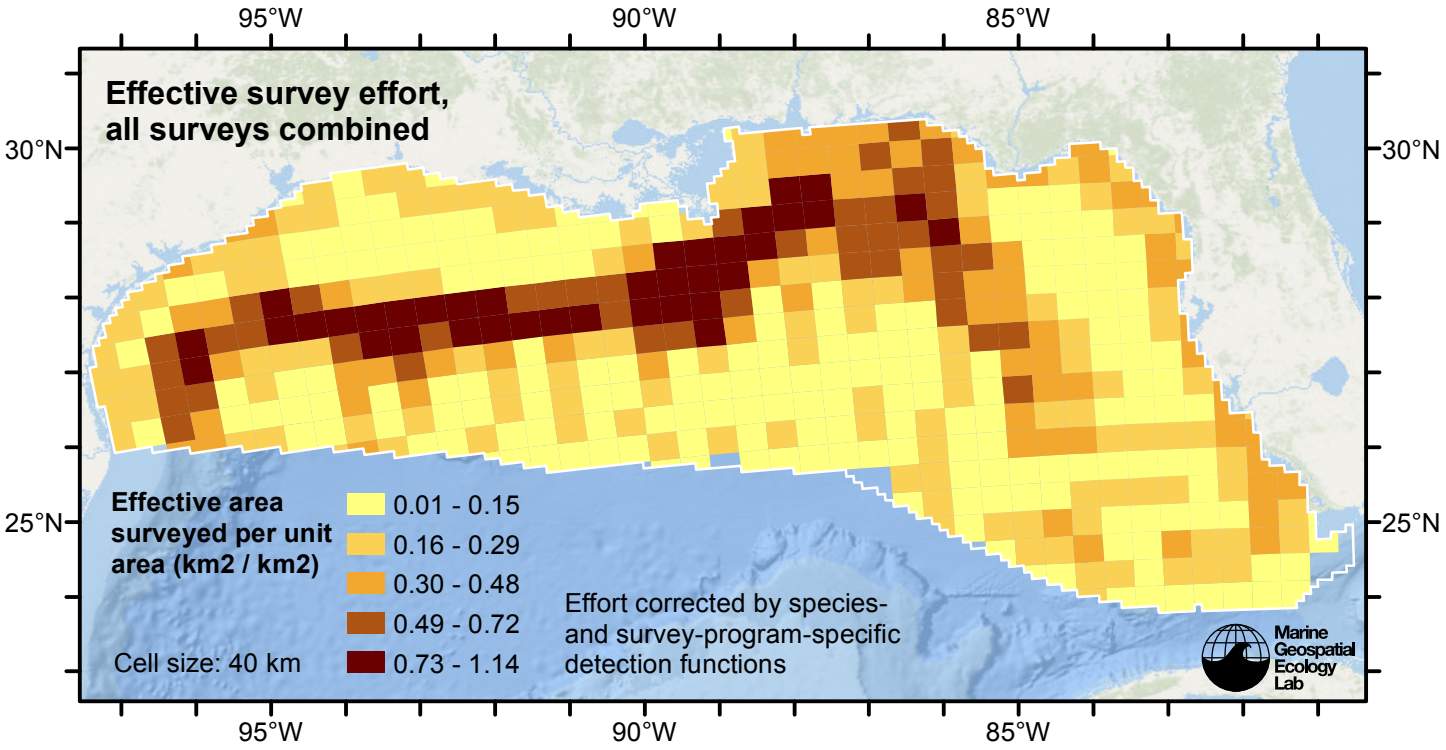

Figure 6: Effective survey effort per unit area, for all surveys combined. Here, effort is corrected by the species- and survey-program-specific detection functions used in fitting the density models.

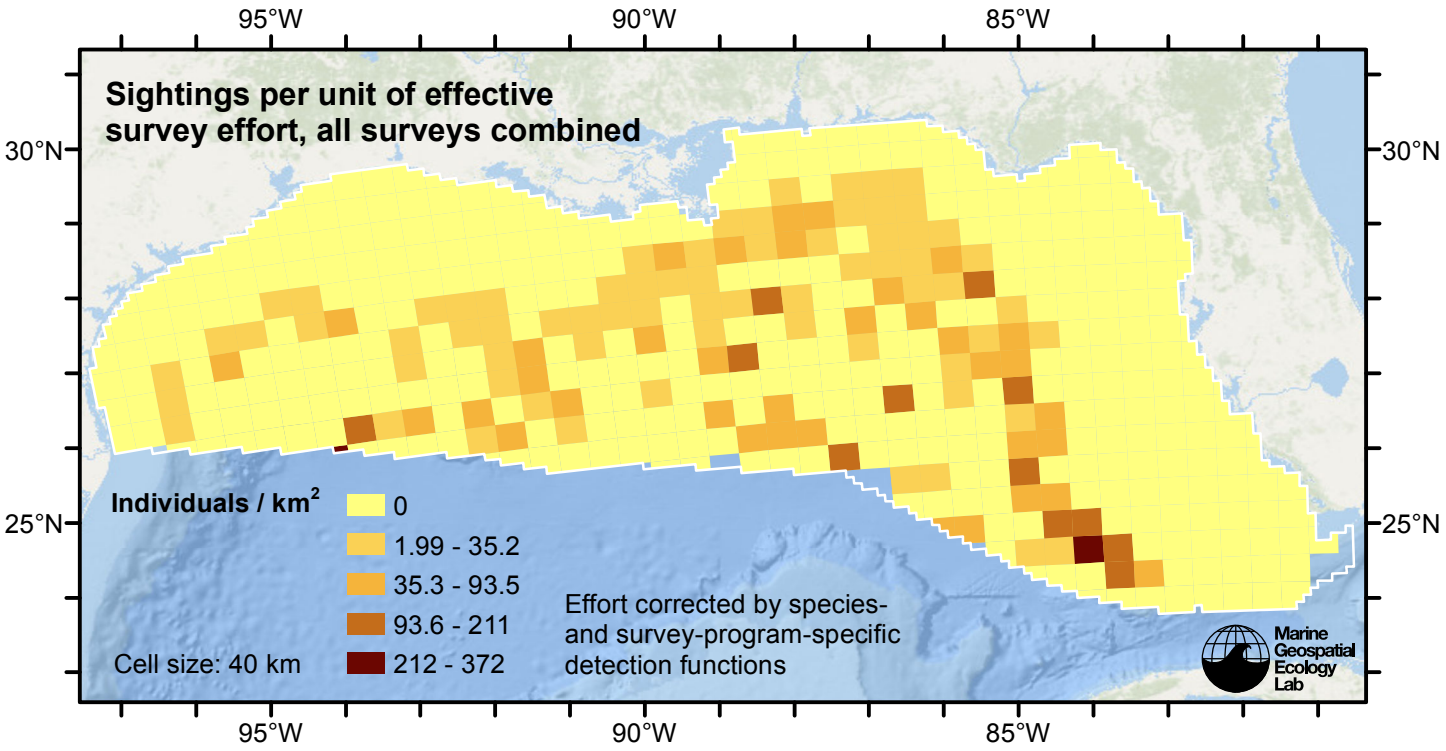

Figure 7: Risso's dolphin sightings per unit of effective survey effort, for all surveys combined. Here, effort is corrected by the species- and survey-program-specific detection functions used in fitting the density models.

Detection Functions

The detection hierarchy figures below show how sightings from multiple surveys were pooled to try to achieve Buckland et. al's (2001) recommendation that at least 60-80 sightings be used to fit a detection function. Leaf nodes, on the right, usually represent individual surveys, while the hierarchy to the left shows how they have been grouped according to how similar we believed the surveys were to each other in their detection performance.

At each node, the red or green number indicates the total number of sightings below that node in the hierarchy, and is colored green if 70 or more sightings were available, and red otherwise. If a grouping node has zero sightings–i.e. all of the surveys within it had zero sightings–it may be collapsed and shown as a leaf to save space.

Each histogram in the figure indicates a node where a detection function was fitted. The actual detection functions do not appear in this figure; they are presented in subsequent sections. The histogram shows the frequency of sightings by perpendicular sighting distance for all surveys contained by that node. Each survey (leaf node) recieves the detection function that is closest to it up the hierarchy. Thus, for common species, sufficient sightings may be available to fit detection functions deep in the hierarchy, with each function applying to only a few surveys, thereby allowing variability in detection performance between surveys to be addressed relatively finely. For rare species, so few sightings may be available that we have to pool many surveys together to try to meet Buckland's recommendation, and fit only a few coarse detection functions high in the hierarchy.

A blue Proxy Species tag indicates that so few sightings were available that, rather than ascend higher in the hierarchy to a point that we would pool grossly-incompatible surveys together, (e.g. shipboard surveys that used big-eye binoculars with those that used only naked eyes) we pooled sightings of similar species together instead. The list of species pooled is given in following sections.

Shipboard Surveys

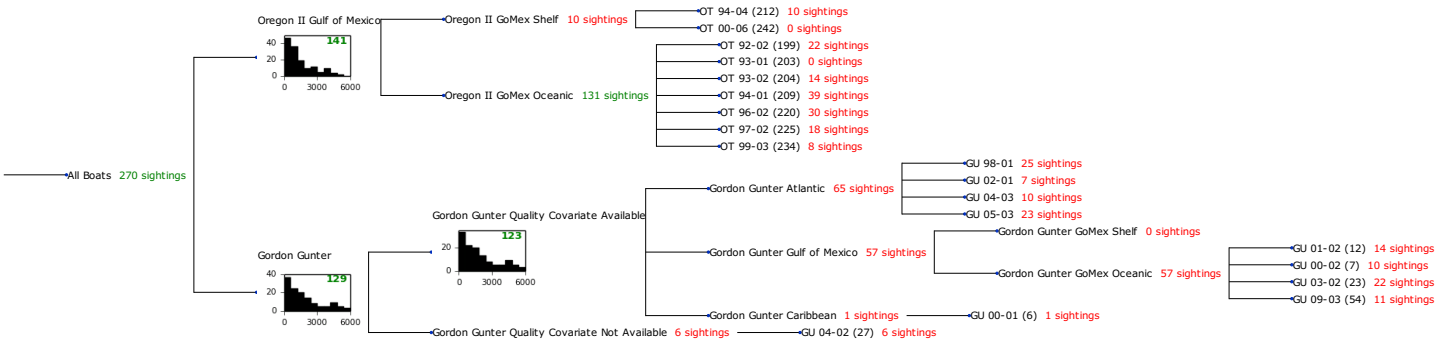

Figure 8: Detection hierarchy for shipboard surveys

Oregon II Gulf of Mexico

The sightings were right truncated at 6000m.

Covariate	Description
beaufort	Beaufort sea state.
quality	Survey-specific index of the quality of observation conditions, utilizing relevant factors other than Beaufort sea state (see methods).
size	Estimated size (number of individuals) of the sighted group.

Table 4: Covariates tested in candidate "multi-covariate distance sampling" (MCDS) detection functions.

Key	Adjustment	Order	Covariates	Succeeded	Δ AIC	Mean ESHW (m)
hr			beaufort, quality, size	Yes	0.00	1915
hn	cos	3		Yes	0.06	1668
hr			quality, size	Yes	0.75	1760
hr	poly	4		Yes	0.81	1221
hr			beaufort, quality	Yes	1.47	1810
hr			quality	Yes	2.59	1701
hr			size	Yes	3.34	1732
hr			beaufort, size	Yes	3.63	1843
hn			beaufort, quality, size	Yes	4.16	2405
hr			beaufort	Yes	4.69	1784
hn			beaufort, size	Yes	4.85	2427
hr				Yes	5.34	1625
hn	cos	2		Yes	6.90	1974
hn			beaufort, quality	Yes	6.92	2424
hr	poly	2		Yes	7.34	1625
hn			beaufort	Yes	10.01	2420
hn			quality, size	Yes	10.49	2406
hn			size	Yes	10.64	2417
hn			quality	Yes	13.79	2413
hn				Yes	14.86	2422
hn	herm	4		Yes	16.72	2417

Table 5: Candidate detection functions for Oregon II Gulf of Mexico. The first one listed was selected for the density model.

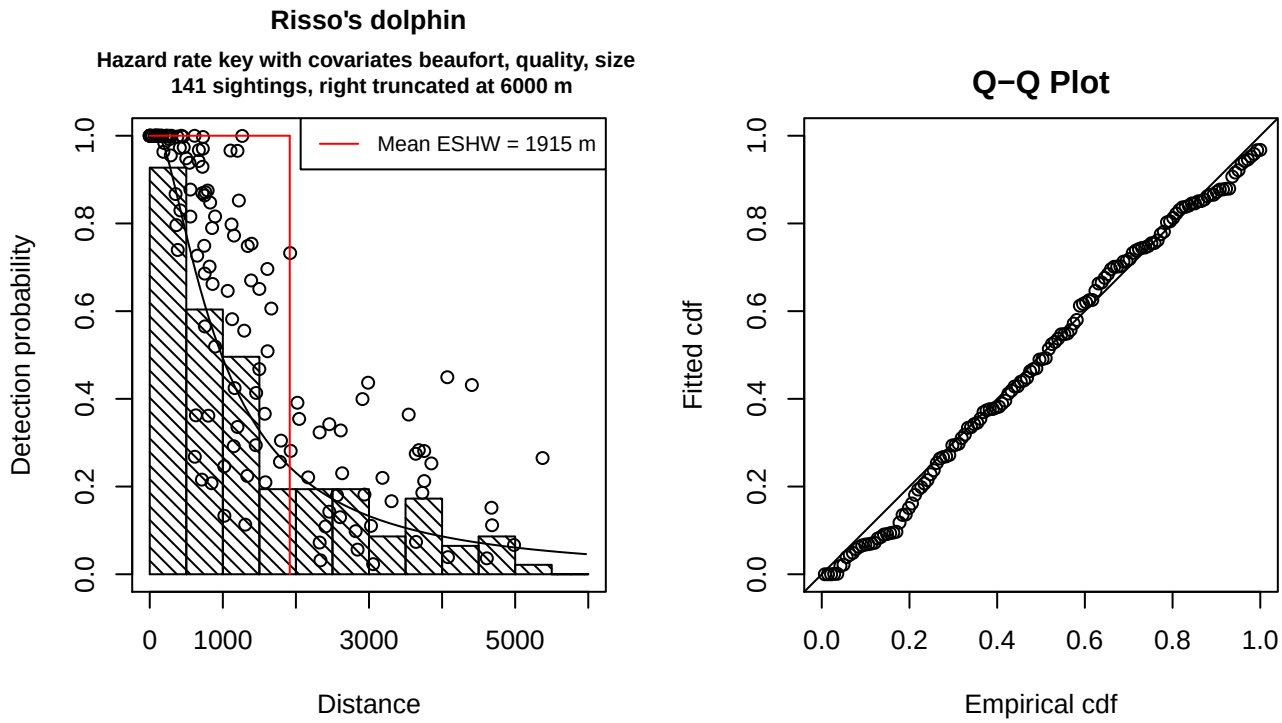

Figure 9: Detection function for Oregon II Gulf of Mexico that was selected for the density model

Statistical output for this detection function:

```
Summary for ds object
Number of observations :  141
Distance range         :  0  -  6000
AIC                    :  2322.728

Detection function:
 Hazard-rate key function

Detection function parameters
Scale Coefficients:
             estimate        se
(Intercept)  7.3916603 0.4586564
beaufort    -0.1906380 0.1085974
quality     -0.2949812 0.1123805
size         0.3227455 0.1397792

Shape parameters:
             estimate        se
(Intercept) 0.5328842 0.1641668

                       Estimate          SE        CV
Average p             0.2533669  0.03723334 0.1469542
N in covered region 556.5051785 92.04741915 0.1654026
```

Additional diagnostic plots:

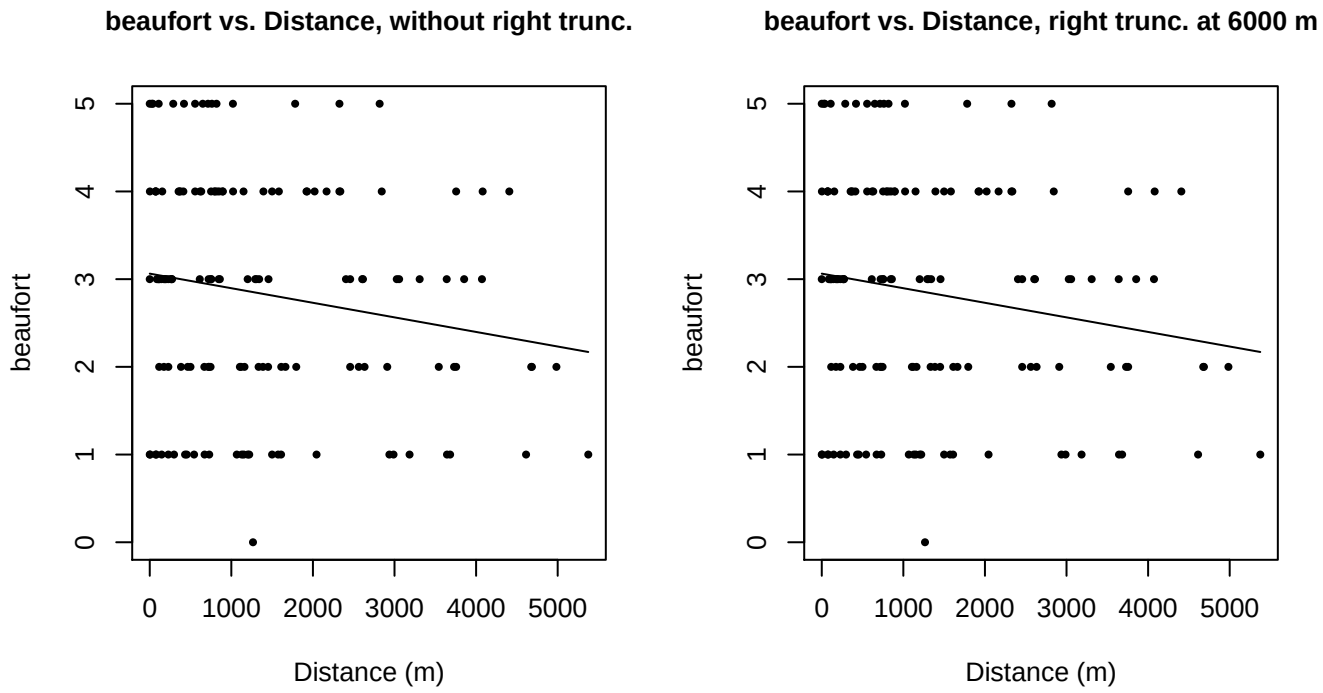

Figure 10: Scatterplots showing the relationship between Beaufort sea state and perpendicular sighting distance, for all sightings (left) and only those not right truncated (right). The line is a simple linear regression.

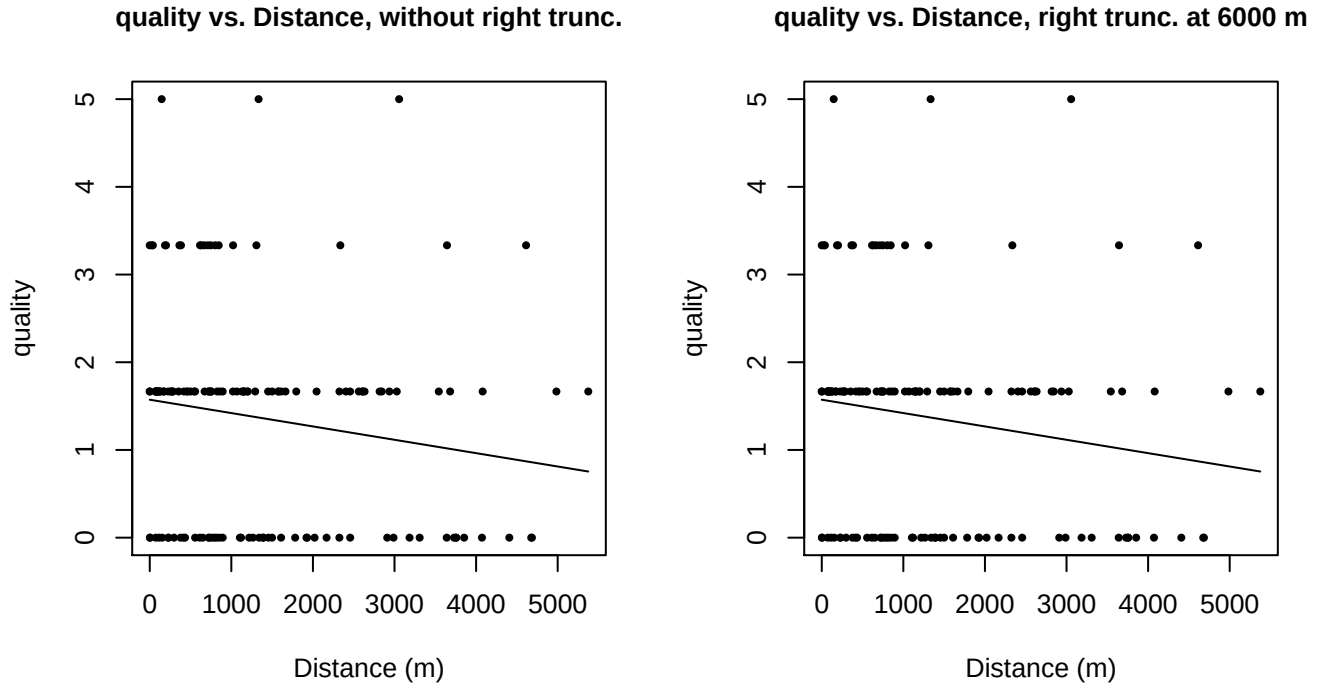

Figure 11: Scatterplots showing the relationship between the survey-specific index of the quality of observation conditions and perpendicular sighting distance, for all sightings (left) and only those not right truncated (right). Low values of the quality index correspond to better observation conditions. The line is a simple linear regression.

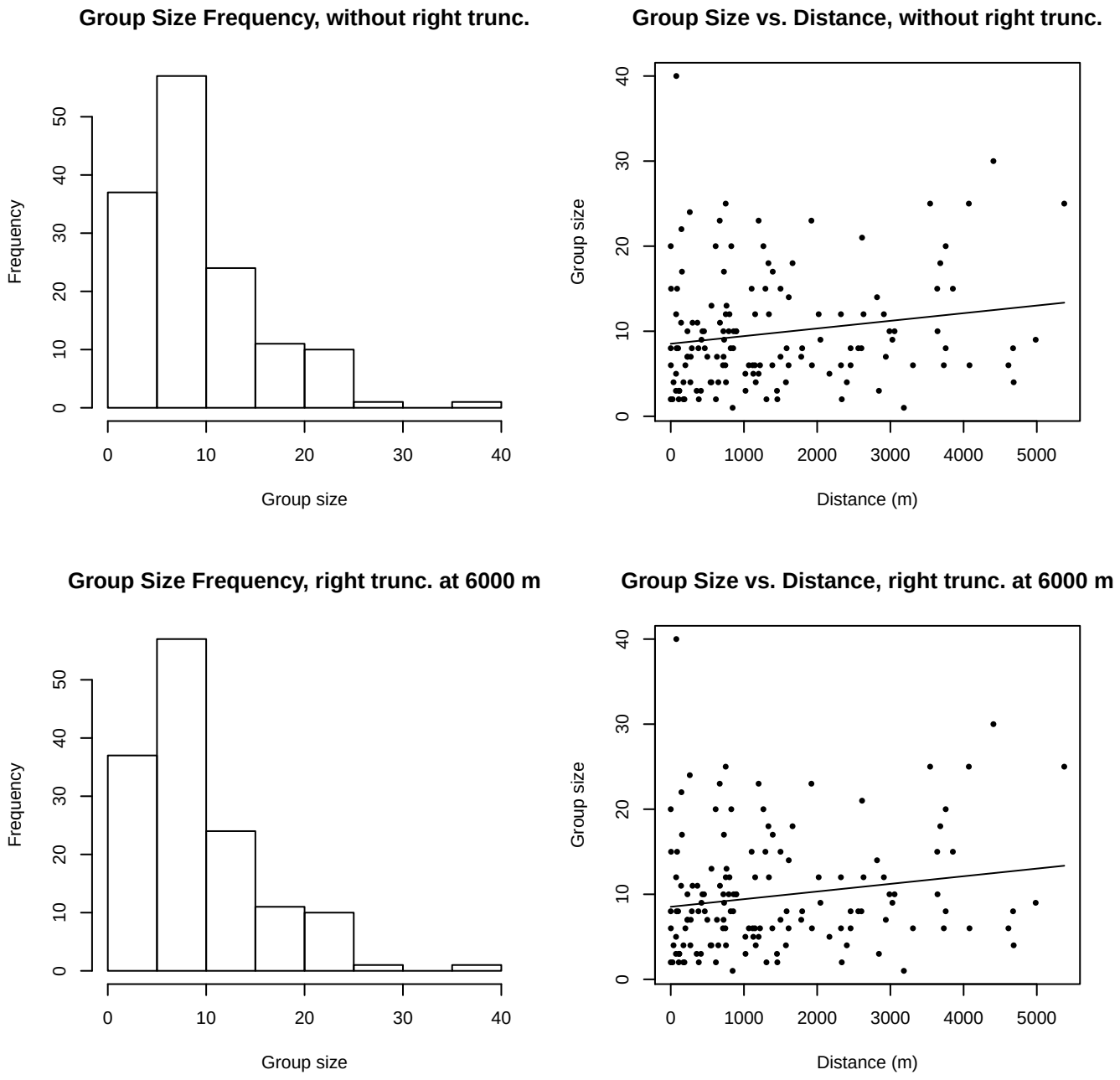

Figure 12: Histograms showing group size frequency and scatterplots showing the relationship between group size and perpendicular sighting distance, for all sightings (top row) and only those not right truncated (bottom row). In the scatterplot, the line is a simple linear regression.

Gordon Gunter

The sightings were right truncated at 6100m.

Covariate	Description
beaufort	Beaufort sea state.
size	Estimated size (number of individuals) of the sighted group.

Table 6: Covariates tested in candidate "multi-covariate distance sampling" (MCDS) detection functions.

Key	Adjustment	Order	Covariates	Succeeded	Δ AIC	Mean ESHW (m)
hr			size	Yes	0.00	2426
hn	cos	2		Yes	0.50	2304
hr				Yes	1.46	2132
hr			beaufort, size	Yes	1.77	2449
hr			beaufort	Yes	2.20	2276
hr	poly	4		Yes	3.43	2095
hr	poly	2		Yes	3.46	2132
hn	cos	3		Yes	10.14	2553
hn				Yes	11.24	3106
hn			beaufort	Yes	11.25	3110
hn			size	Yes	12.15	3141
hn			beaufort, size	Yes	12.90	3119
hn	herm	4		Yes	12.90	3095

Table 7: Candidate detection functions for Gordon Gunter. The first one listed was selected for the density model.

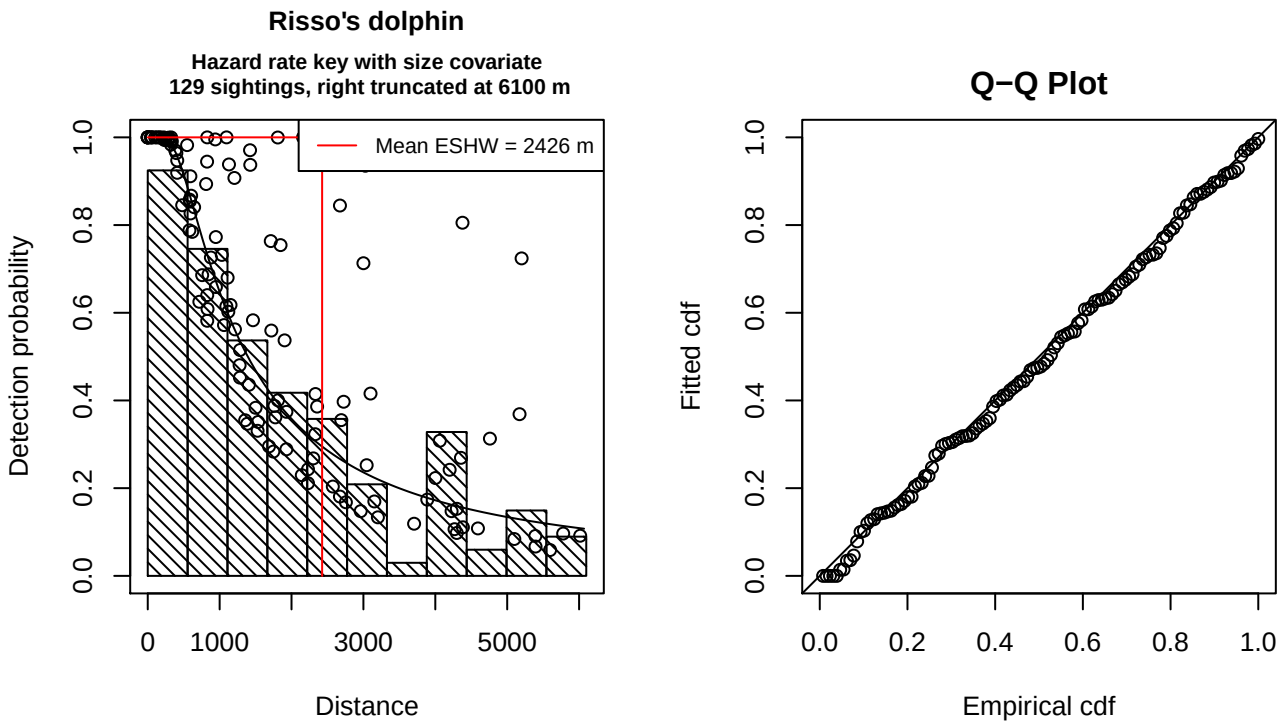

Figure 13: Detection function for Gordon Gunter that was selected for the density model

Statistical output for this detection function:

```
Summary for ds object
```

```
Number of observations :  129
Distance range         :  0  -  6100
AIC                    :  2180.94

Detection function:
 Hazard-rate key function

Detection function parameters
Scale Coefficients:
             estimate        se
(Intercept) 6.4483550 0.4532456
size        0.7370187 0.3673670

Shape parameters:
             estimate        se
(Intercept) 0.3317178 0.1958107

                       Estimate          SE        CV
Average p             0.3498014  0.05748444 0.1643345
N in covered region 368.7807069 66.39806619 0.1800476
```

Additional diagnostic plots:

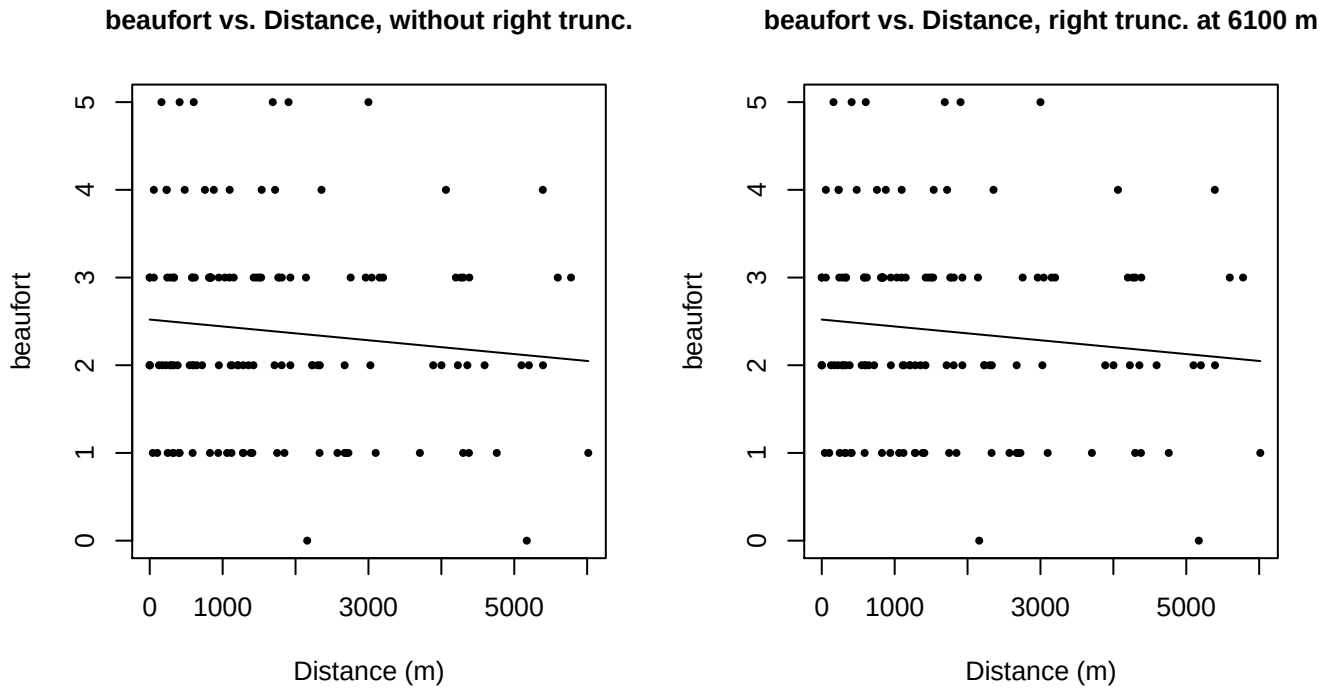

Figure 14: Scatterplots showing the relationship between Beaufort sea state and perpendicular sighting distance, for all sightings (left) and only those not right truncated (right). The line is a simple linear regression.

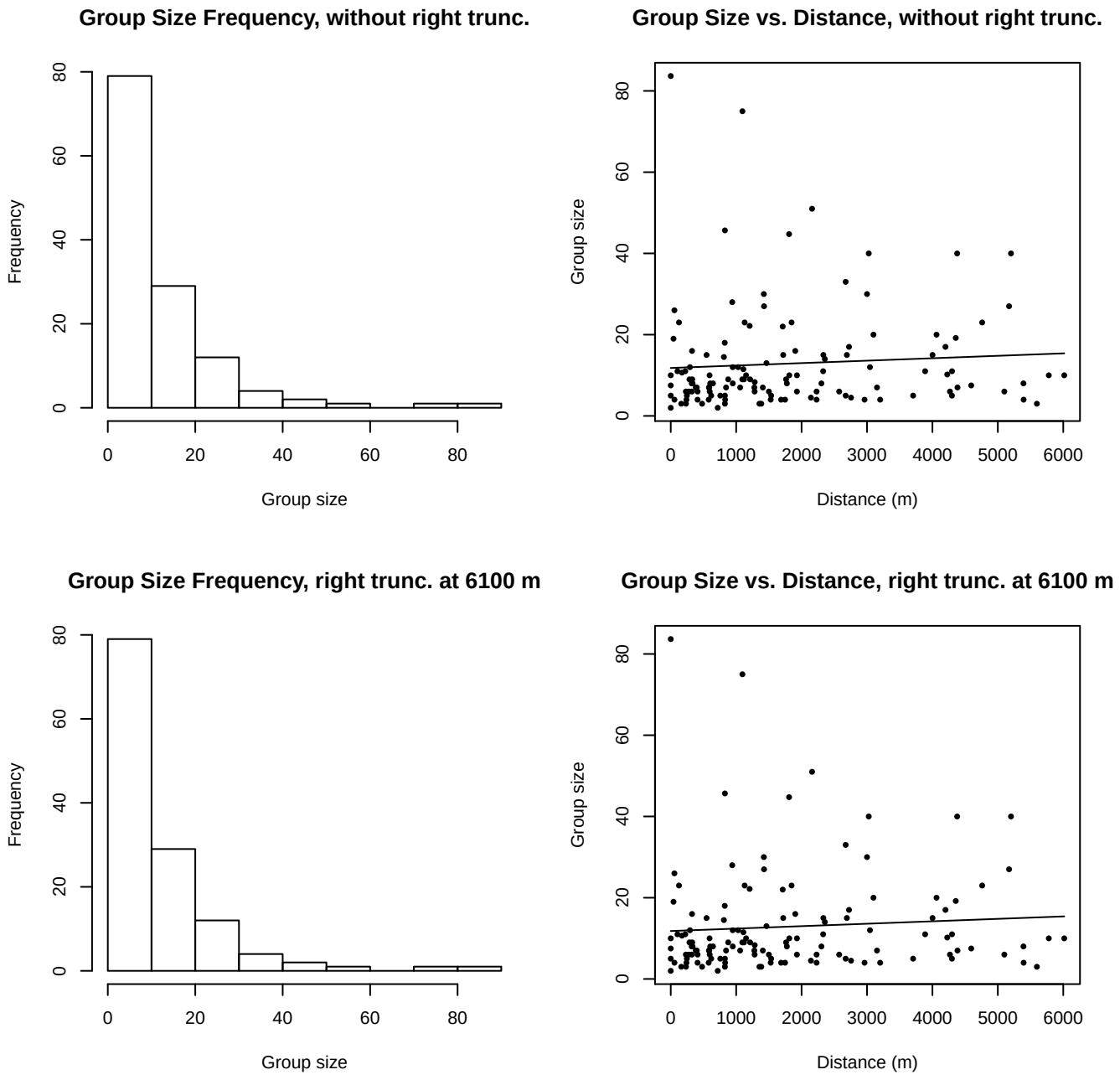

Figure 15: Histograms showing group size frequency and scatterplots showing the relationship between group size and perpendicular sighting distance, for all sightings (top row) and only those not right truncated (bottom row). In the scatterplot, the line is a simple linear regression.

Gordon Gunter Quality Covariate Available

The sightings were right truncated at 6100m.

Covariate	Description
beaufort	Beaufort sea state.
quality	Survey-specific index of the quality of observation conditions, utilizing relevant factors other than Beaufort sea state (see methods).
size	Estimated size (number of individuals) of the sighted group.

Table 8: Covariates tested in candidate "multi-covariate distance sampling" (MCDS) detection functions.

Key	Adjustment	Order	Covariates	Succeeded	Δ AIC	Mean ESHW (m)
hr			quality, size	Yes	0.00	2676
hr			size	Yes	0.37	2549
hr			quality	Yes	0.80	2472
hn	cos	2		Yes	1.45	2360
hr			beaufort, quality, size	Yes	1.83	2702
hr			beaufort, quality	Yes	1.86	2551
hr			beaufort, size	Yes	2.03	2600
hr				Yes	2.47	2168
hr			beaufort	Yes	2.82	2430
hr	poly	4		Yes	4.41	2091
hr	poly	2		Yes	4.47	2168
hn	cos	3		Yes	10.26	2636
hn			beaufort	Yes	10.63	3185
hn				Yes	10.93	3178
hn			size	Yes	11.58	3240
hn			quality	Yes	11.84	3203
hn			beaufort, size	Yes	12.23	3204
hn			beaufort, quality	Yes	12.25	3199
hn			quality, size	Yes	12.42	3268
hn	herm	4		Yes	12.62	3166
hn			beaufort, quality, size	Yes	13.61	3243

Table 9: Candidate detection functions for Gordon Gunter Quality Covariate Available. The first one listed was selected for the density model.

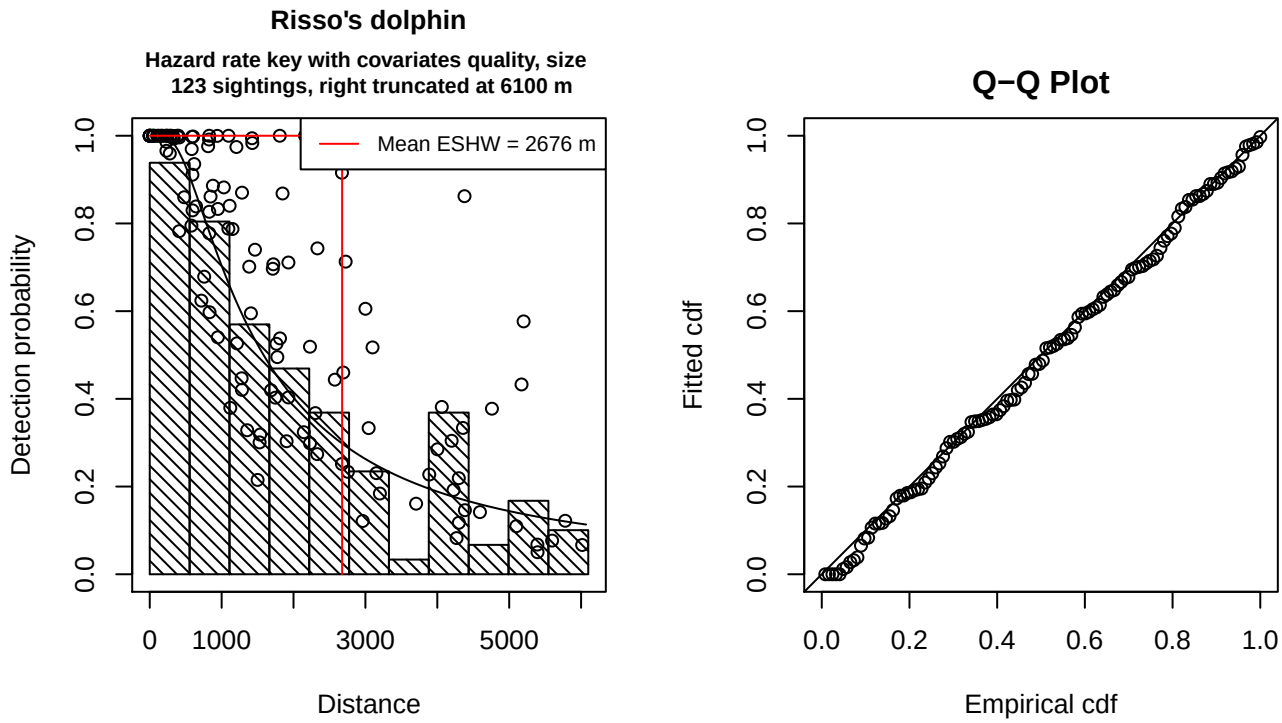

Figure 16: Detection function for Gordon Gunter Quality Covariate Available that was selected for the density model

Statistical output for this detection function:

```
Summary for ds object
Number of observations :  123
Distance range         :  0  -  6100
AIC                    :  2083.318

Detection function:
 Hazard-rate key function

Detection function parameters
Scale Coefficients:
             estimate        se
(Intercept)  7.2066038 0.4736353
quality     -0.2232128 0.1419035
size         0.6553273 0.3184299

Shape parameters:
             estimate        se
(Intercept) 0.4285349 0.2031903

                       Estimate          SE        CV
Average p             0.3747365  0.06095815 0.1626694
N in covered region 328.2306433 58.77494296 0.1790660
```

Additional diagnostic plots:

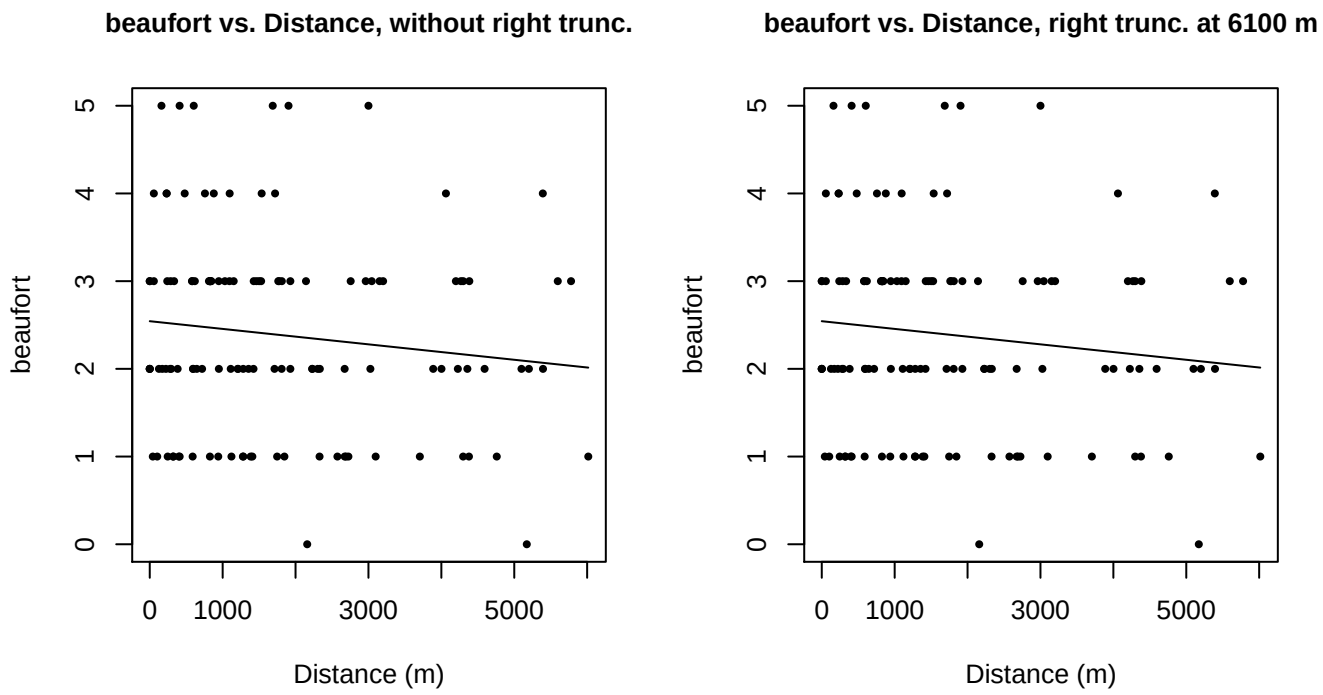

Figure 17: Scatterplots showing the relationship between Beaufort sea state and perpendicular sighting distance, for all sightings (left) and only those not right truncated (right). The line is a simple linear regression.

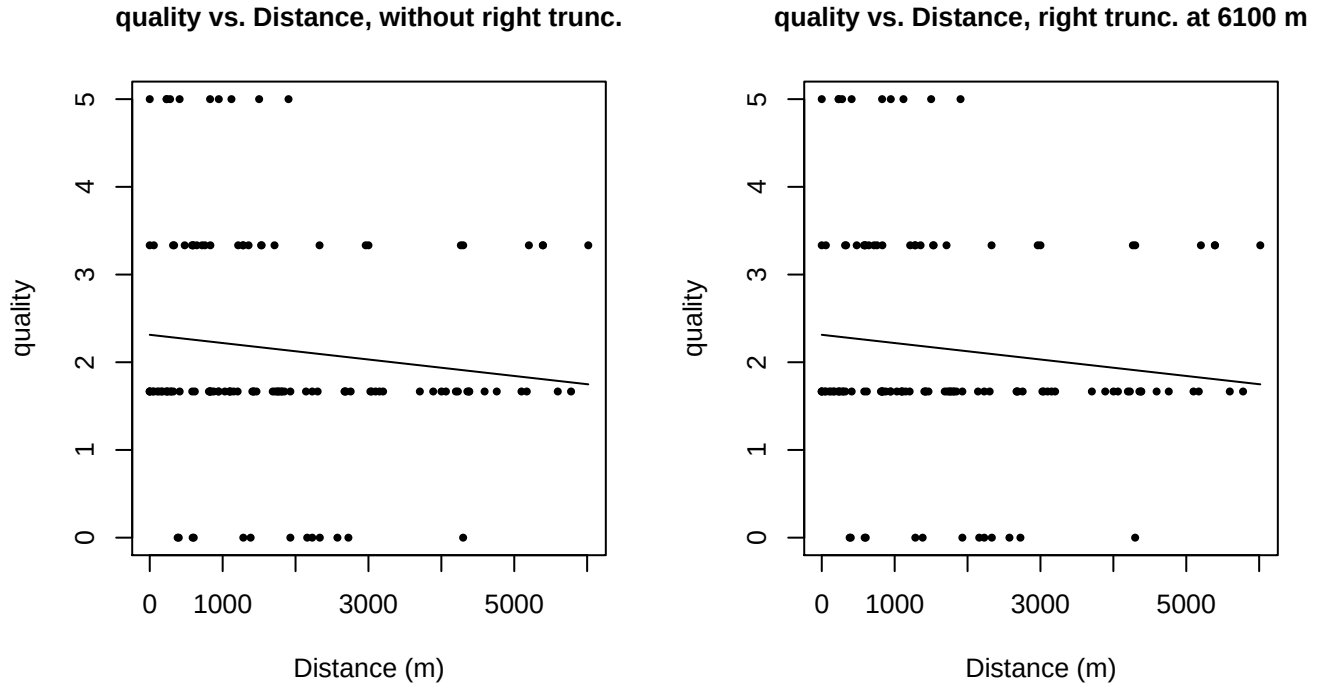

Figure 18: Scatterplots showing the relationship between the survey-specific index of the quality of observation conditions and perpendicular sighting distance, for all sightings (left) and only those not right truncated (right). Low values of the quality index correspond to better observation conditions. The line is a simple linear regression.

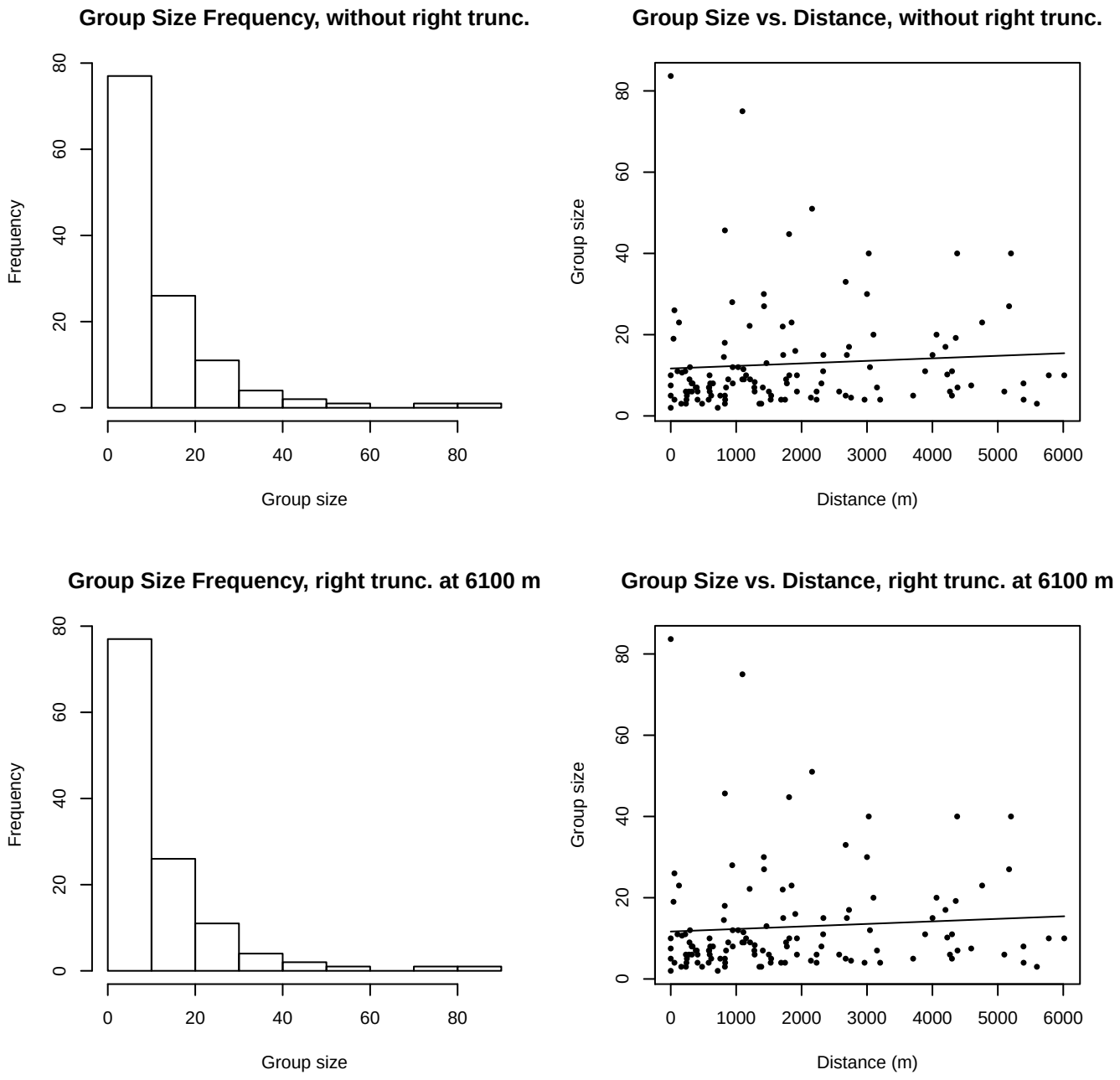

Figure 19: Histograms showing group size frequency and scatterplots showing the relationship between group size and perpendicular sighting distance, for all sightings (top row) and only those not right truncated (bottom row). In the scatterplot, the line is a simple linear regression.

Aerial Surveys

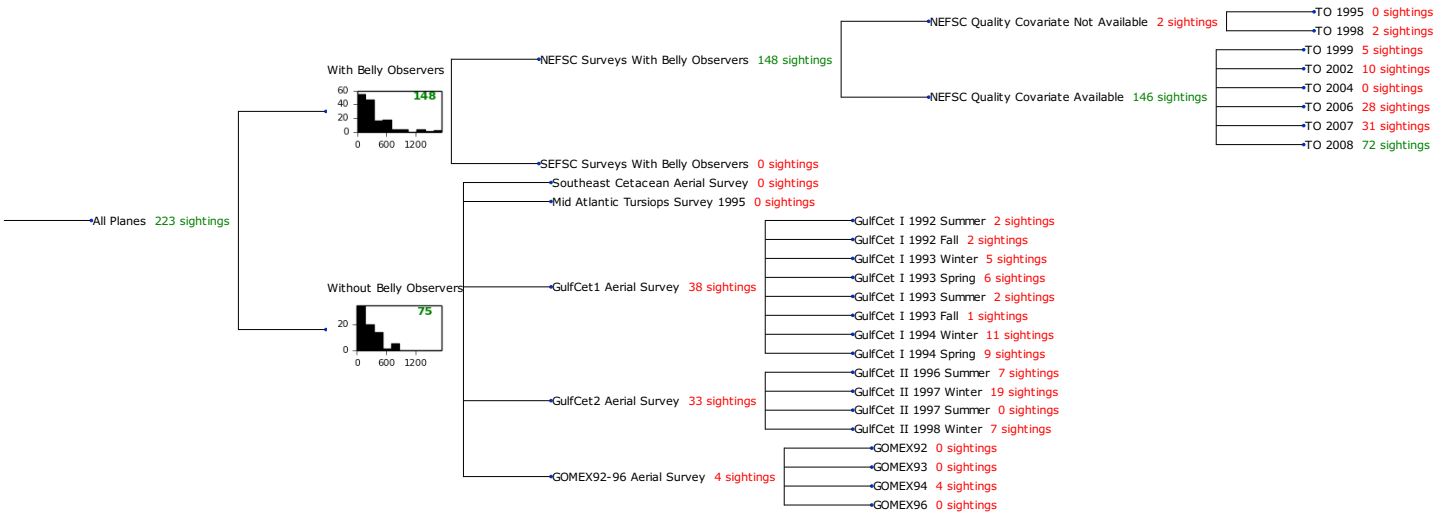

Figure 20: Detection hierarchy for aerial surveys

With Belly Observers

The sightings were right truncated at 1500m.

Covariate	Description
beaufort	Beaufort sea state.
size	Estimated size (number of individuals) of the sighted group.

Table 10: Covariates tested in candidate "multi-covariate distance sampling" (MCDS) detection functions.

Key	Adjustment	Order	Covariates	Succeeded	Δ AIC	Mean ESHW (m)
hr				Yes	0.00	474
hn	cos	2		Yes	0.96	436
hr			size	Yes	1.85	477
hr			beaufort	Yes	1.92	476
hr	poly	2		Yes	2.00	474
hr	poly	4		Yes	2.00	474
hr			beaufort, size	Yes	3.74	478
hn	cos	3		Yes	10.33	460
hn				Yes	10.66	533
hn			beaufort	Yes	11.82	533
hn			size	Yes	11.89	533
hn	herm	4		Yes	12.36	532
hn			beaufort, size	Yes	12.82	533

Table 11: Candidate detection functions for With Belly Observers. The first one listed was selected for the density model.

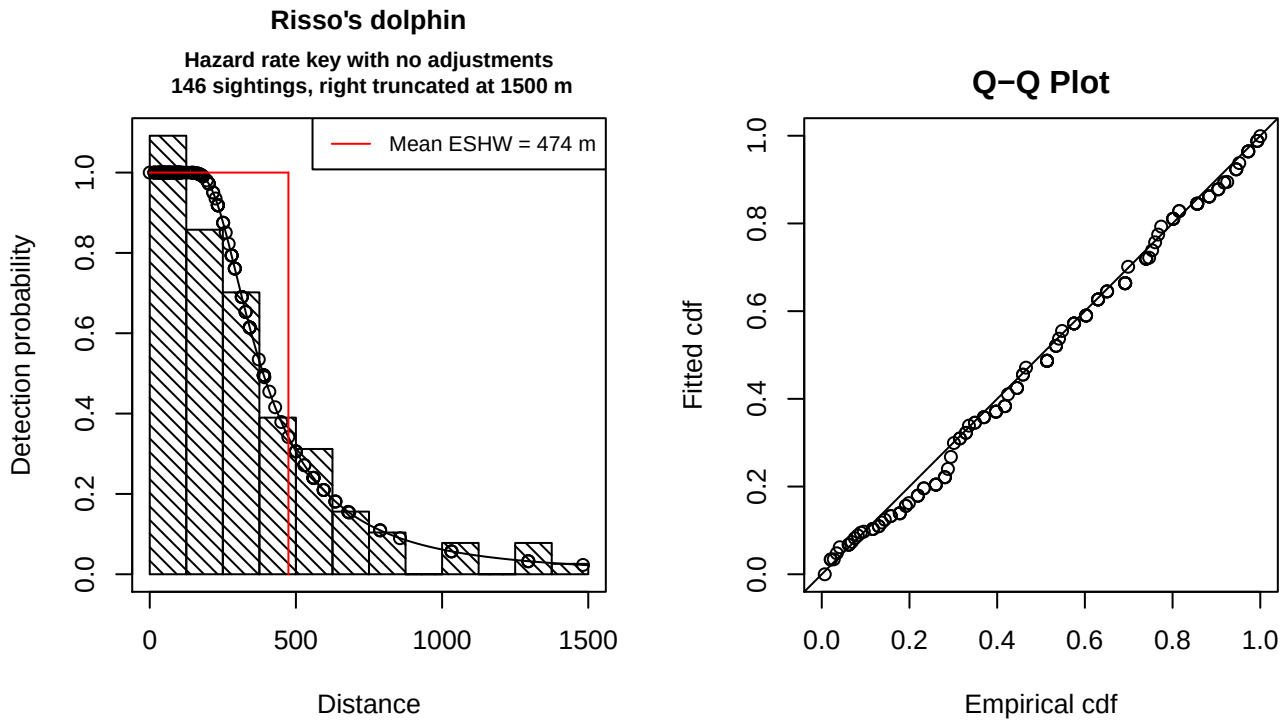

Figure 21: Detection function for With Belly Observers that was selected for the density model

Statistical output for this detection function:

```
Summary for ds object
Number of observations :  146
Distance range         :  0  -  1500
AIC                    :  1969.719

Detection function:
 Hazard-rate key function

Detection function parameters
Scale Coefficients:
            estimate       se
(Intercept) 5.815632 0.132012

Shape parameters:
             estimate        se
(Intercept) 0.9257516 0.1478857

                       Estimate          SE         CV
Average p             0.3162475  0.02818735 0.08913069
N in covered region 461.6637948 51.87818782 0.11237222
```

Additional diagnostic plots:

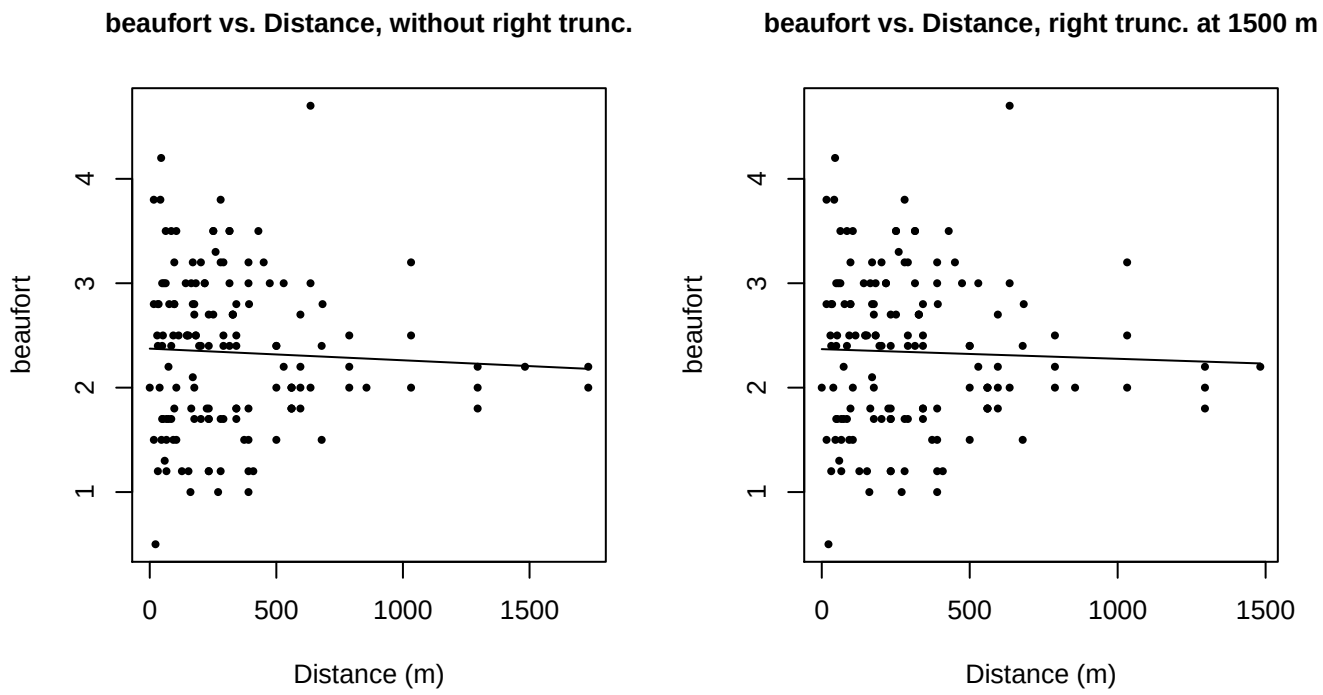

Figure 22: Scatterplots showing the relationship between Beaufort sea state and perpendicular sighting distance, for all sightings (left) and only those not right truncated (right). The line is a simple linear regression.

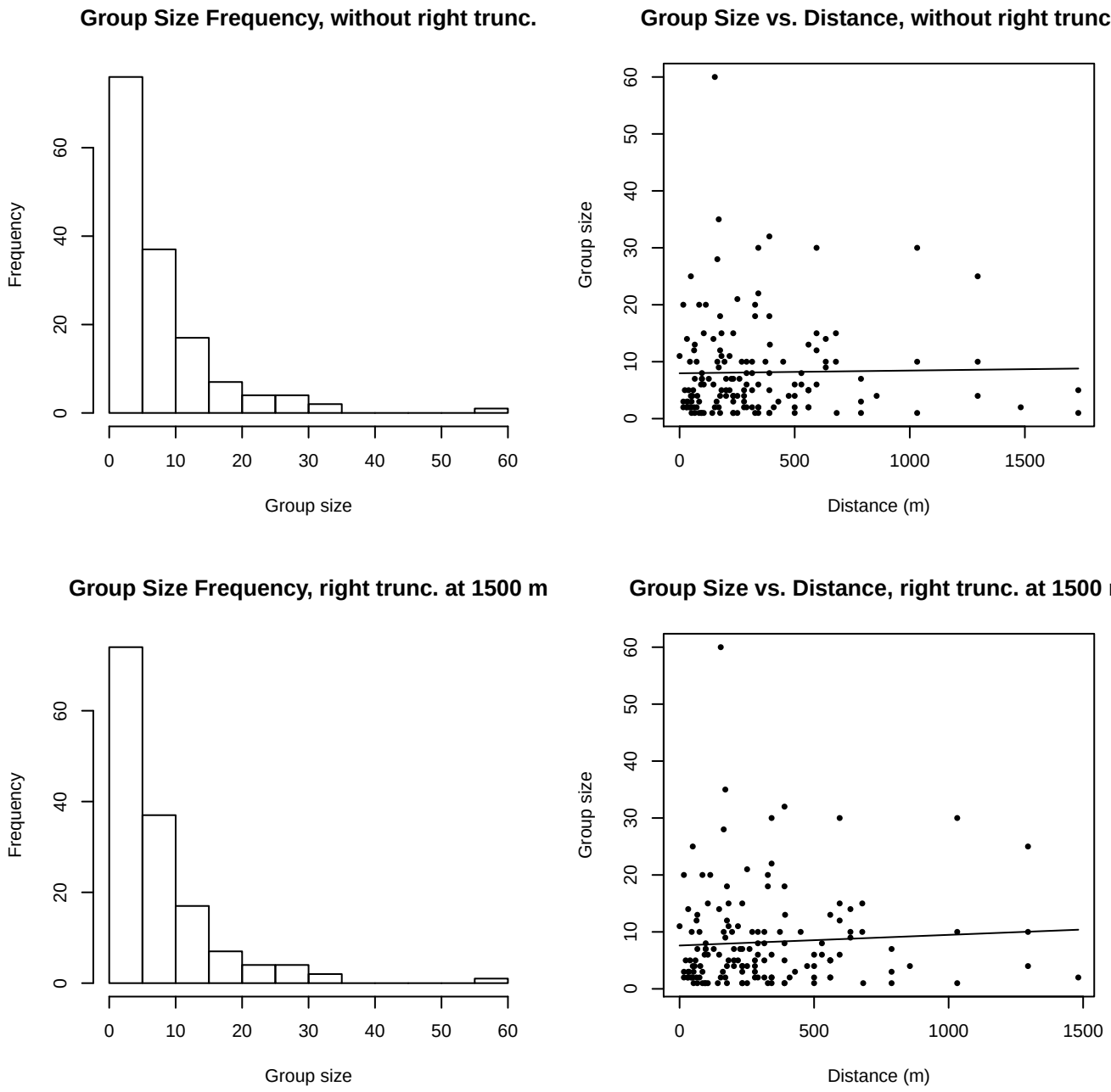

Figure 23: Histograms showing group size frequency and scatterplots showing the relationship between group size and perpendicular sighting distance, for all sightings (top row) and only those not right truncated (bottom row). In the scatterplot, the line is a simple linear regression.

Without Belly Observers

The sightings were right truncated at 1296m. The vertical sighting angles were heaped at 10 degree increments, so the candidate detection functions were fitted using linear bins scaled accordingly.

Covariate	Description
beaufort	Beaufort sea state.
size	Estimated size (number of individuals) of the sighted group.

Table 12: Covariates tested in candidate "multi-covariate distance sampling" (MCDS) detection functions.

Key	Adjustment	Order	Covariates	Succeeded	Δ AIC	Mean ESHW (m)
hr				Yes	0.00	379
hr	poly	2		Yes	2.00	379
hr	poly	4		Yes	2.00	379
hn	cos	2		Yes	2.15	360
hn	cos	3		Yes	2.20	332
hn				Yes	2.97	410
hn	herm	4		Yes	4.94	410
hr			beaufort	No		
hn			beaufort	No		
hr			size	No		
hn			size	No		
hr			beaufort, size	No		
hn			beaufort, size	No		

Table 13: Candidate detection functions for Without Belly Observers. The first one listed was selected for the density model.

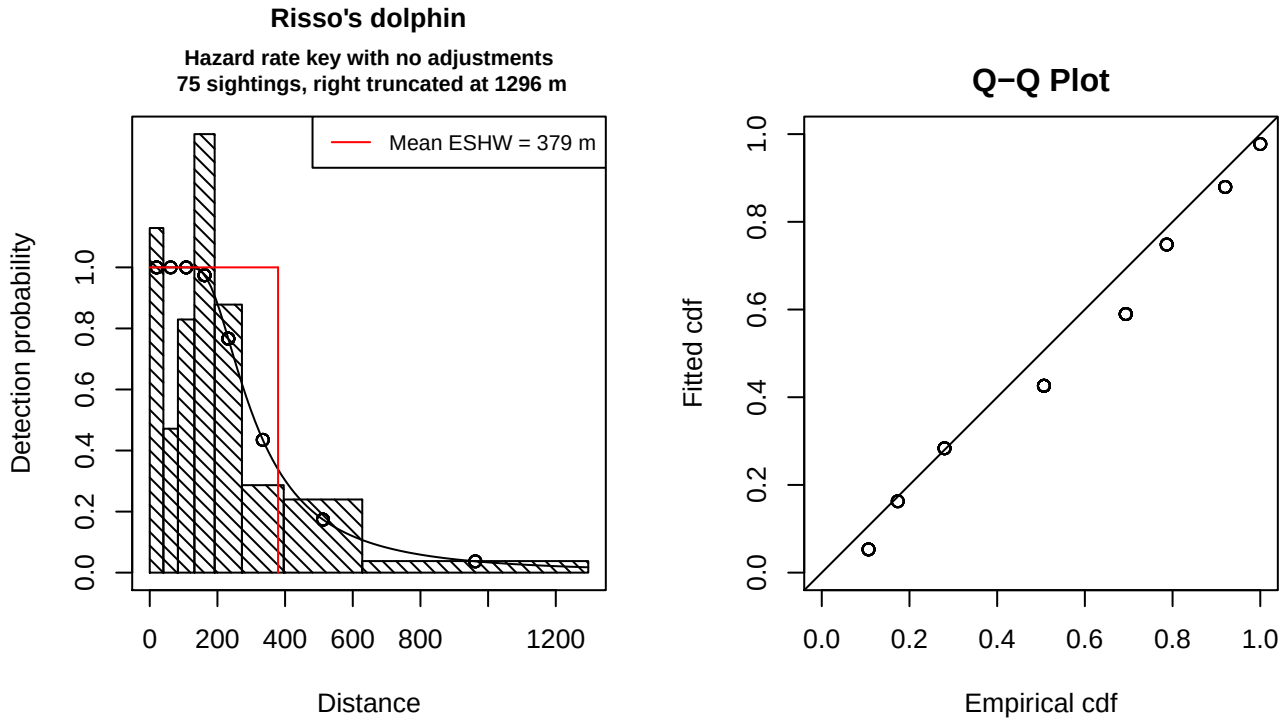

Figure 24: Detection function for Without Belly Observers that was selected for the density model

Statistical output for this detection function:

```
Summary for ds object
Number of observations :  75
Distance range         :  0  -  1296
AIC                    :  310.3741

Detection function:
 Hazard-rate key function

Detection function parameters
Scale Coefficients:
            estimate        se
(Intercept) 5.593342 0.2033349

Shape parameters:
             estimate       se
(Intercept) 0.9427326 0.214553

                        Estimate          SE        CV
Average p               0.2926147  0.03947708 0.1349115
N in covered region 256.3097146 42.60674510 0.1662315
```

Additional diagnostic plots:

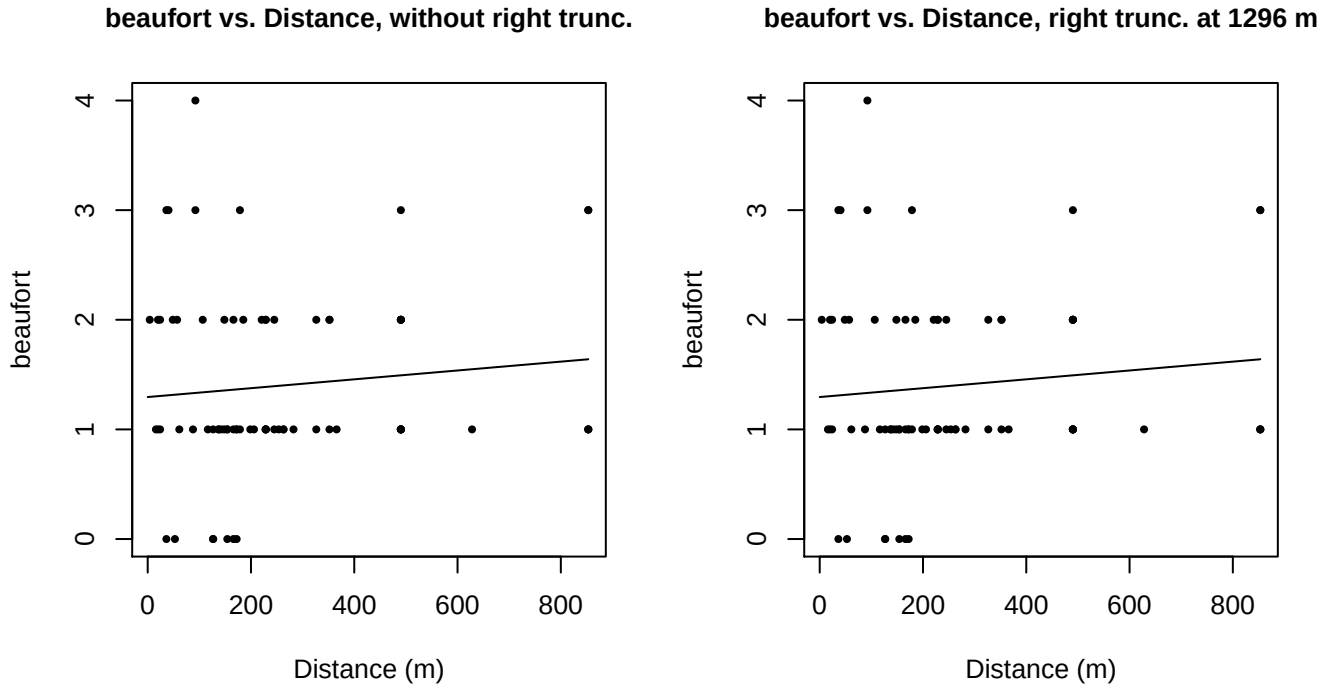

Figure 25: Scatterplots showing the relationship between Beaufort sea state and perpendicular sighting distance, for all sightings (left) and only those not right truncated (right). The line is a simple linear regression.

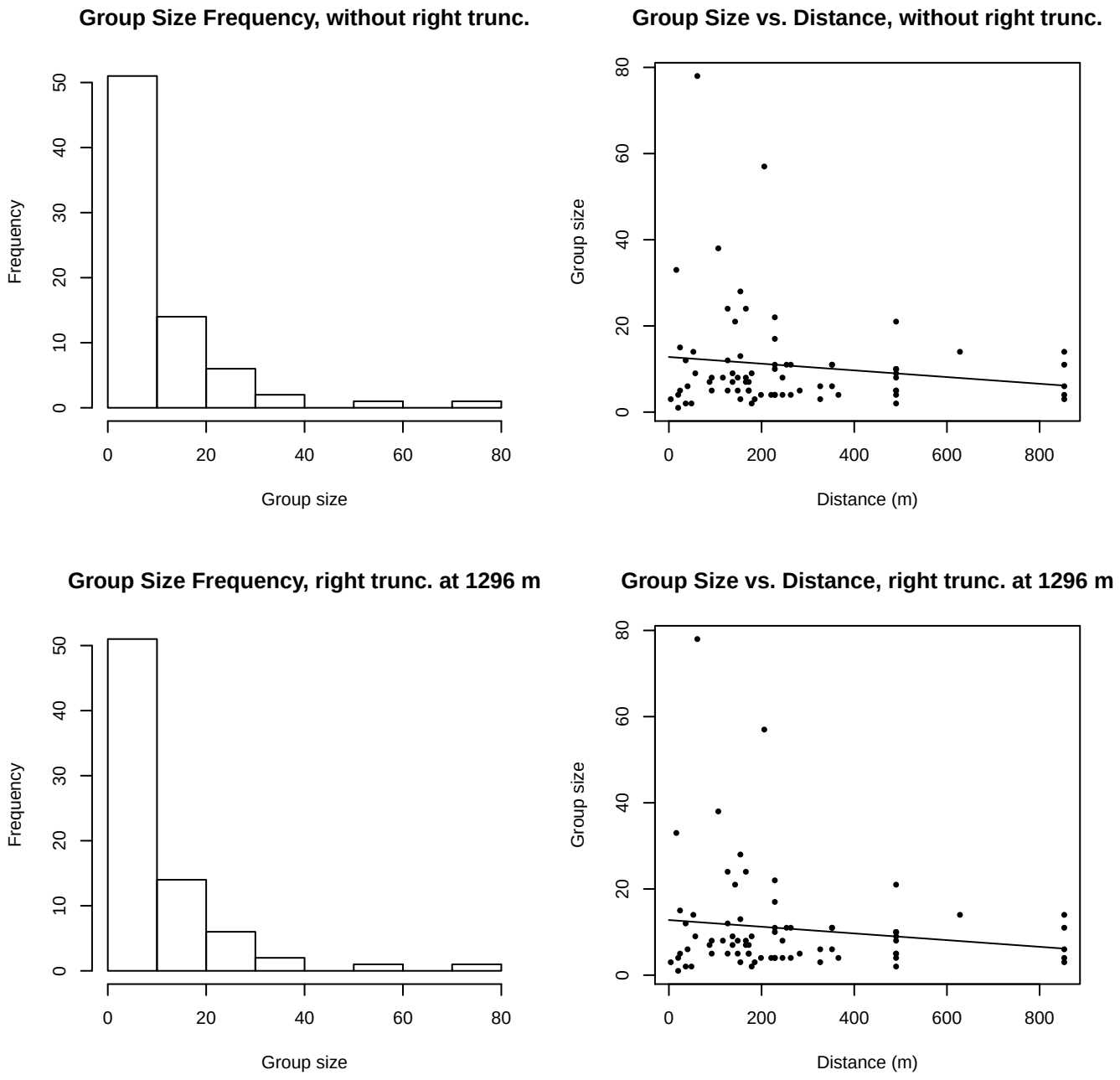

Figure 26: Histograms showing group size frequency and scatterplots showing the relationship between group size and perpendicular sighting distance, for all sightings (top row) and only those not right truncated (bottom row). In the scatterplot, the line is a simple linear regression.

g(0) Estimates

Platform	Surveys	Group Size	*g(0)*	Biases Addressed	Source
Shipboard	All	1-20	0.856	Perception	Barlow and Forney (2007)
		>20	0.970	Perception	Barlow and Forney (2007)
Aerial	All	1-5	0.43	Both	Palka (2006)
		>5	0.960	Both	Carretta et al. (2000)

Table 14: Estimates of *g(0)* used in this density model.

No g(0) estimates were published for any of the shipboard surveys available to us from this region. Instead, we utilized Barlow and Forney's (2007) estimates for delphinids, produced from several years of dual-team surveys that used bigeye binoculars and similar protocols to the surveys in our study. This study provided separate estimates for small and large groups, but pooled sightings of several species together to provide a generic estimate for all delphinids, due to sample-size limitations. To our knowledge, there is no species-specific shipboard g(0) estimate that treats small and large groups separately, so we believe Barlow and Forney (2007) provide the best general-purpose alternative. Their estimate accounted for perception bias but not availability bias; dive times for dolphins are short enough that availability bias is not expected to be significant for dolphins observed from shipboard surveys.

For aerial surveys, we were unable to locate species-specific g(0) estimates in the literature. For small groups, defined here as 1-5 individuals, we used Palka's (2006) estimate of g(0) for groups of 1-5 small cetaceans, estimated from two years of aerial surveys using the Hiby (1999) circle-back method. This estimate accounted for both availability and perception bias, but pooled sightings of several species together to provide a generic estimate for all delphinids, due to sample-size limitations. For large groups, defined here as greater than 5 individuals, Palka (2006) assumed that g(0) was 1. When we discussed this with NOAA SWFSC reviewers, they agreed that it was safe to assume that the availability bias component of g(0) was 1 but insisted that perception bias should be slightly less than 1, because it was possible to miss large groups. We agreed to take a conservative approach and obtained our g(0) for large groups from Carretta et al. (2000), who estimated g(0) for both small and large groups of delphinids. We used Carretta et al.'s g(0) estimate for groups of 1-25 individuals (0.960), rather than their larger one for more than 25 individuals (0.994), to account for the fact that we were using Palka's definition of large groups as those with more than 5 individuals.

Density Models

A recent comprehensive review of the global distribution reported that Risso's dolphins "occur in all habitats from coastal to oceanic [but] show a strong preference for the mid-temperate waters of the continental shelf and slope between 30-45 degrees latitude", (Jefferson et al. 2014). While the Gulf of Mexico occurs at lower latitudes, Risso's dolphins are not rare here; the surveys utilized in this model reported 282 sightings between 1992-2009. Prior habitat analysis suggested density is highest on steep sections of the upper continental slope (Baumgartner 1997). Many of the sightings reported by the surveys we utilized occurred in these areas; none occurred over the continental shelf. We found no definitive descriptions in the literature of seasonal movements by Risso's dolphins in the Gulf of Mexico. Accordingly we fitted a year-round model to off-shelf waters, defined here as those deeper than the 100m isobath.

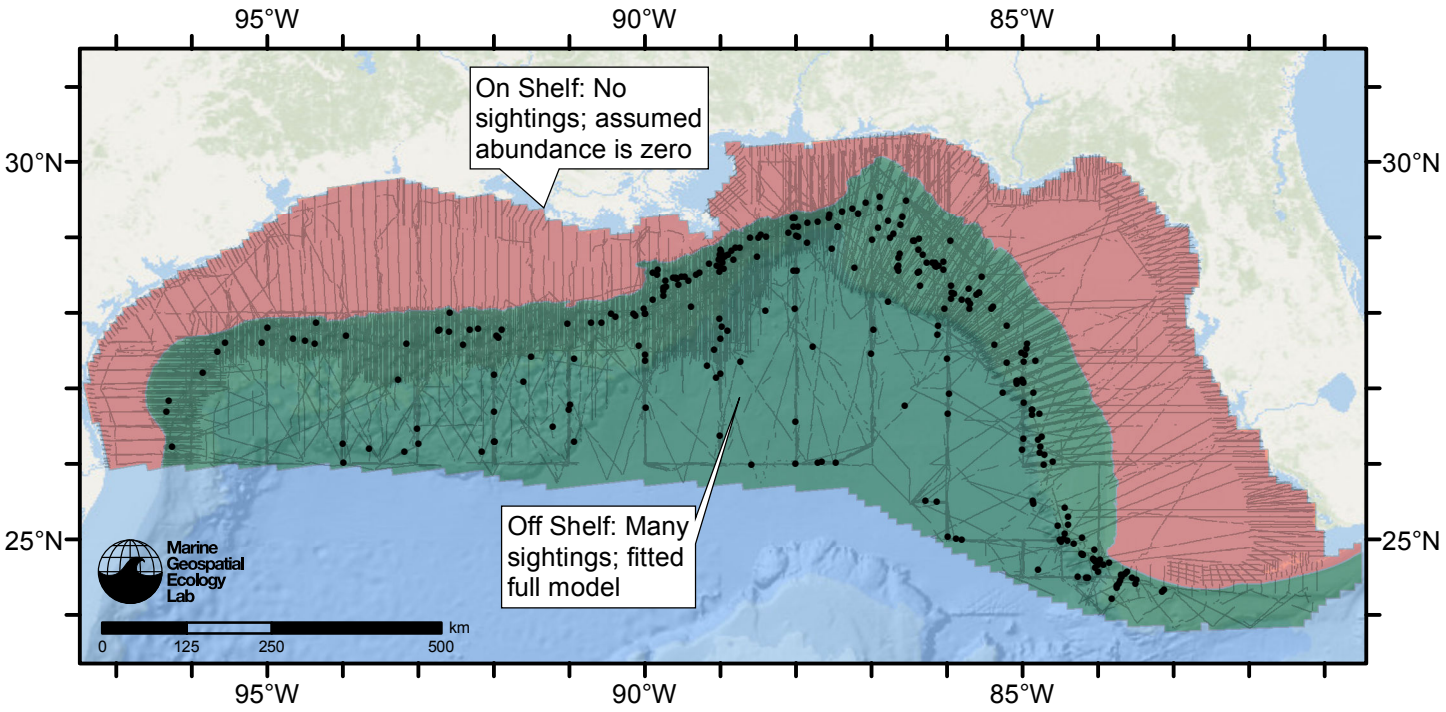

Figure 27: Risso's dolphin density model schematic. All on-effort sightings are shown, including those that were truncated when detection functions were fitted.

Climatological Model

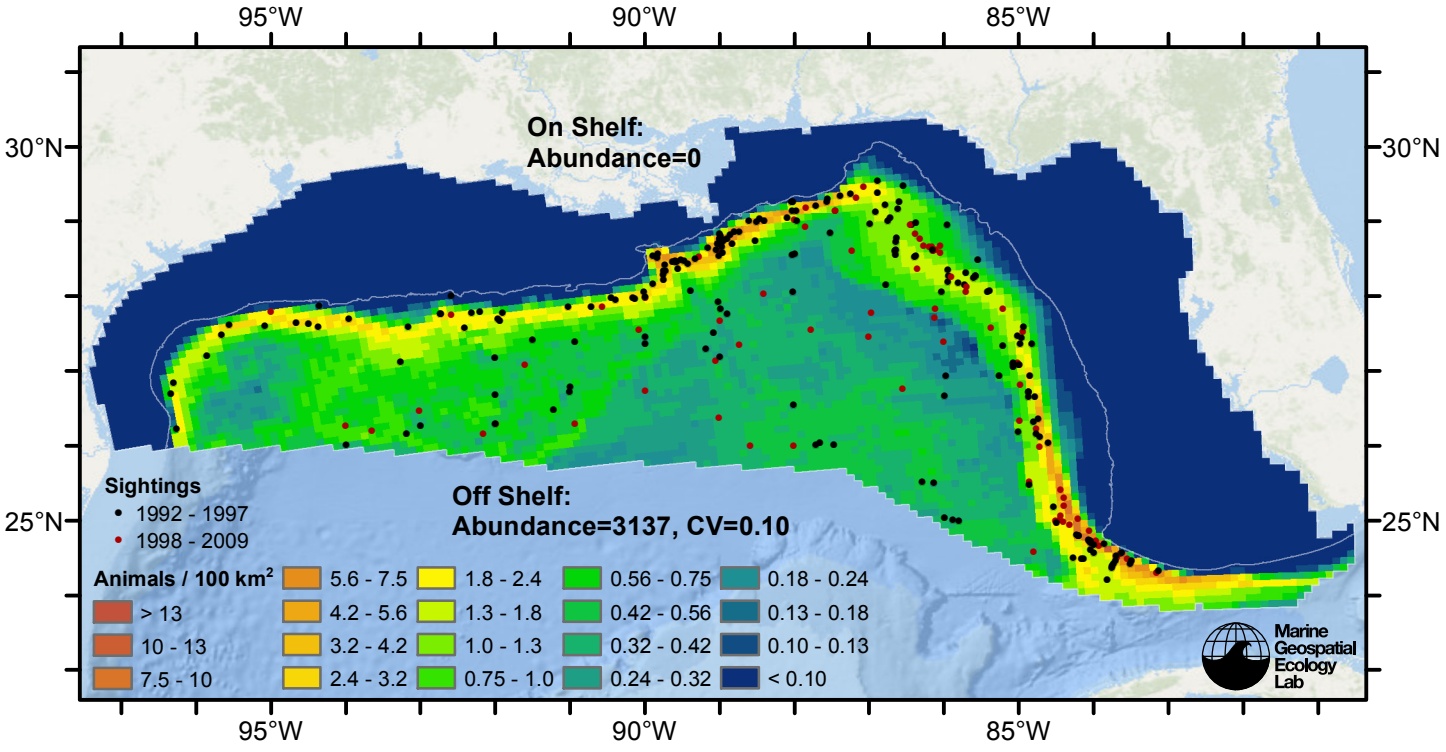

Figure 28: Risso's dolphin density predicted by the climatological model that explained the most deviance. Pixels are 10x10 km. The legend gives the estimated individuals per pixel; breaks are logarithmic. Abundance for each region was computed by summing the density cells occuring in that region.

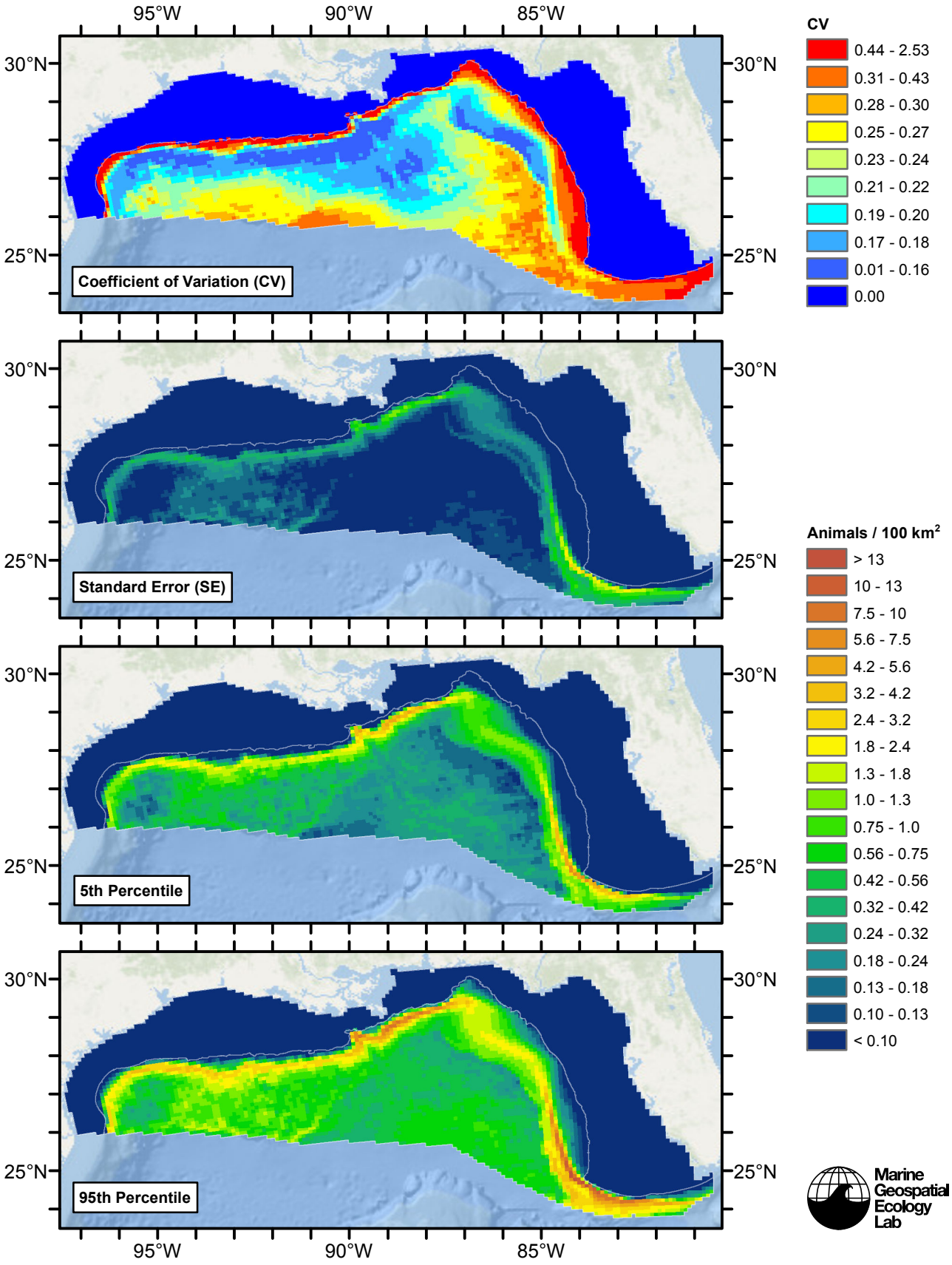

Figure 29: Estimated uncertainty for the climatological model that explained the most deviance. These estimates only incorporate the statistical uncertainty estimated for the spatial model (by the R mgcv package). They do not incorporate uncertainty in the detection functions, g(0) estimates, predictor variables, and so on.

Off Shelf

Statistical output

```
Rscript.exe: This is mgcv 1.8-2. For overview type 'help("mgcv-package")'.


Family: Tweedie(p=1.202)
Link function: log

Formula:
abundance ~ offset(log(area_km2)) + s(log10(Depth), bs = "ts",
    k = 5) + s(log10(pmax(Slope, 1e-05)), bs = "ts", k = 5) +
    s(ClimSST, bs = "ts", k = 5) + s(pmin(I(ClimDistToFront2/1000),
    250), bs = "ts", k = 5) + s(pmin(I(ClimDistToAEddy/1000),
    250), bs = "ts", k = 5) + s(log10(pmax(ClimEpiMnkPP, 1e-06)),
    bs = "ts", k = 5)

Parametric coefficients:
            Estimate Std. Error t value Pr(>|t|)
(Intercept)  -5.1824     0.1084  -47.83   <2e-16 ***
---
Signif. codes:  0 '***' 0.001 '**' 0.01 '*' 0.05 '.' 0.1 ' ' 1

Approximate significance of smooth terms:
                                       edf Ref.df      F  p-value
s(log10(Depth))                      3.650      4 25.532  < 2e-16 ***
s(log10(pmax(Slope, 1e-05)))         1.102      4  6.439 1.40e-07 ***
s(ClimSST)                           3.188      4  8.183 5.62e-08 ***
s(pmin(I(ClimDistToFront2/1000), 250)) 1.173      4  5.018 1.24e-06 ***
s(pmin(I(ClimDistToAEddy/1000), 250))  1.125      4  5.027 3.16e-06 ***
s(log10(pmax(ClimEpiMnkPP, 1e-06)))    2.529      4  5.196 1.36e-05 ***
---
Signif. codes:  0 '***' 0.001 '**' 0.01 '*' 0.05 '.' 0.1 ' ' 1

R-sq.(adj) =  0.0202   Deviance explained = 13.2%
-REML = 2339.4  Scale est. = 48.466    n = 14455

All predictors were significant. This is the final model.
Creating term plots.
Diagnostic output from gam.check():

Method: REML   Optimizer: outer newton
full convergence after 11 iterations.
Gradient range [-2.624525e-06,2.075236e-06]
(score 2339.441 & scale 48.46584).
Hessian positive definite, eigenvalue range [0.4797732,1258.518].
Model rank =  25 / 25

Basis dimension (k) checking results. Low p-value (k-index<1) may
indicate that k is too low, especially if edf is close to k'.

                                       k'   edf k-index p-value
s(log10(Depth))                      4.000 3.650   0.780    0.06
s(log10(pmax(Slope, 1e-05)))         4.000 1.102   0.799    0.44
s(ClimSST)                           4.000 3.188   0.796    0.31
s(pmin(I(ClimDistToFront2/1000), 250)) 4.000 1.173   0.798    0.40
s(pmin(I(ClimDistToAEddy/1000), 250))  4.000 1.125   0.795    0.34
s(log10(pmax(ClimEpiMnkPP, 1e-06)))    4.000 2.529   0.811    0.86
```

Predictors retained during the model selection procedure: Depth, Slope, ClimSST, ClimDistToFront2, ClimDistToAEddy, ClimEpiMnkPP

Predictors dropped during the model selection procedure: DistTo300m, ClimTKE, ClimDistToCEddy

Model term plots

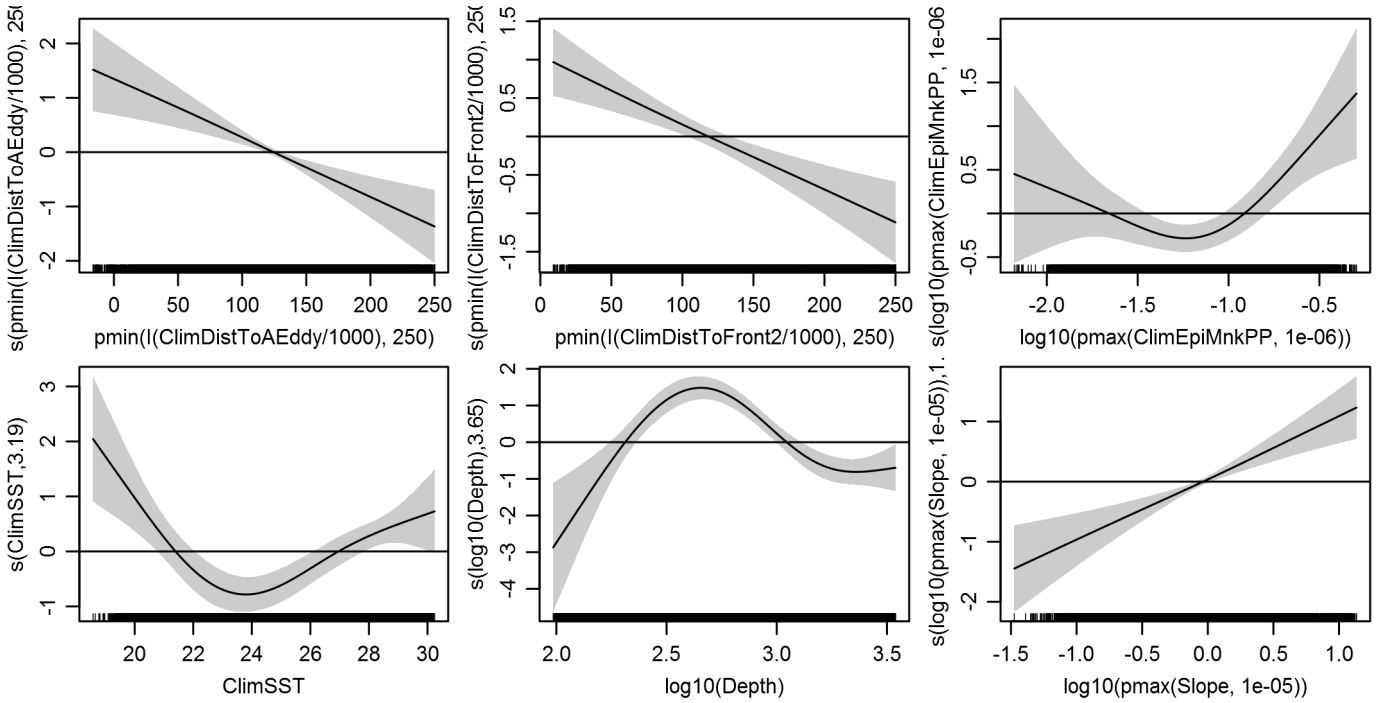

Diagnostic plots

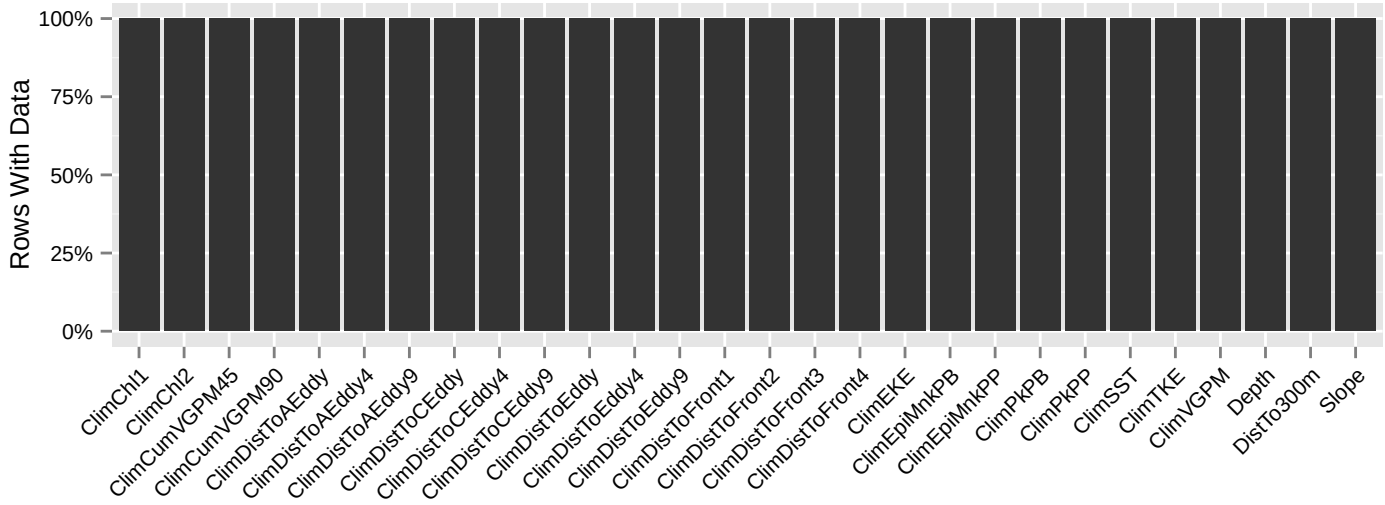

Figure 30: Segments with predictor values for the Risso's dolphin Climatological model, Off Shelf. This plot is used to assess how many segments would be lost by including a given predictor in a model.

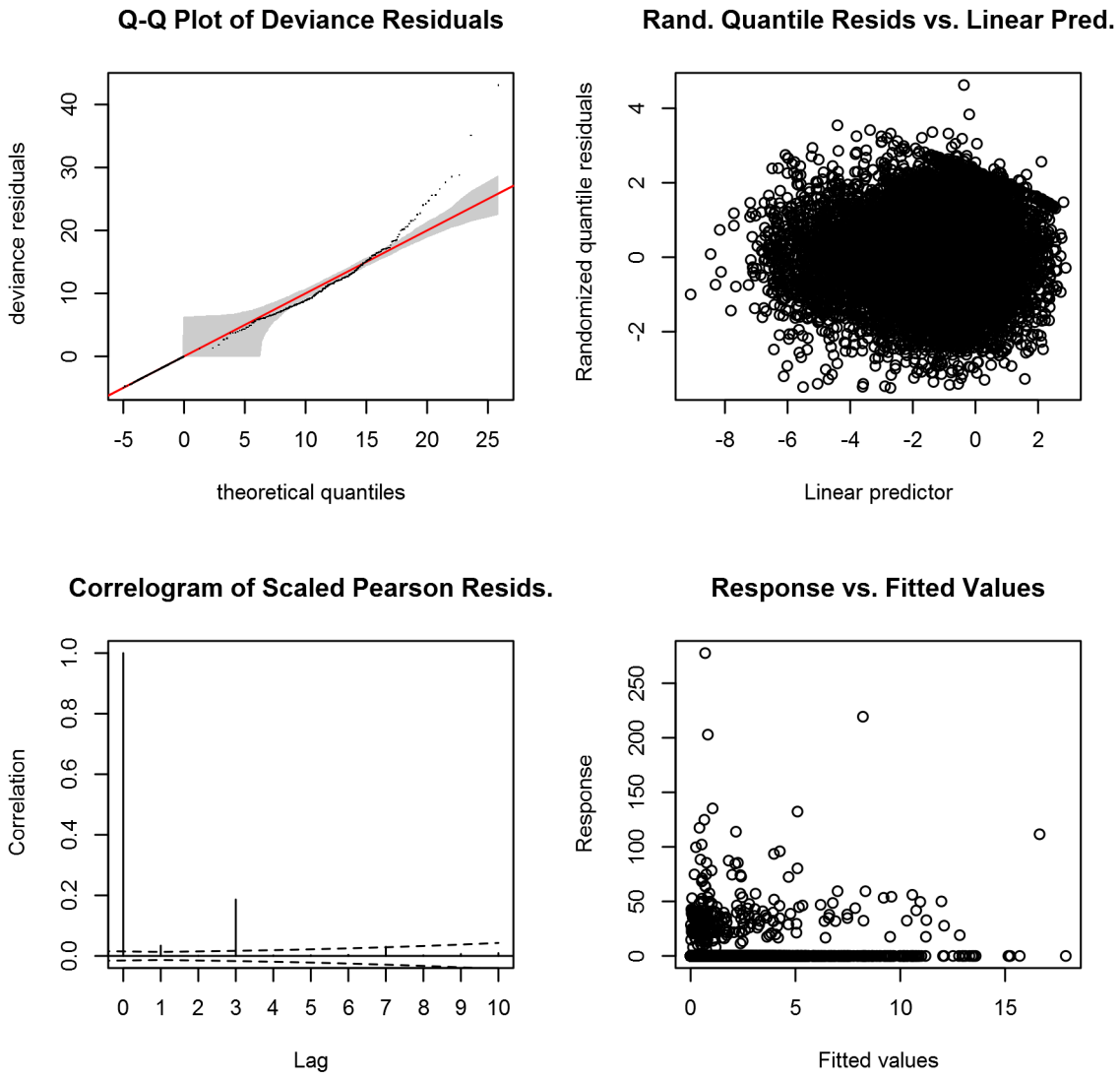

Figure 31: Statistical diagnostic plots for the Risso's dolphin Climatological model, Off Shelf.

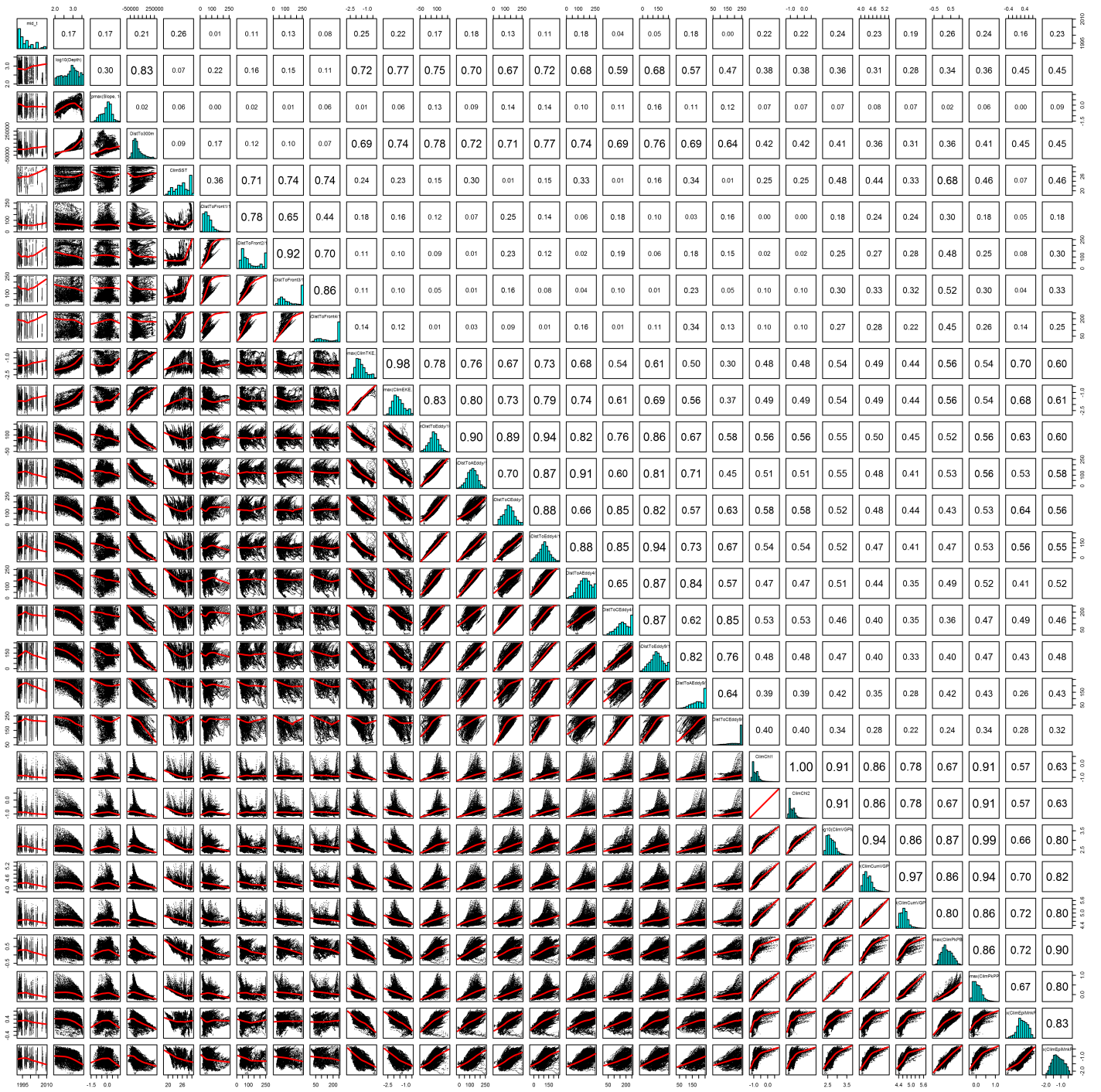

Figure 32: Scatterplot matrix for the Risso's dolphin Climatological model, Off Shelf. This plot is used to inspect the distribution of predictors (via histograms along the diagonal), simple correlation between predictors (via pairwise Pearson coefficients above the diagonal), and linearity of predictor correlations (via scatterplots below the diagonal). This plot is best viewed at high magnification.

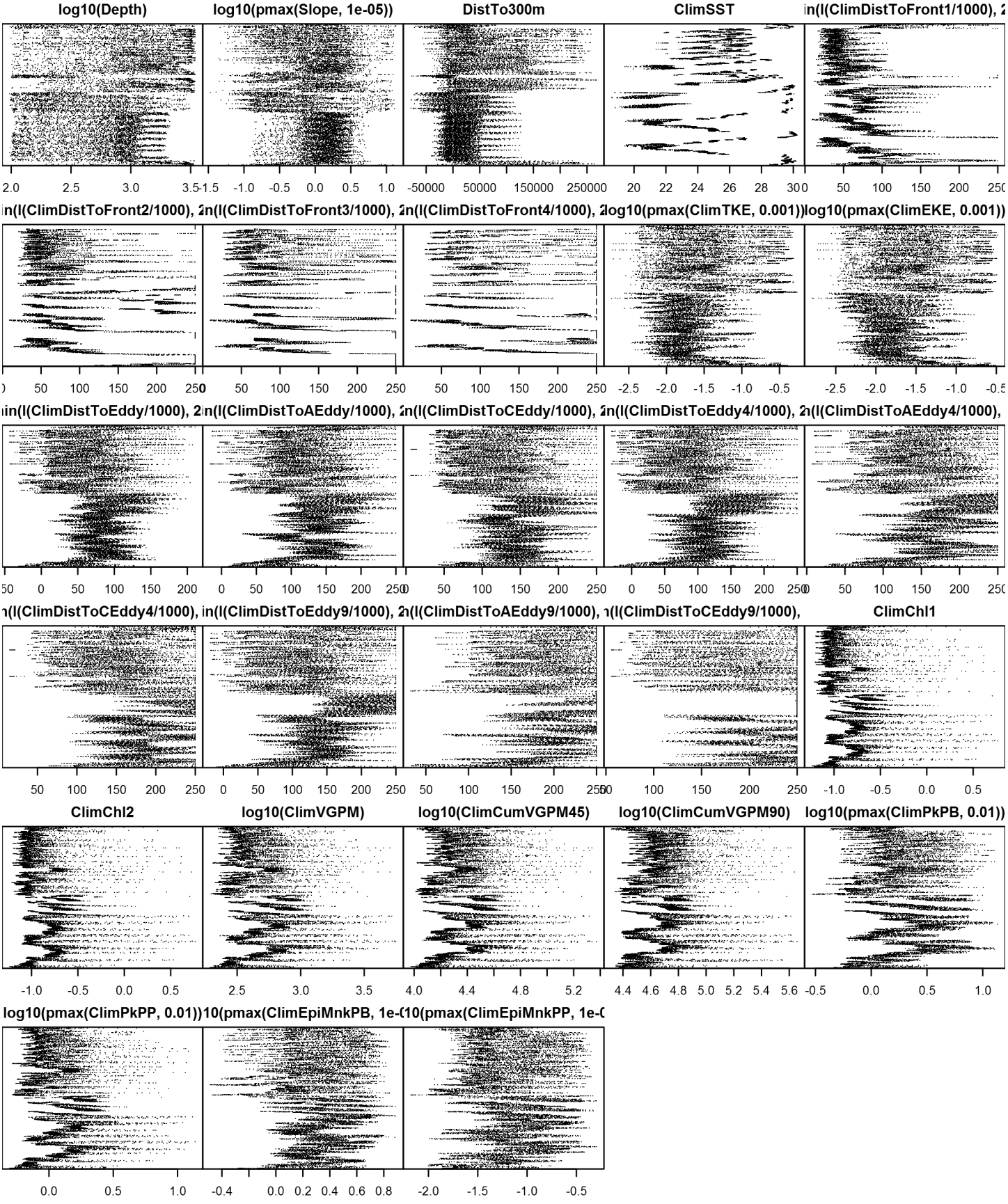

Figure 33: Dotplot for the Risso's dolphin Climatological model, Off Shelf. This plot is used to check for suspicious patterns and outliers in the data. Points are ordered vertically by transect ID, sequentially in time.

On Shelf

Density assumed to be 0 in this region.

Contemporaneous Model

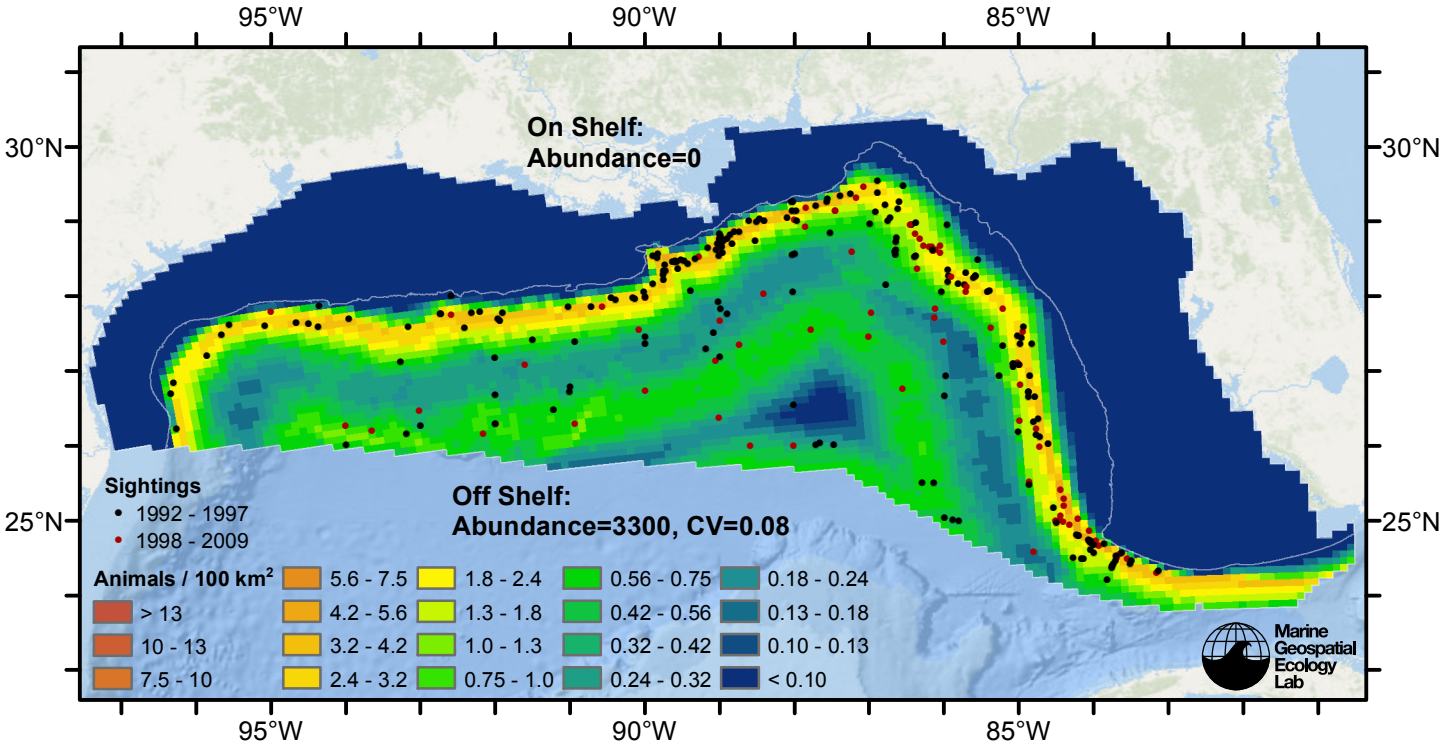

Figure 34: Risso's dolphin density predicted by the contemporaneous model that explained the most deviance. Pixels are 10x10 km. The legend gives the estimated individuals per pixel; breaks are logarithmic. Abundance for each region was computed by summing the density cells occuring in that region.

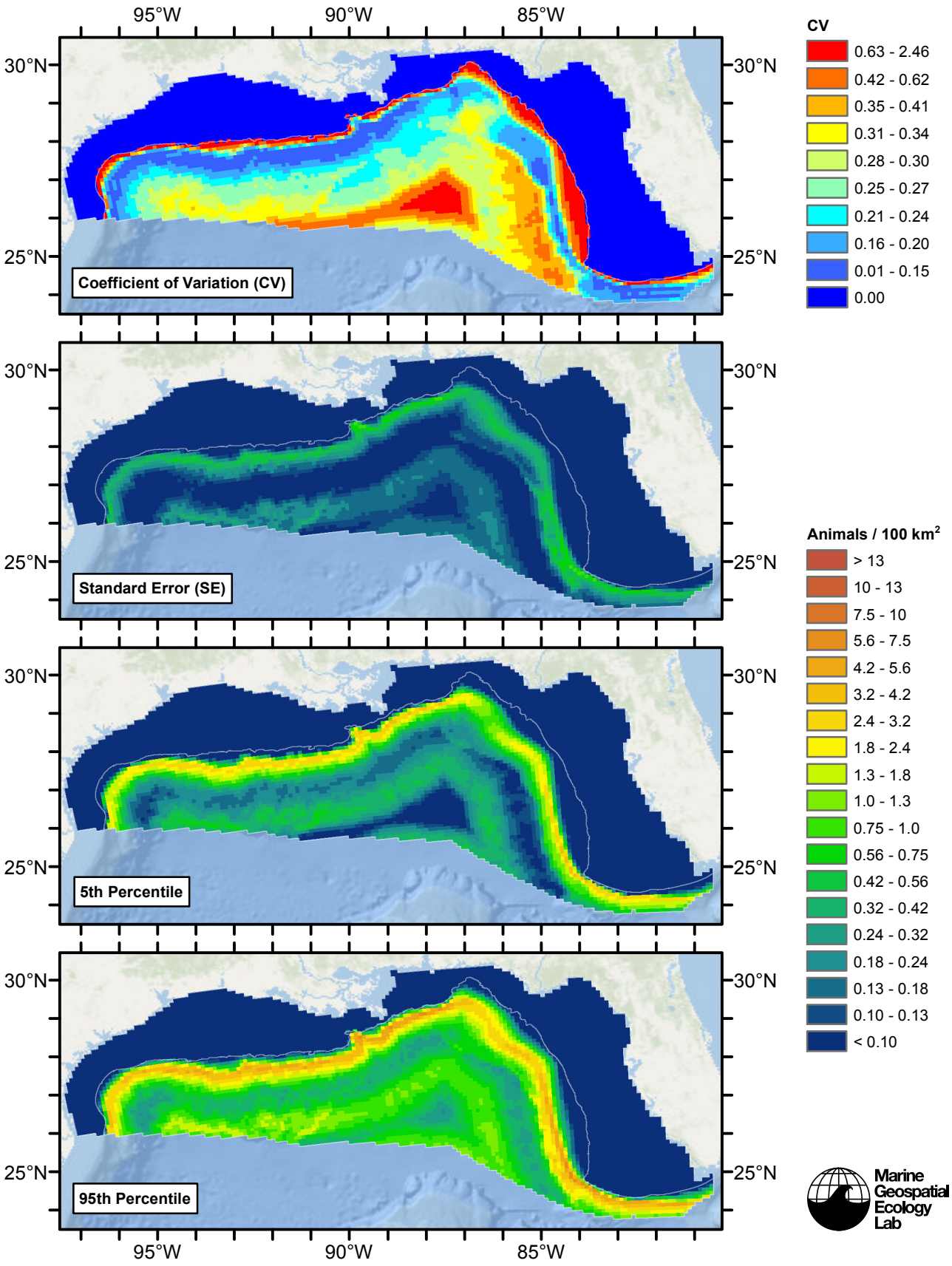

Figure 35: Estimated uncertainty for the contemporaneous model that explained the most deviance. These estimates only incorporate the statistical uncertainty estimated for the spatial model (by the R mgcv package). They do not incorporate uncertainty in the detection functions, g(0) estimates, predictor variables, and so on.

Off Shelf

Statistical output

```
Rscript.exe: This is mgcv 1.8-2. For overview type 'help("mgcv-package")'.


Family: Tweedie(p=1.214)
Link function: log

Formula:
abundance ~ offset(log(area_km2)) + s(log10(Depth), bs = "ts",
    k = 5) + s(log10(pmax(Slope, 1e-05)), bs = "ts", k = 5) +
    s(DistTo300m, bs = "ts", k = 5) + s(SST, bs = "ts", k = 5) +
    s(pmin(I(DistToFront1/1000), 250), bs = "ts", k = 5) + s(pmin(I(DistToEddy/1000),
    250), bs = "ts", k = 5)

Parametric coefficients:
            Estimate Std. Error t value Pr(>|t|)
(Intercept)  -5.1545     0.1159  -44.48   <2e-16 ***
---
Signif. codes:  0 '***' 0.001 '**' 0.01 '*' 0.05 '.' 0.1 ' ' 1

Approximate significance of smooth terms:
                                   edf Ref.df     F  p-value
s(log10(Depth))                 3.3413      4 6.140 5.93e-06 ***
s(log10(pmax(Slope, 1e-05)))    0.9686      4 2.245 0.001437 **
s(DistTo300m)                   3.7168      4 5.810 4.16e-05 ***
s(SST)                          3.5610      4 9.362 2.47e-08 ***
s(pmin(I(DistToFront1/1000), 250)) 1.0559      4 3.511 0.000127 ***
s(pmin(I(DistToEddy/1000), 250))   0.8909      4 1.288 0.014211 *
---
Signif. codes:  0 '***' 0.001 '**' 0.01 '*' 0.05 '.' 0.1 ' ' 1

R-sq.(adj) =  0.00774   Deviance explained = 10.8%
-REML = 2129.7  Scale est. = 49.394    n = 12621

All predictors were significant. This is the final model.
Creating term plots.
Diagnostic output from gam.check():

Method: REML   Optimizer: outer newton
full convergence after 14 iterations.
Gradient range [-0.000154868,3.081681e-05]
(score 2129.665 & scale 49.3944).
Hessian positive definite, eigenvalue range [0.1307249,1089.128].
Model rank =  25 / 25

Basis dimension (k) checking results. Low p-value (k-index<1) may
indicate that k is too low, especially if edf is close to k'.

                                   k'   edf k-index p-value
s(log10(Depth))                 4.000 3.341   0.806    0.05
s(log10(pmax(Slope, 1e-05)))    4.000 0.969   0.835    0.70
s(DistTo300m)                   4.000 3.717   0.814    0.11
s(SST)                          4.000 3.561   0.829    0.44
s(pmin(I(DistToFront1/1000), 250)) 4.000 1.056   0.811    0.10
s(pmin(I(DistToEddy/1000), 250))   4.000 0.891   0.820    0.21
```

```
Predictors retained during the model selection procedure: Depth, Slope, DistTo300m, SST,
DistToFront1, DistToEddy

Predictors dropped during the model selection procedure: TKE
```

Model term plots

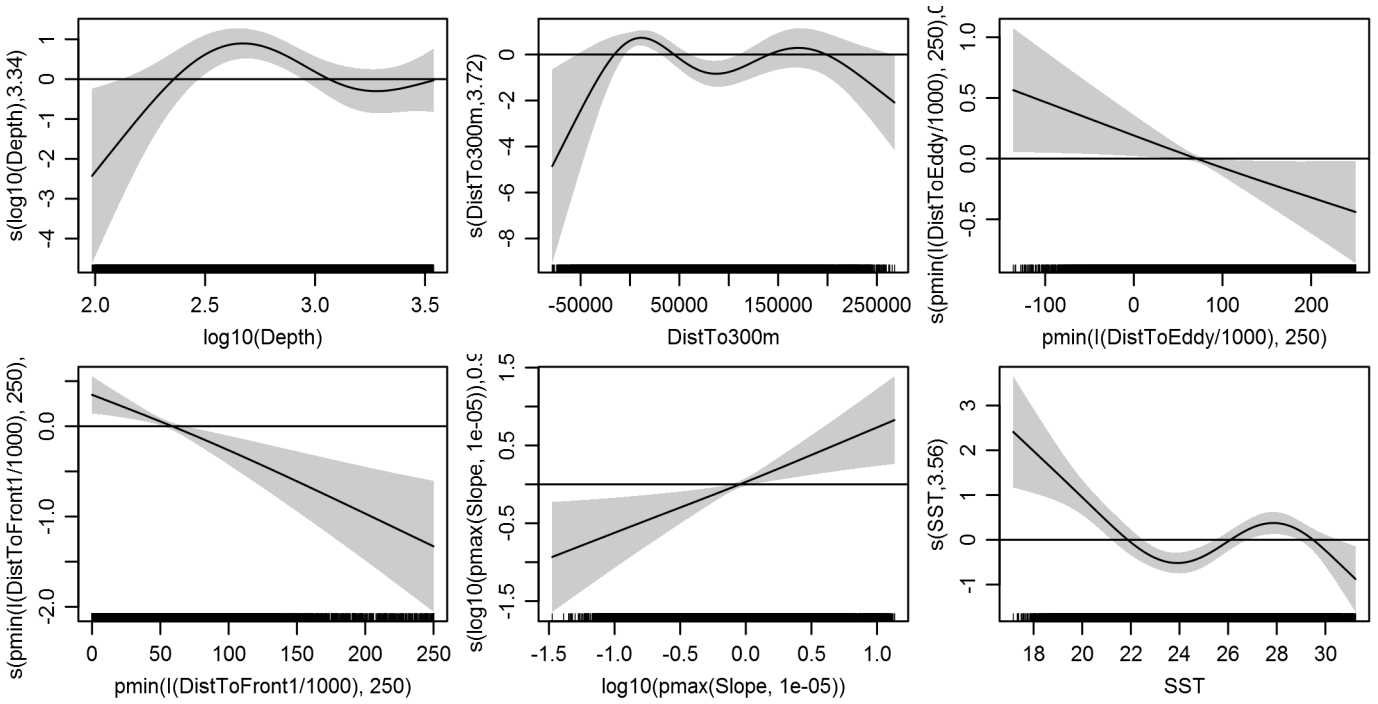

Diagnostic plots

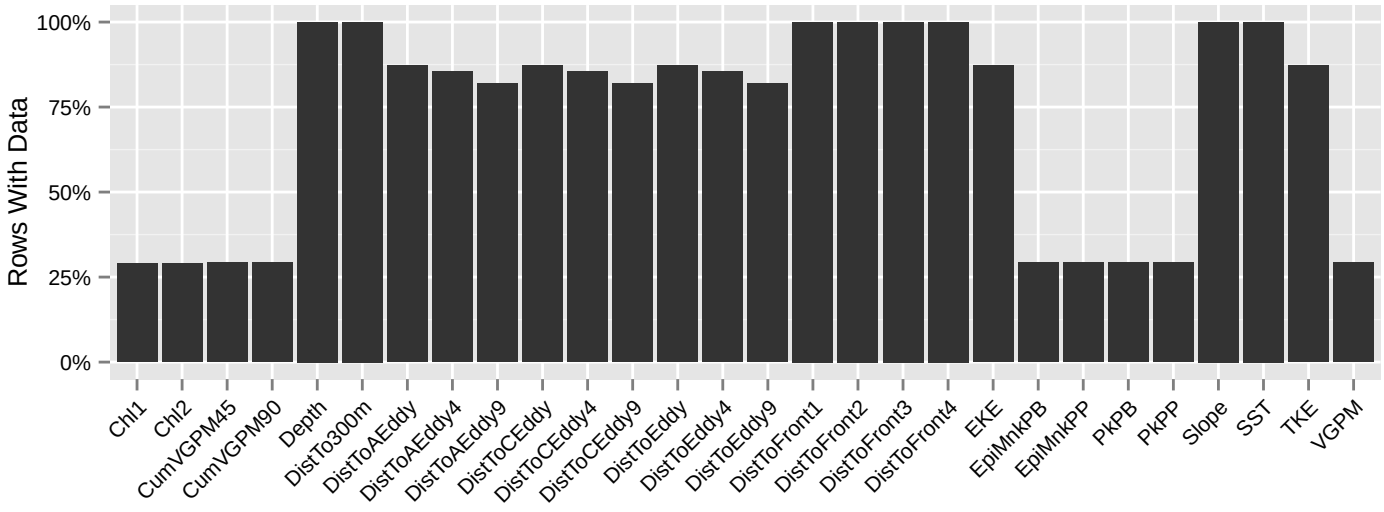

Figure 36: Segments with predictor values for the Risso's dolphin Contemporaneous model, Off Shelf. This plot is used to assess how many segments would be lost by including a given predictor in a model.

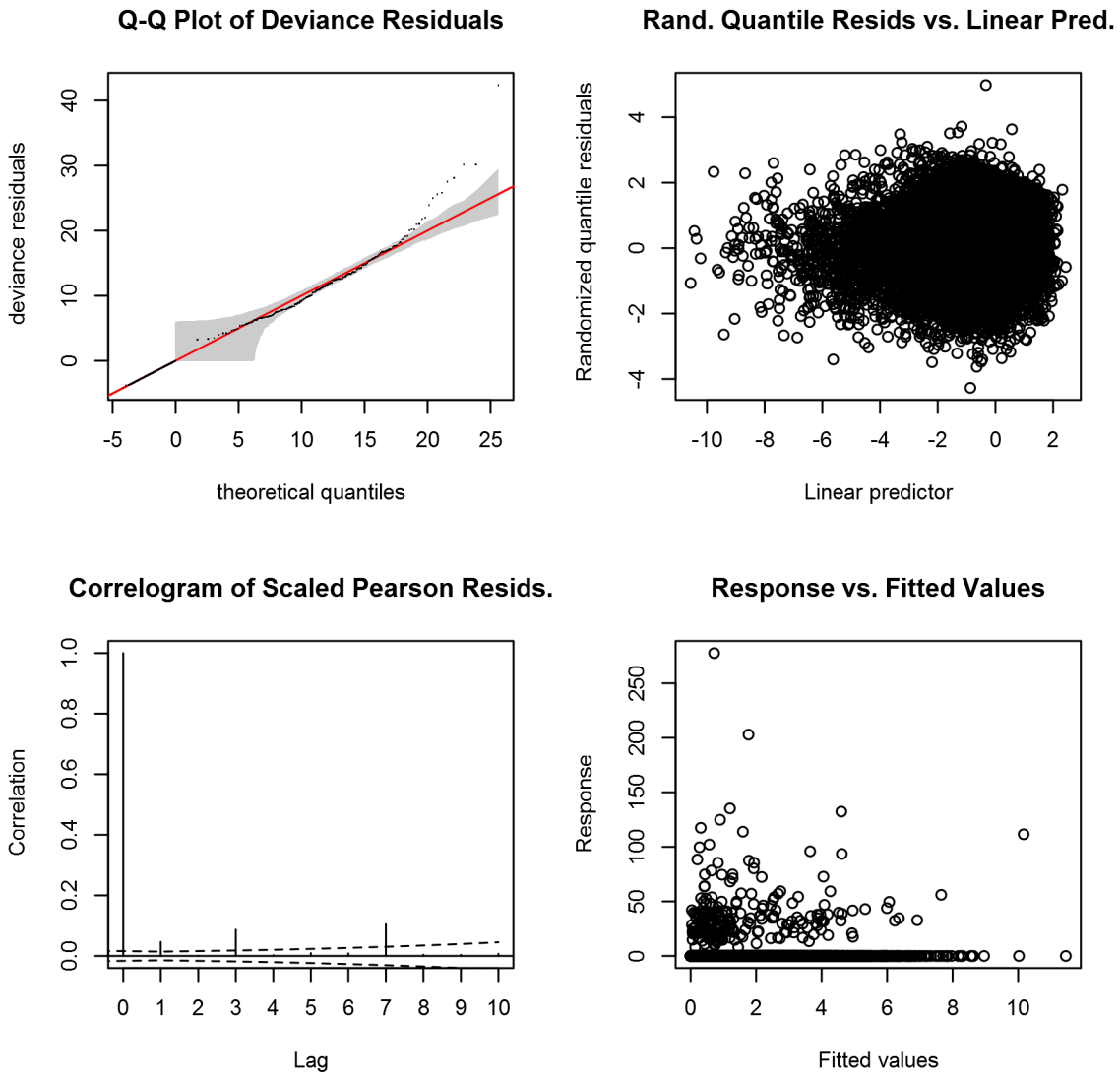

Figure 37: Statistical diagnostic plots for the Risso's dolphin Contemporaneous model, Off Shelf.

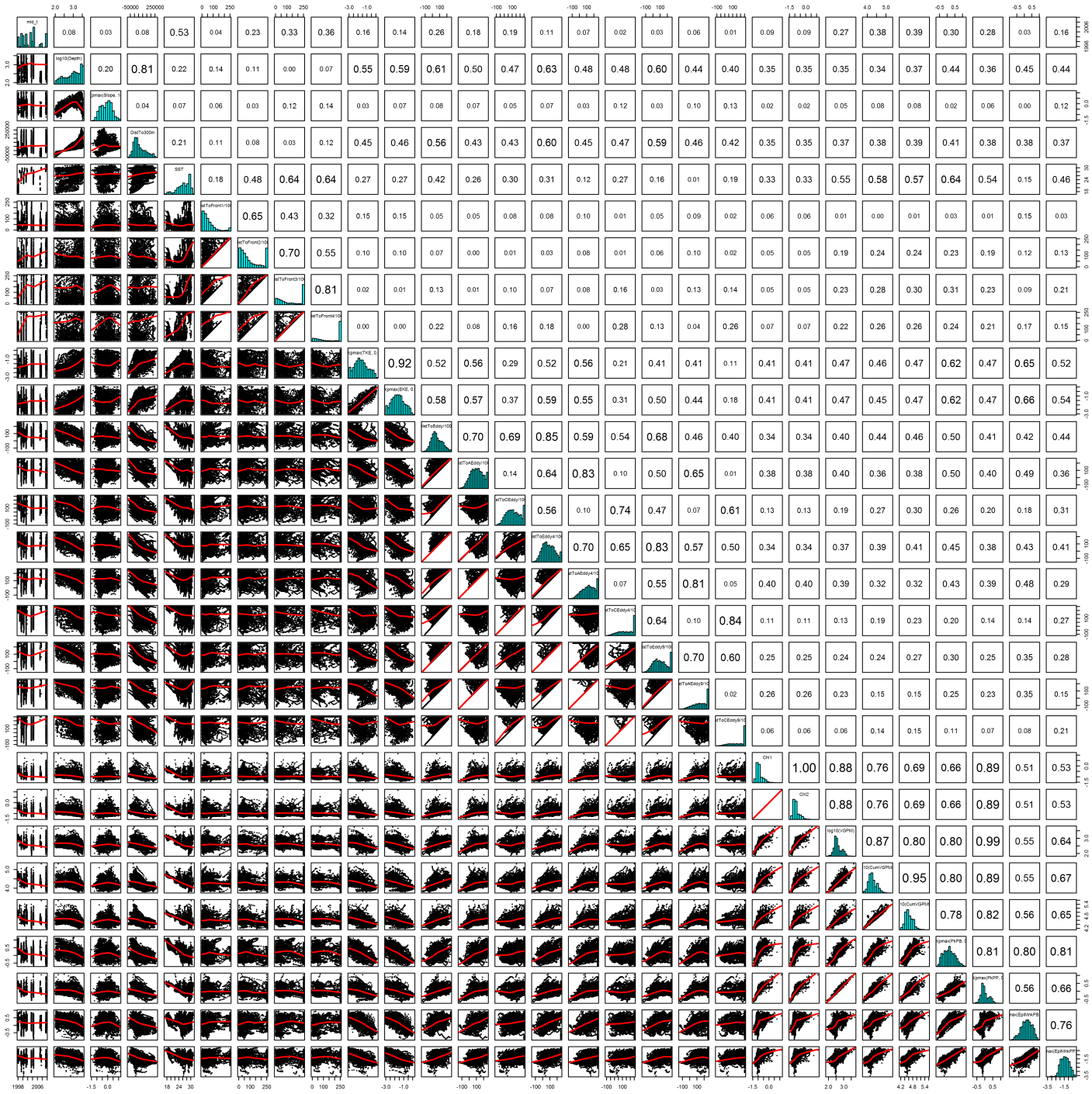

Figure 38: Scatterplot matrix for the Risso's dolphin Contemporaneous model, Off Shelf. This plot is used to inspect the distribution of predictors (via histograms along the diagonal), simple correlation between predictors (via pairwise Pearson coefficients above the diagonal), and linearity of predictor correlations (via scatterplots below the diagonal). This plot is best viewed at high magnification.

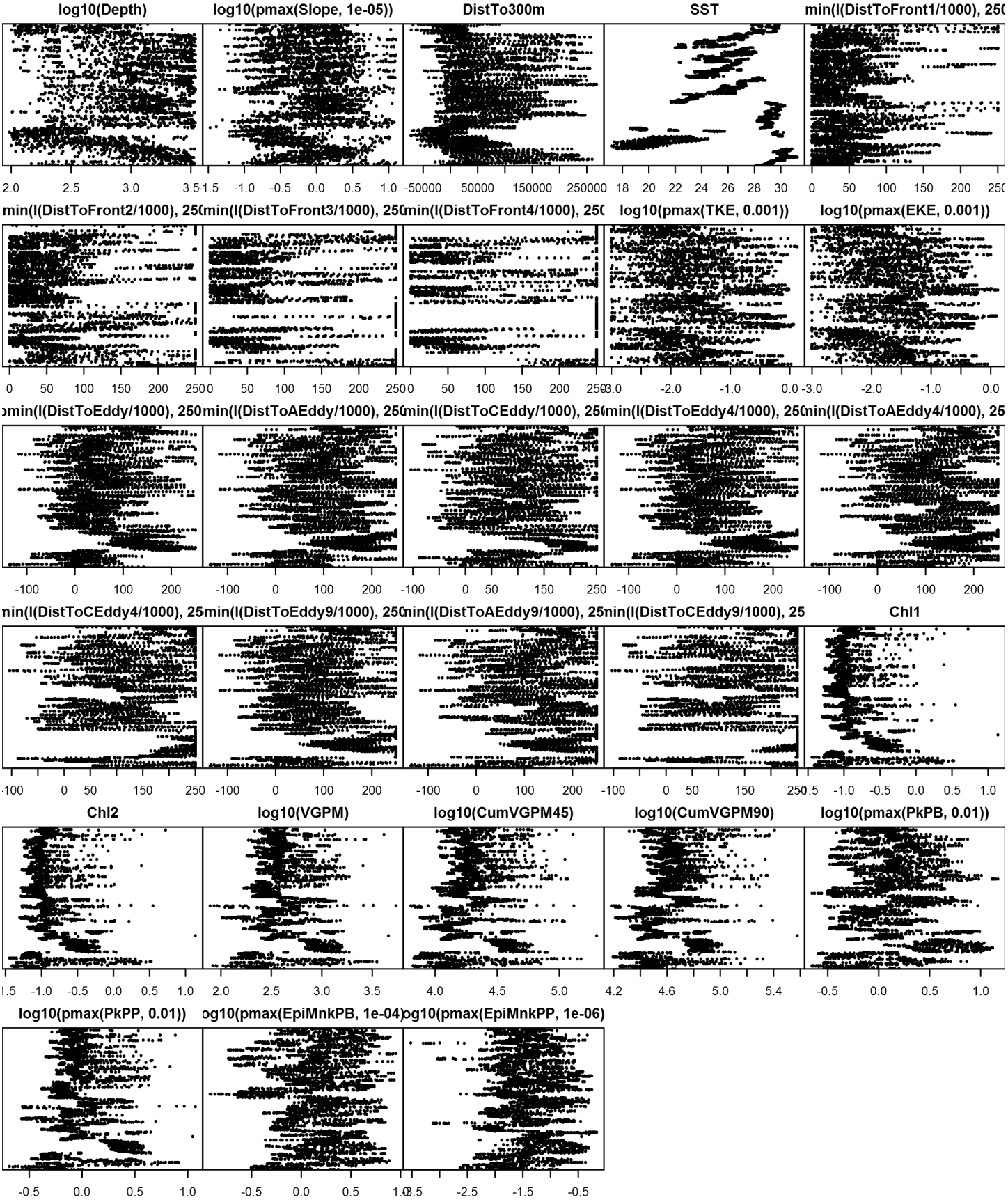

Figure 39: Dotplot for the Risso's dolphin Contemporaneous model, Off Shelf. This plot is used to check for suspicious patterns and outliers in the data. Points are ordered vertically by transect ID, sequentially in time.

On Shelf

Density assumed to be 0 in this region.

Climatological Same Segments Model

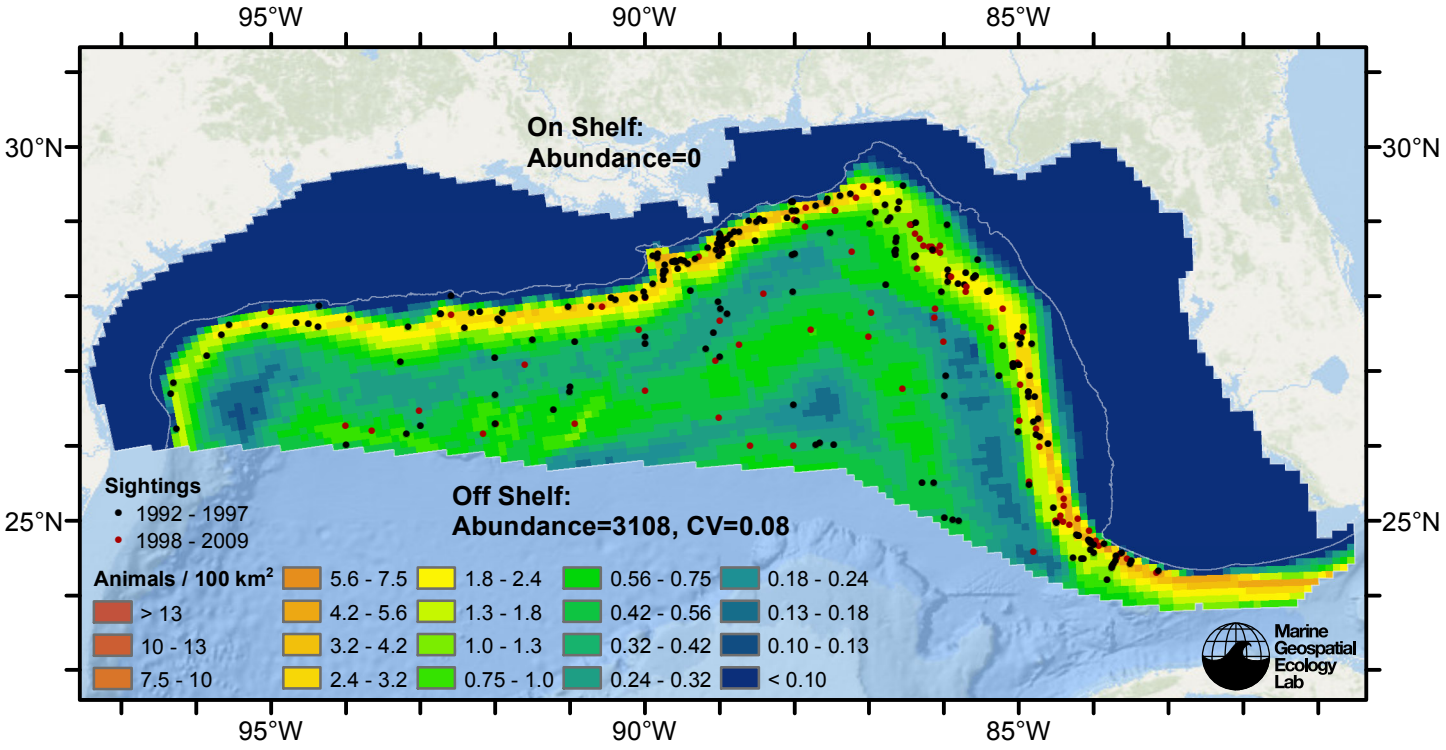

Figure 40: Risso's dolphin density predicted by the climatological same segments model that explained the most deviance. Pixels are 10x10 km. The legend gives the estimated individuals per pixel; breaks are logarithmic. Abundance for each region was computed by summing the density cells occuring in that region.

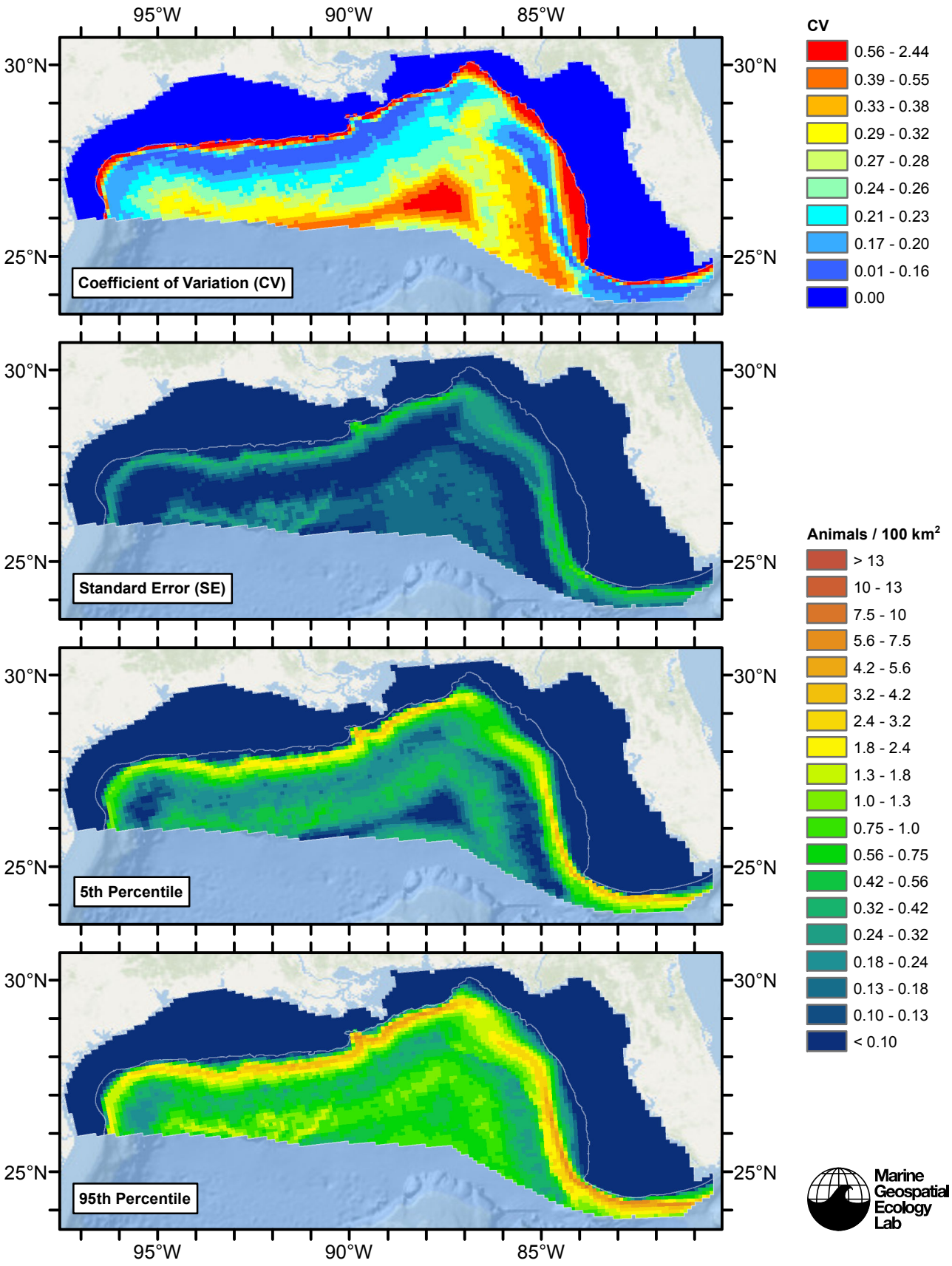

Figure 41: Estimated uncertainty for the climatological same segments model that explained the most deviance. These estimates only incorporate the statistical uncertainty estimated for the spatial model (by the R mgcv package). They do not incorporate uncertainty in the detection functions, g(0) estimates, predictor variables, and so on.

Off Shelf

Statistical output

```
Rscript.exe: This is mgcv 1.8-2. For overview type 'help("mgcv-package")'.


Family: Tweedie(p=1.208)
Link function: log

Formula:
abundance ~ offset(log(area_km2)) + s(log10(Depth), bs = "ts",
    k = 5) + s(log10(pmax(Slope, 1e-05)), bs = "ts", k = 5) +
    s(DistTo300m, bs = "ts", k = 5) + s(ClimSST, bs = "ts", k = 5) +
    s(pmin(I(ClimDistToFront2/1000), 250), bs = "ts", k = 5)

Parametric coefficients:
            Estimate Std. Error t value Pr(>|t|)
(Intercept)  -5.1160     0.1057   -48.4   <2e-16 ***
---
Signif. codes:  0 '***' 0.001 '**' 0.01 '*' 0.05 '.' 0.1 ' ' 1

Approximate significance of smooth terms:
                                       edf Ref.df     F  p-value
s(log10(Depth))                      3.459      4 9.546 3.26e-09 ***
s(log10(pmax(Slope, 1e-05)))         1.026      4 3.580 7.45e-05 ***
s(DistTo300m)                        3.470      4 3.656  0.00206 **
s(ClimSST)                           3.187      4 9.300 6.50e-09 ***
s(pmin(I(ClimDistToFront2/1000), 250)) 1.350      4 8.077 1.03e-09 ***
---
Signif. codes:  0 '***' 0.001 '**' 0.01 '*' 0.05 '.' 0.1 ' ' 1

R-sq.(adj) =  0.0123   Deviance explained =   12%
-REML = 2349.8  Scale est. = 49.288    n = 14455

All predictors were significant. This is the final model.
Creating term plots.
Diagnostic output from gam.check():

Method: REML   Optimizer: outer newton
full convergence after 11 iterations.
Gradient range [-0.0007394192,0.0003224075]
(score 2349.823 & scale 49.28802).
Hessian positive definite, eigenvalue range [0.3942366,1236.182].
Model rank =  21 / 21

Basis dimension (k) checking results. Low p-value (k-index<1) may
indicate that k is too low, especially if edf is close to k'.

                                       k'   edf k-index p-value
s(log10(Depth))                      4.000 3.459   0.795    0.23
s(log10(pmax(Slope, 1e-05)))         4.000 1.026   0.788    0.10
s(DistTo300m)                        4.000 3.470   0.780    0.04
s(ClimSST)                           4.000 3.187   0.777    0.04
s(pmin(I(ClimDistToFront2/1000), 250)) 4.000 1.350   0.810    0.72

Predictors retained during the model selection procedure: Depth, Slope, DistTo300m, ClimSST,
ClimDistToFront2
```

```
Predictors dropped during the model selection procedure:
```

Model term plots

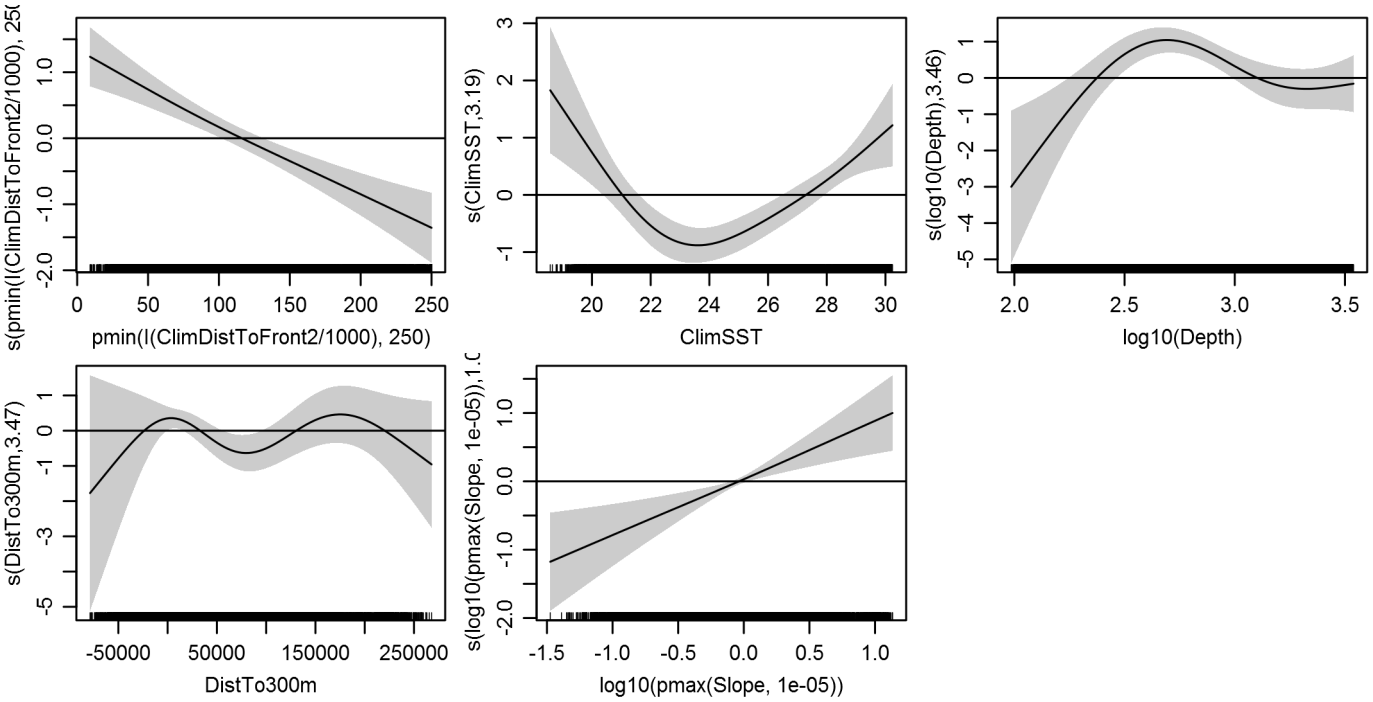

Diagnostic plots

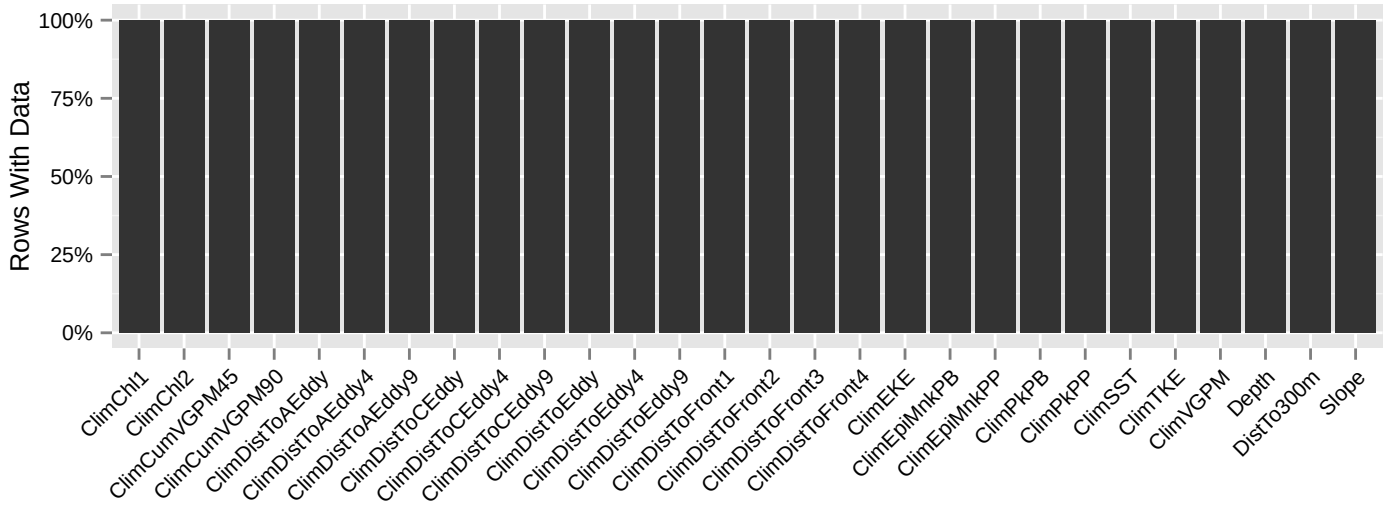

Figure 42: Segments with predictor values for the Risso's dolphin Climatological model, Off Shelf. This plot is used to assess how many segments would be lost by including a given predictor in a model.

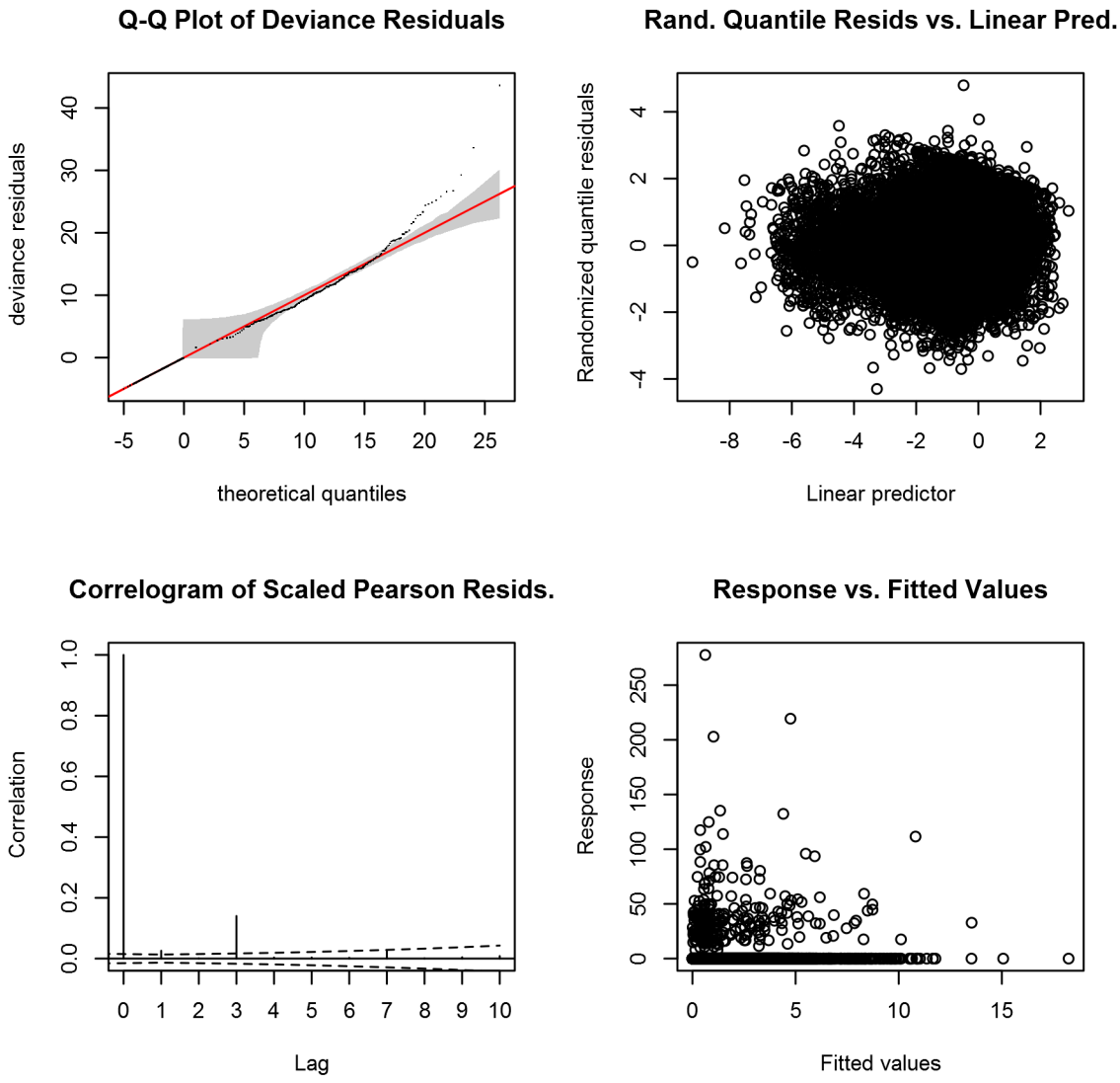

Figure 43: Statistical diagnostic plots for the Risso's dolphin Climatological model, Off Shelf.

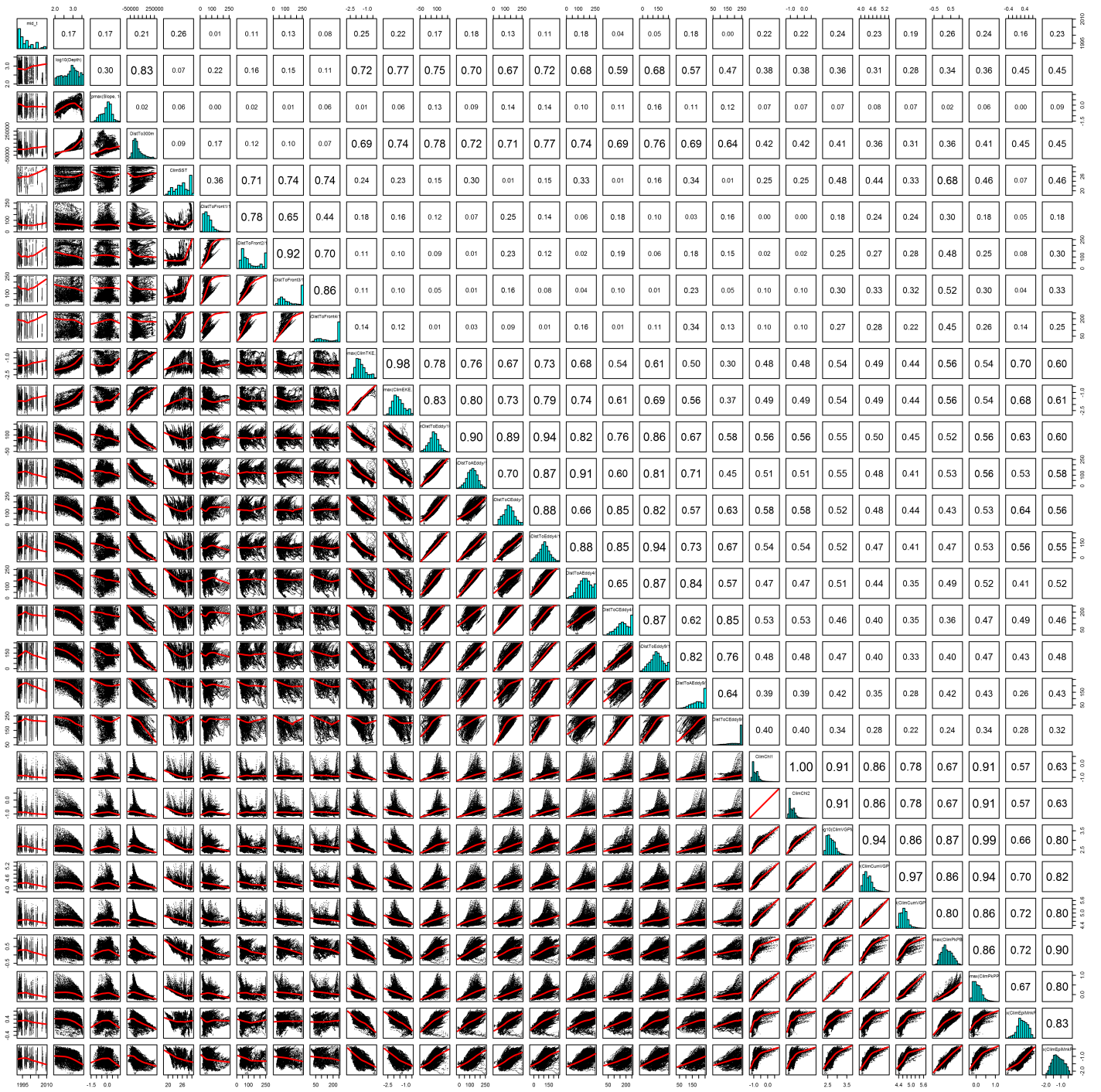

Figure 44: Scatterplot matrix for the Risso's dolphin Climatological model, Off Shelf. This plot is used to inspect the distribution of predictors (via histograms along the diagonal), simple correlation between predictors (via pairwise Pearson coefficients above the diagonal), and linearity of predictor correlations (via scatterplots below the diagonal). This plot is best viewed at high magnification.

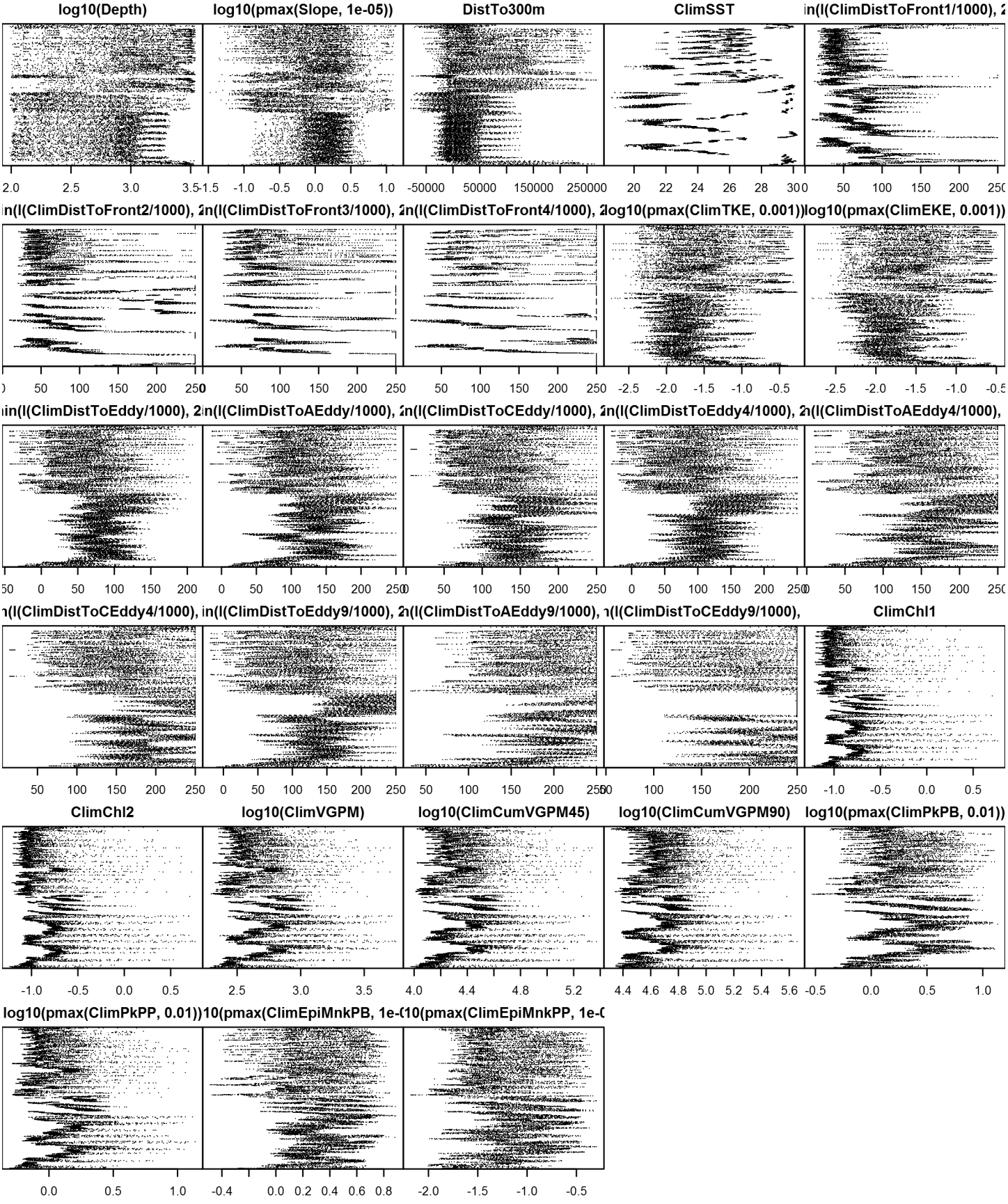

Figure 45: Dotplot for the Risso's dolphin Climatological model, Off Shelf. This plot is used to check for suspicious patterns and outliers in the data. Points are ordered vertically by transect ID, sequentially in time.

On Shelf

Density assumed to be 0 in this region.

Model Comparison

Spatial Model Performance

The table below summarizes the performance of the candidate spatial models that were tested. The first model contained only physiographic predictors. Subsequent models added additional suites of predictors of based on when they became available via remote sensing.

For each model, three versions were fitted; the % Dev Expl columns give the % deviance explained by each one. The "climatological" models were fitted to 8-day climatologies of the environmental predictors. Because the environmental predictors were always available, no segments were lost, allowing these models to consider the maximal amount of survey data. The "contemporaneous" models were fitted to day-of-sighting images of the environmental predictors; these were smoothed to reduce data loss due to clouds, but some segments still failed to retrieve environmental values and were lost. Finally, the "climatological same segments" models fitted climatological predictors to the segments retained by the contemporaneous model, so that the explantory power of the two types of predictors could be directly compared. For each of the three models, predictors were selected independently via shrinkage smoothers; thus the three models did not necessarily utilize the same predictors.

Predictors derived from ocean currents first became available in January 1993 after the launch of the TOPEX/Poseidon satellite; productivity predictors first became available in September 1997 after the launch of the SeaWiFS sensor. Contemporaneous and climatological same segments models considering these predictors usually suffered data loss. Date Range shows the years spanned by the retained segments. The Segments column gives the number of segments retained; % Lost gives the percentage lost.

Predictors	Climatol % Dev Expl	Contemp % Dev Expl	Climatol Same Segs % Dev Expl	Segments	% Lost	Date Range
Phys	8.1			14455		1992-2009
Phys+SST	12.0	10.8	12.0	14455	0.0	1992-2009
Phys+SST+Curr	12.8	10.8	11.5	12621	12.7	1993-2009
Phys+SST+Curr+Prod	13.2	5.1	5.2	4219	70.8	1998-2009

Table 15: Deviance explained by the candidate density models.

Abundance Estimates

The table below shows the estimated mean abundance (number of animals) within the study area, for the models that explained the most deviance for each model type. Mean abundance was calculated by first predicting density maps for a series of time steps, then computing the abundance for each map, and then averaging the abundances. For the climatological models, we used 8-day climatologies, resulting in 46 abundance maps. For the contemporaneous models, we used daily images, resulting in 365 predicted abundance maps per year that the prediction spanned. The Dates column gives the dates to which the estimates apply. For our models, these are the years for which both survey data and remote sensing data were available.

The Assumed g(0)=1 column specifies whether the abundance estimate assumed that detection was certain along the survey trackline. Studies that assumed this did not correct for availability or perception bias, and therefore underestimated abundance. The In our models column specifies whether the survey data from the study was also used in our models. If not, the study provides a completely independent estimate of abundance.

Dates	Model or study	Estimated abundance	CV	Assumed g(0)=1	In our models

1992-2009	Climatological model*	3137	0.10	No	
1993-2009	Contemporaneous model	3300	0.08	No	
1992-2009	Climatological same segments model	3108	0.08	No	
2009	Oceanic waters, Jun-Aug (Waring et al. 2013)	2442	0.57	Yes	Yes
2003-2004	Oceanic waters, Jun-Aug (Mullin 2007)	1589	0.27	Yes	Yes
1996-2001	Oceanic waters, Apr-Jun (Mullin and Fulling 2004)	2169	0.32	Yes	Yes
1991-1994	Oceanic waters, Apr-Jun (Hansen et al. 1995)	2749	0.27	Yes	Yes

Table 16: Estimated mean abundance within the study area. We selected the model marked with * as our best estimate of the abundance and distribution of this taxon. For comparison, independent abundance estimates from NOAA technical reports and/or the scientific literature are shown. Please see the Discussion section below for our evaluation of our models compared to the other estimates. Note that our abundance estimates are averaged over the whole year, while the other studies may have estimated abundance for specific months or seasons. Our coefficients of variation (CVs) underestimate the true uncertainty in our estimates, as they only incorporated the uncertainty of the GAM stage of our models. Other sources of uncertainty include the detection functions and g(0) estimates. It was not possible to incorporate these into our CVs without undertaking a computationally-prohibitive bootstrap; we hope to attempt that in a future version of our models.

Density Maps

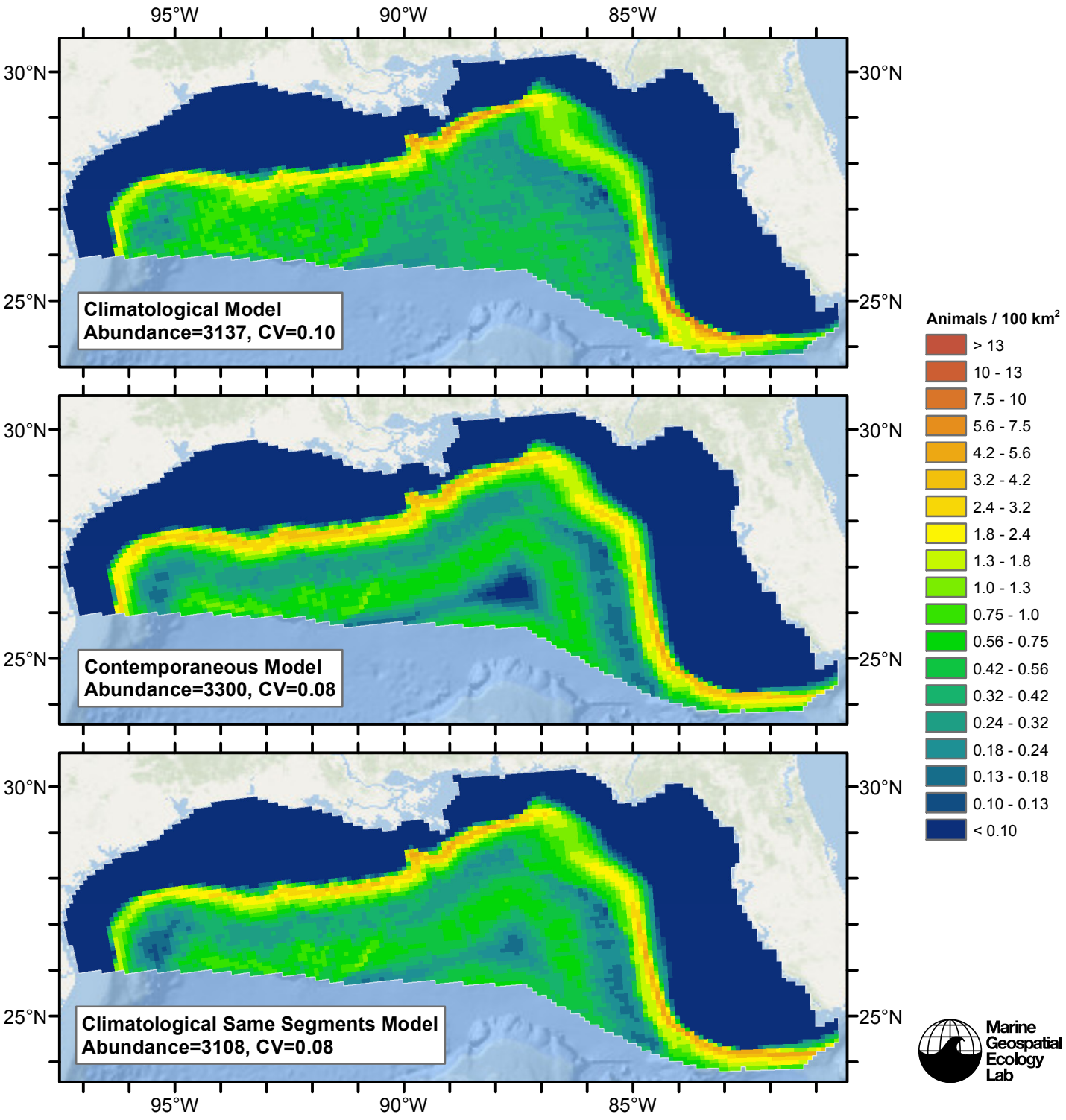

Figure 46: Risso's dolphin density and abundance predicted by the models that explained the most deviance. Regions inside the study area (white line) where the background map is visible are areas we did not model (see text).

Temporal Variability

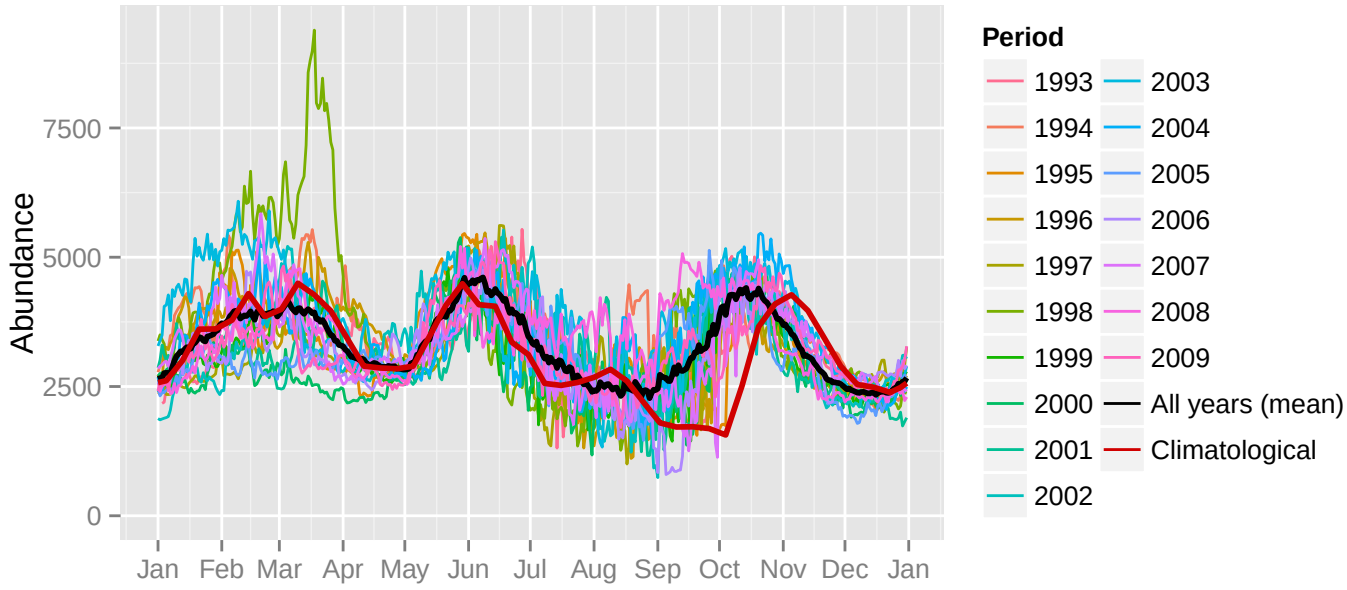

Figure 47: Comparison of Risso's dolphin abundance predicted at a daily time step for different time periods. Individual years were predicted using contemporaneous models. "All years (mean)" averages the individual years, giving the mean annual abundance of the contemporaneous model. "Climatological" was predicted using the climatological model. The results for the climatological same segments model are not shown.

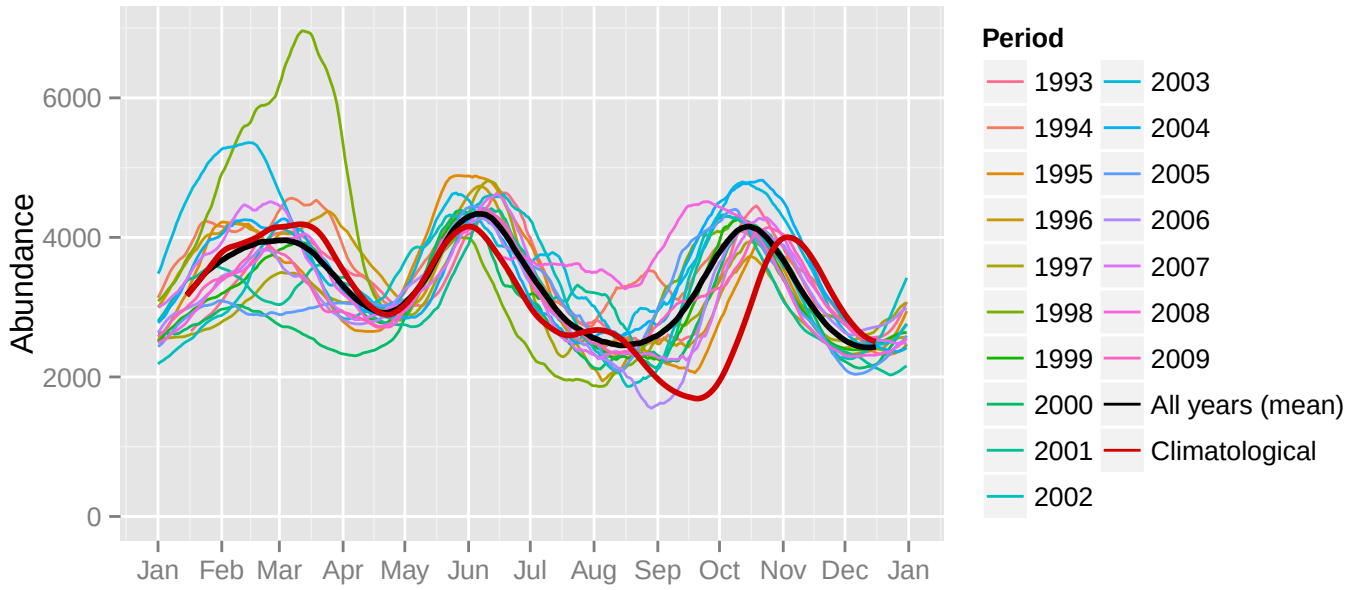

Figure 48: The same data as the preceding figure, but with a 30-day moving average applied.

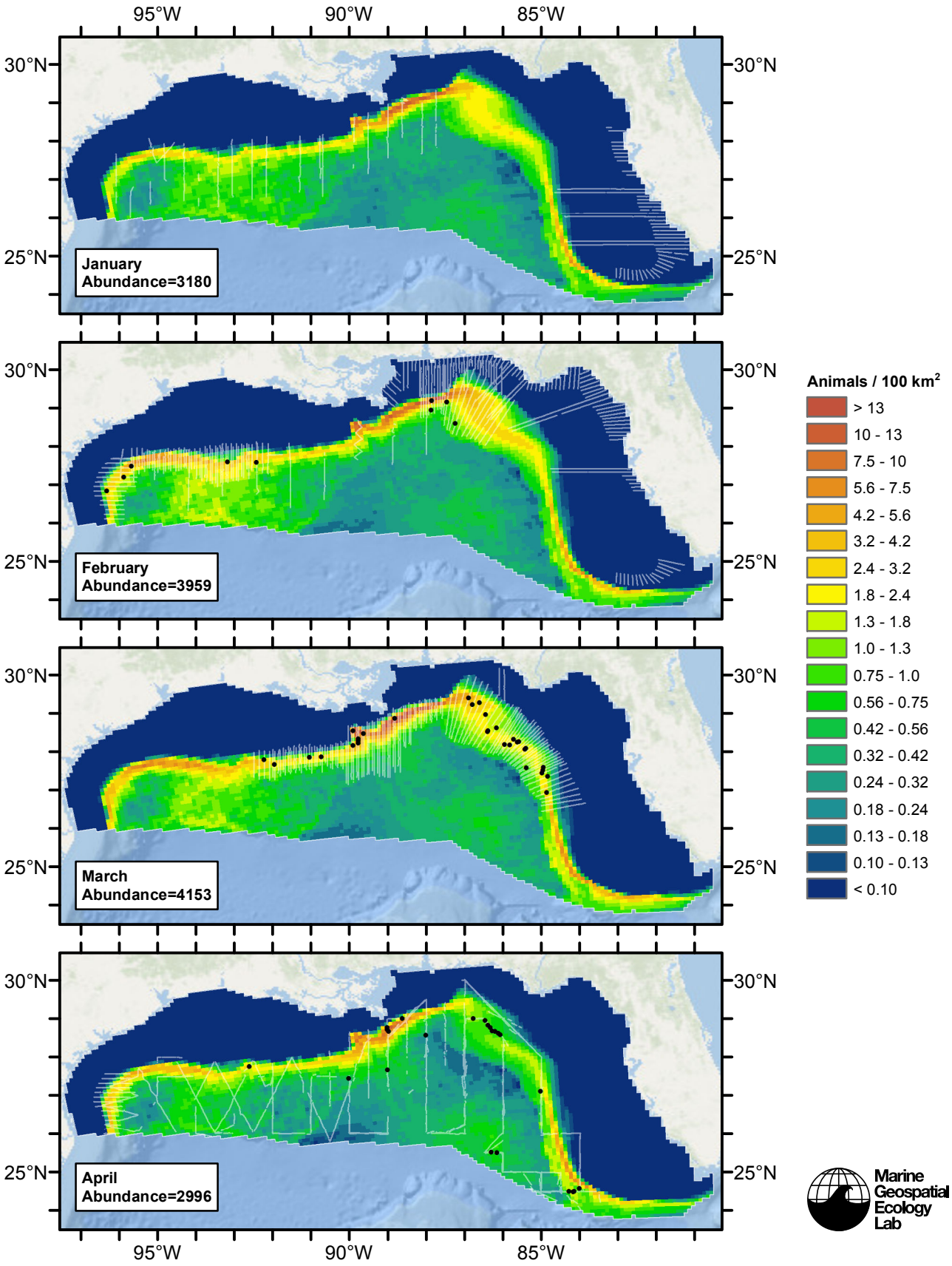
95°W
90°W
85°W
30°N
25°N
January
Abundance=3180
February
Abundance=3959
March
Abundance=4153
April
Abundance=2996
Animals / 100 km²
> 13
10 - 13
7.5 - 10
5.6 - 7.5
4.2 - 5.6
3.2 - 4.2
2.4 - 3.2
1.8 - 2.4
1.3 - 1.8
1.0 - 1.3
0.75 - 1.0
0.56 - 0.75
0.42 - 0.56
0.32 - 0.42
0.24 - 0.32
0.18 - 0.24
0.13 - 0.18
0.10 - 0.13
< 0.10
Marine
Geospatial
Ecology
Lab

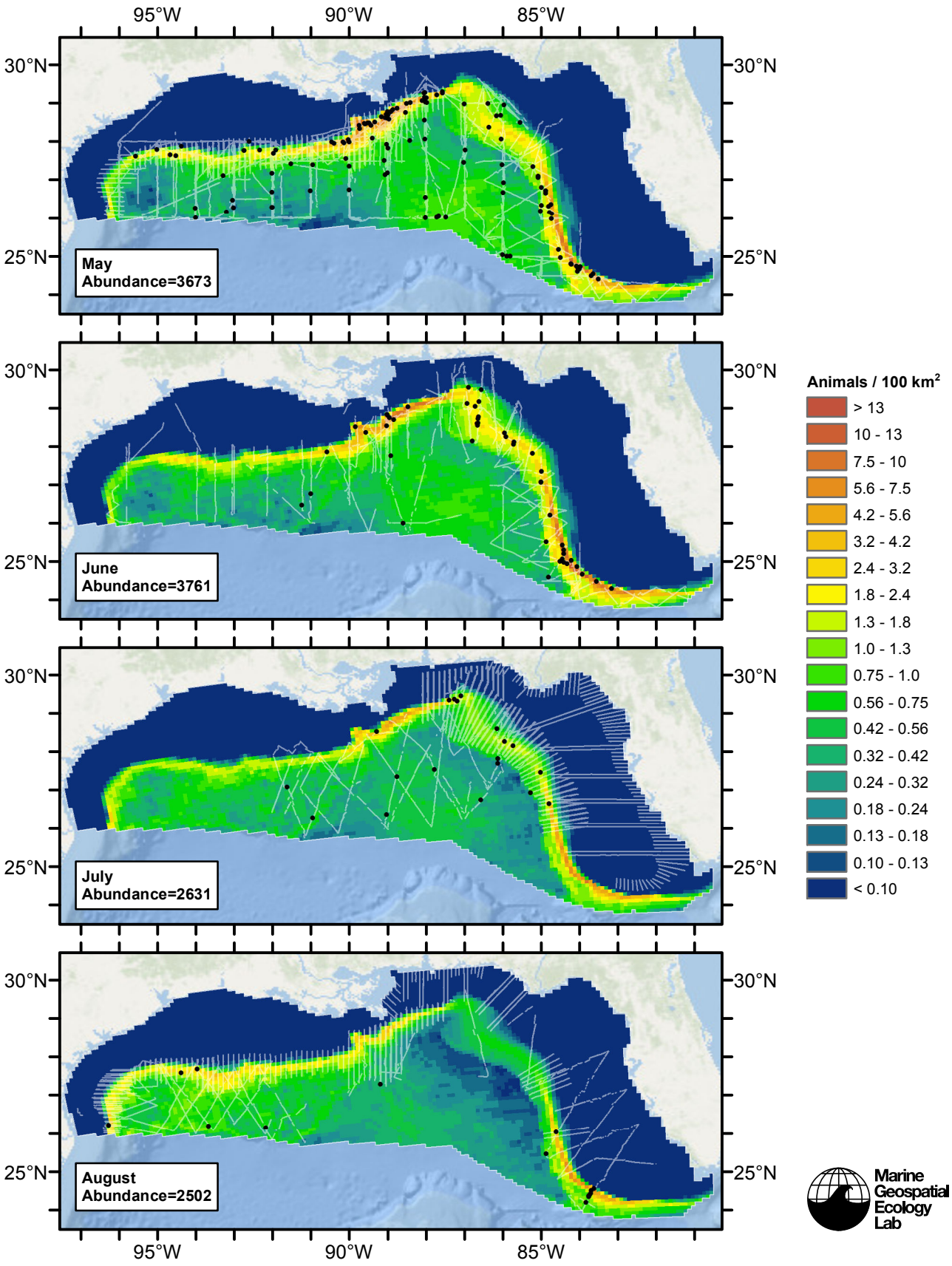
95°W
90°W
85°W
30°N
25°N
May
Abundance=3673
June
Abundance=3761
July
Abundance=2631
August
Abundance=2502
Animals / 100 km²
> 13
10 - 13
7.5 - 10
5.6 - 7.5
4.2 - 5.6
3.2 - 4.2
2.4 - 3.2
1.8 - 2.4
1.3 - 1.8
1.0 - 1.3
0.75 - 1.0
0.56 - 0.75
0.42 - 0.56
0.32 - 0.42
0.24 - 0.32
0.18 - 0.24
0.13 - 0.18
0.10 - 0.13
< 0.10
Marine
Geospatial
Ecology
Lab

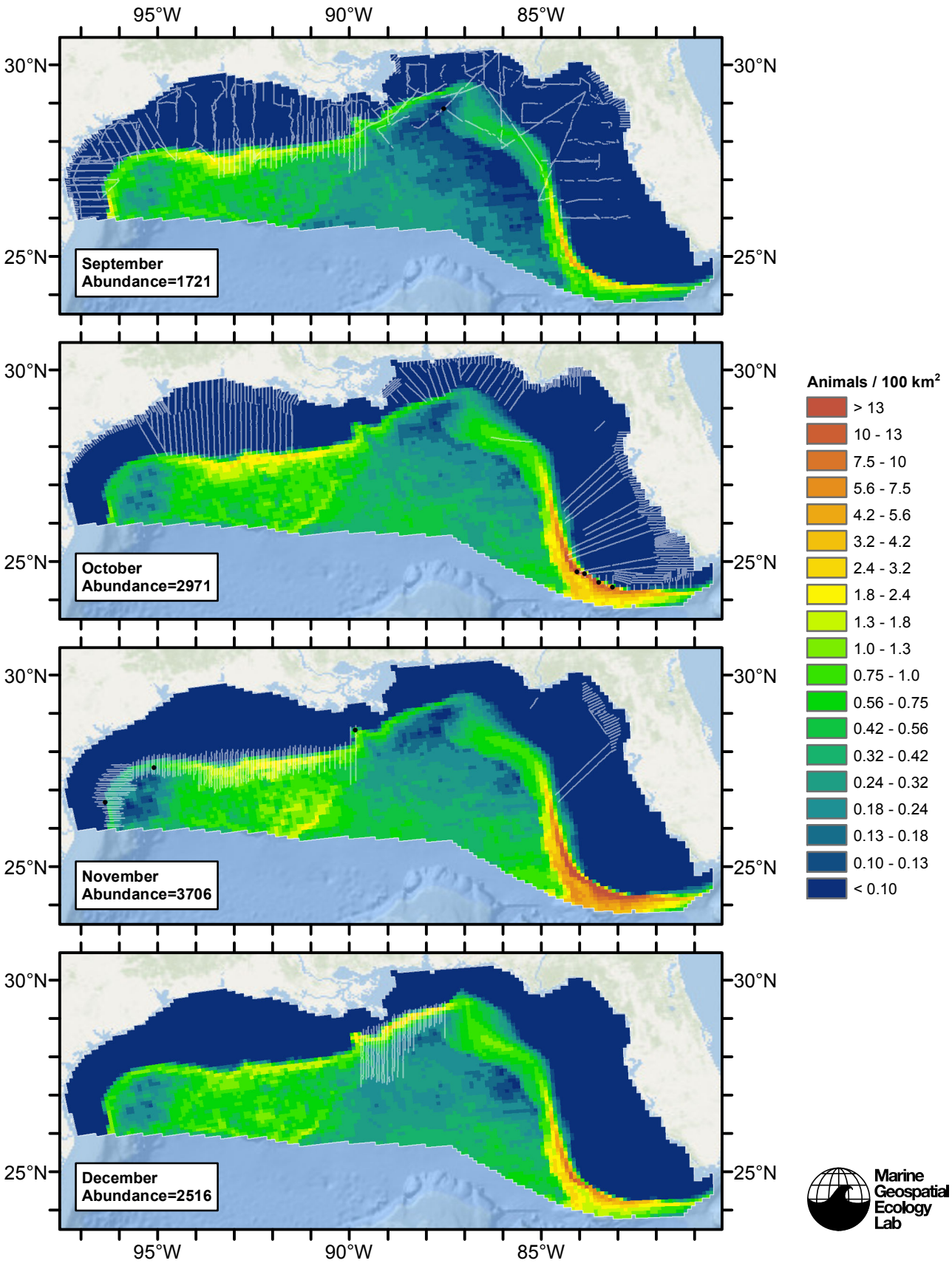
95°W
90°W
85°W
30°N
25°N
September
Abundance=1721
October
Abundance=2971
November
Abundance=3706
December
Abundance=2516
Animals / 100 km²
> 13
10 - 13
7.5 - 10
5.6 - 7.5
4.2 - 5.6
3.2 - 4.2
2.4 - 3.2
1.8 - 2.4
1.3 - 1.8
1.0 - 1.3
0.75 - 1.0
0.56 - 0.75
0.42 - 0.56
0.32 - 0.42
0.24 - 0.32
0.18 - 0.24
0.13 - 0.18
0.10 - 0.13
< 0.10
Marine
Geospatial
Ecology
Lab

Contemporaneous Model

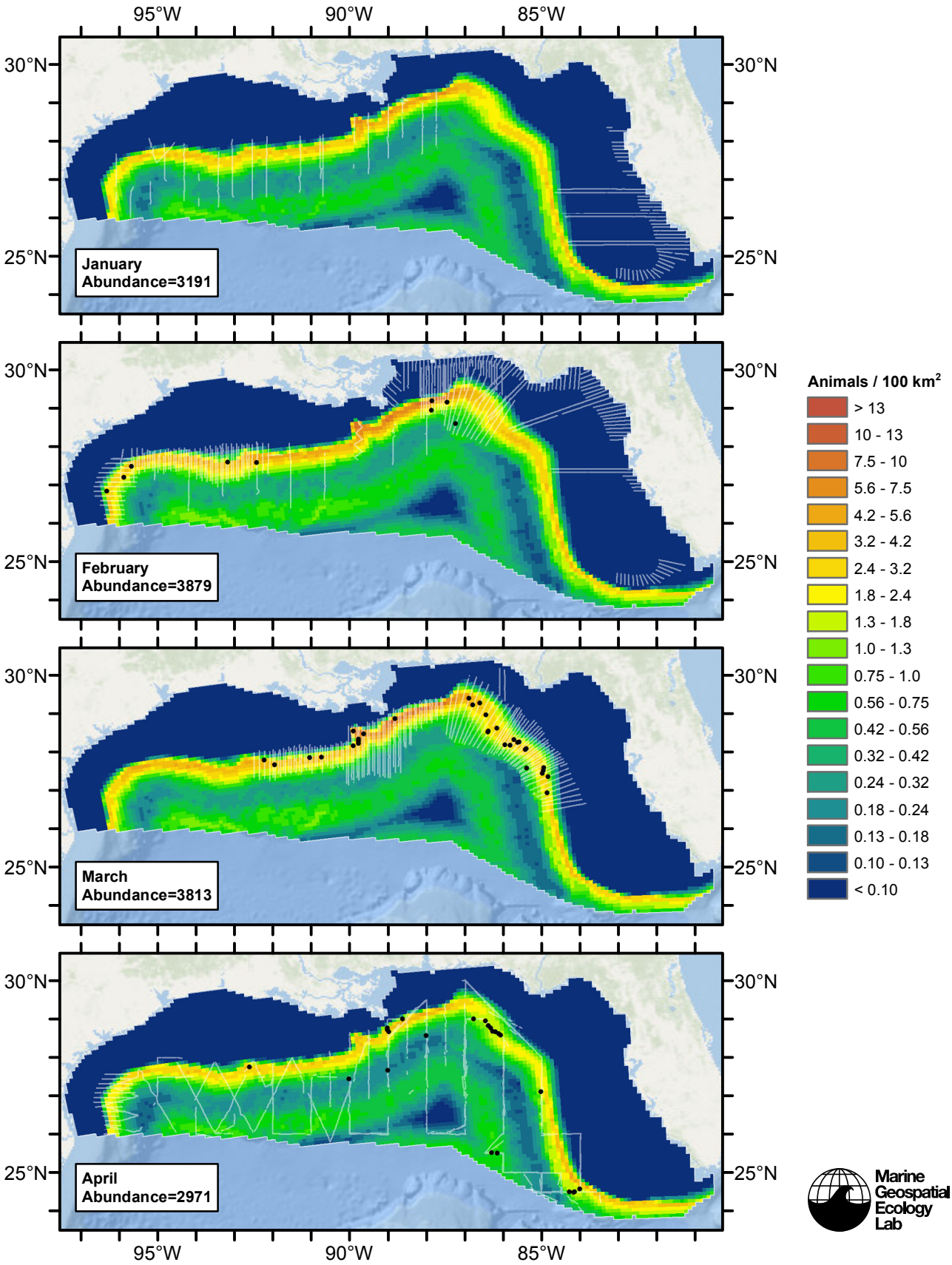

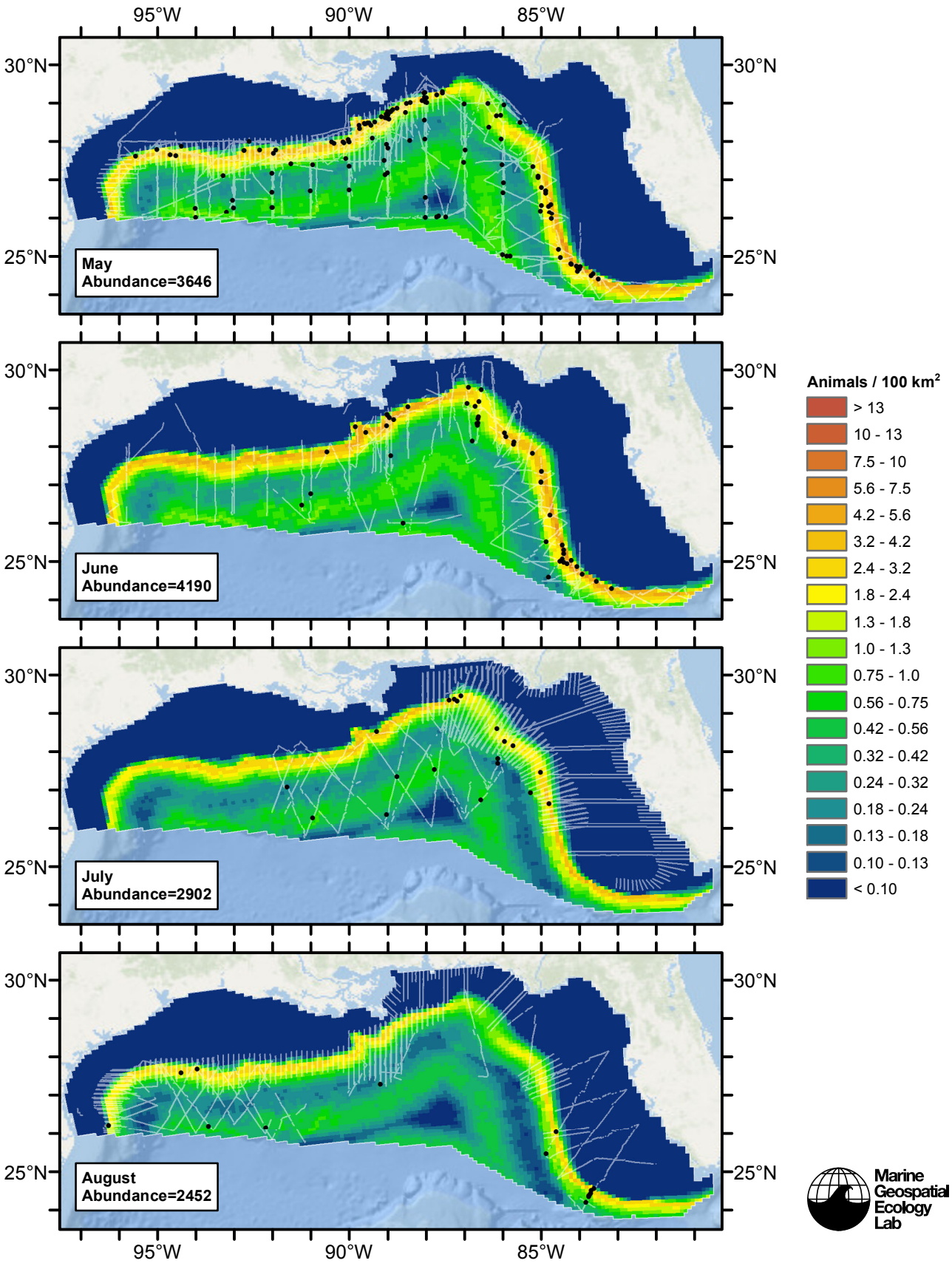
95°W
90°W
85°W
30°N
25°N
May
Abundance=3646
June
Abundance=4190
July
Abundance=2902
August
Abundance=2452
Animals / 100 km²
> 13
10 - 13
7.5 - 10
5.6 - 7.5
4.2 - 5.6
3.2 - 4.2
2.4 - 3.2
1.8 - 2.4
1.3 - 1.8
1.0 - 1.3
0.75 - 1.0
0.56 - 0.75
0.42 - 0.56
0.32 - 0.42
0.24 - 0.32
0.18 - 0.24
0.13 - 0.18
0.10 - 0.13
< 0.10
Marine
Geospatial
Ecology
Lab

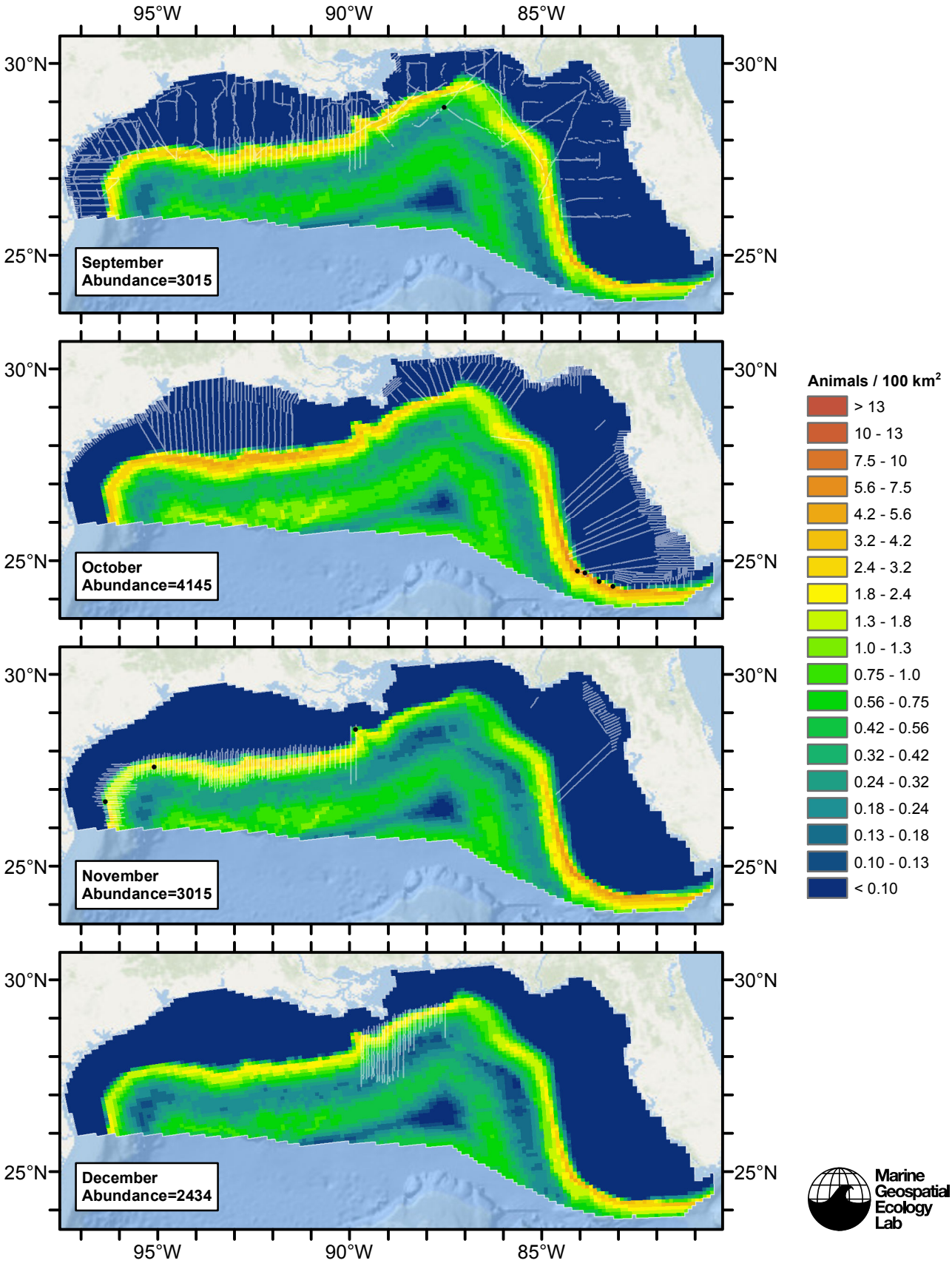
95°W
90°W
85°W
30°N
25°N
September
Abundance=3015
October
Abundance=4145
November
Abundance=3015
December
Abundance=2434
Animals / 100 km²
> 13
10 - 13
7.5 - 10
5.6 - 7.5
4.2 - 5.6
3.2 - 4.2
2.4 - 3.2
1.8 - 2.4
1.3 - 1.8
1.0 - 1.3
0.75 - 1.0
0.56 - 0.75
0.42 - 0.56
0.32 - 0.42
0.24 - 0.32
0.18 - 0.24
0.13 - 0.18
0.10 - 0.13
< 0.10
Marine
Geospatial
Ecology
Lab

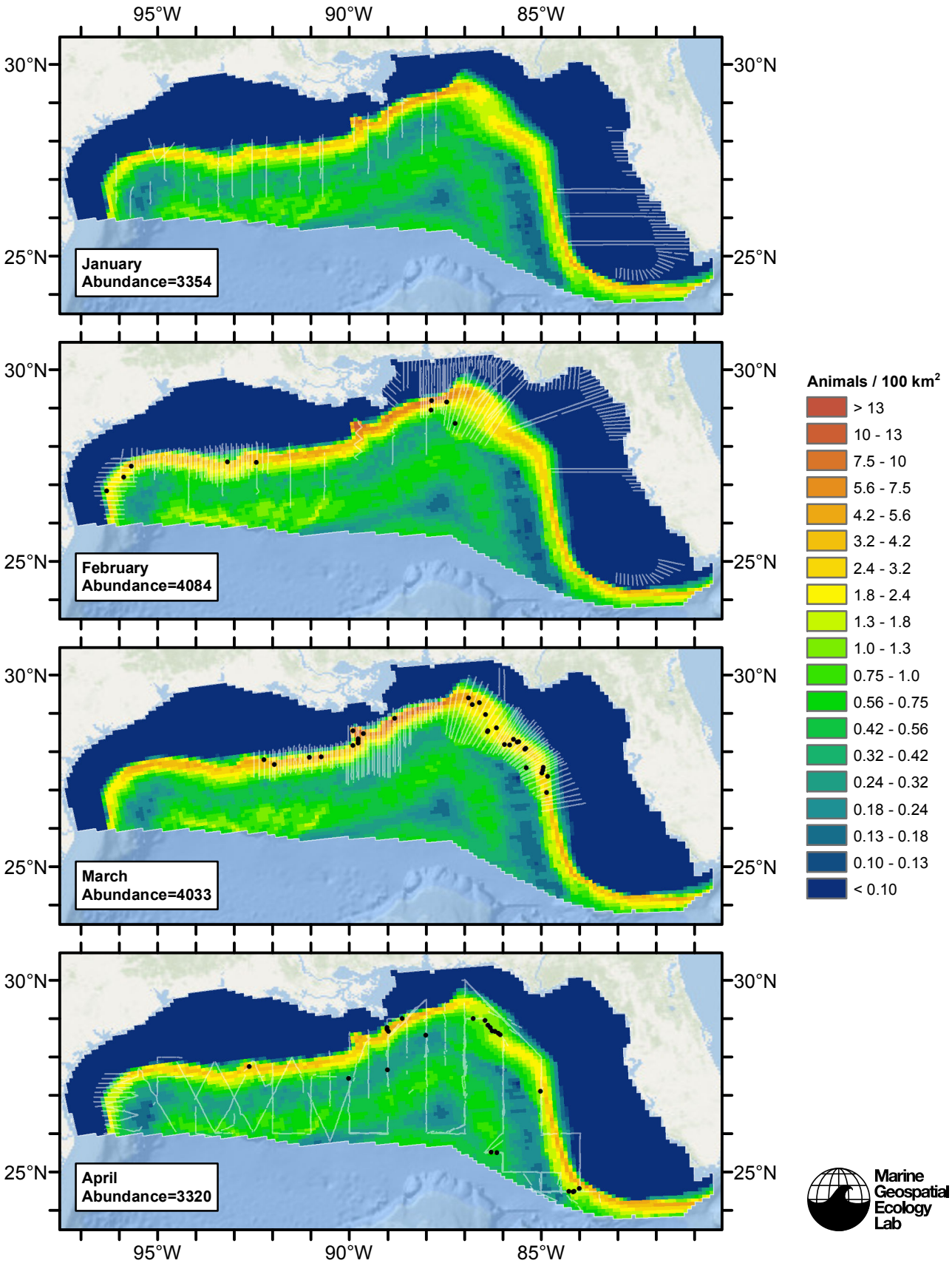
95°W
90°W
85°W
30°N
25°N
January
Abundance=3354
February
Abundance=4084
March
Abundance=4033
April
Abundance=3320
Animals / 100 km²
> 13
10 - 13
7.5 - 10
5.6 - 7.5
4.2 - 5.6
3.2 - 4.2
2.4 - 3.2
1.8 - 2.4
1.3 - 1.8
1.0 - 1.3
0.75 - 1.0
0.56 - 0.75
0.42 - 0.56
0.32 - 0.42
0.24 - 0.32
0.18 - 0.24
0.13 - 0.18
0.10 - 0.13
< 0.10
Marine
Geospatial
Ecology
Lab

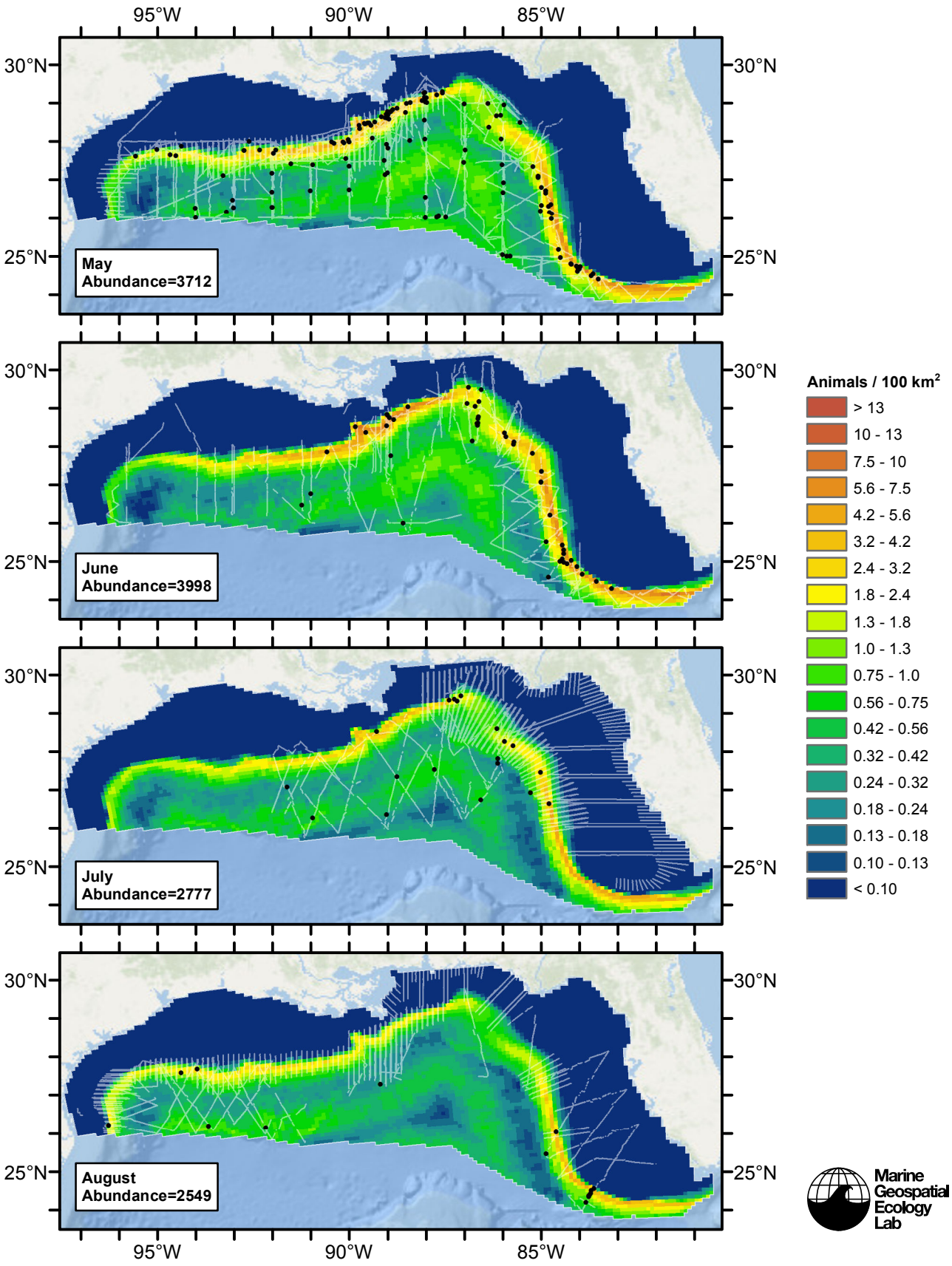
95°W
90°W
85°W
30°N
25°N
May
Abundance=3712
June
Abundance=3998
July
Abundance=2777
August
Abundance=2549
Animals / 100 km²
> 13
10 - 13
7.5 - 10
5.6 - 7.5
4.2 - 5.6
3.2 - 4.2
2.4 - 3.2
1.8 - 2.4
1.3 - 1.8
1.0 - 1.3
0.75 - 1.0
0.56 - 0.75
0.42 - 0.56
0.32 - 0.42
0.24 - 0.32
0.18 - 0.24
0.13 - 0.18
0.10 - 0.13
< 0.10
Marine
Geospatial
Ecology
Lab

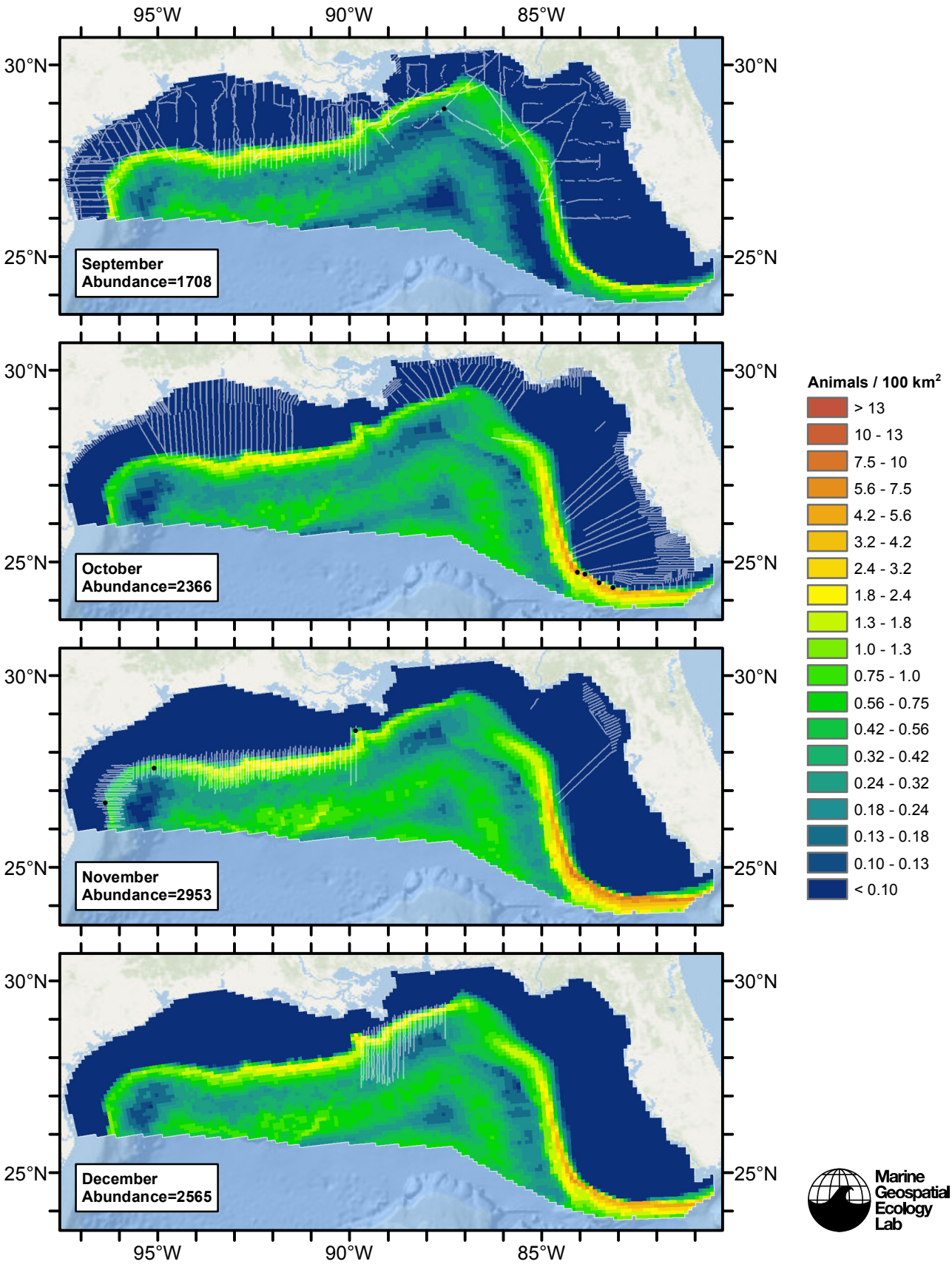
95°W
90°W
85°W
30°N
25°N
September
Abundance=1708
October
Abundance=2366
November
Abundance=2953
December
Abundance=2565
Animals / 100 km²
> 13
10 - 13
7.5 - 10
5.6 - 7.5
4.2 - 5.6
3.2 - 4.2
2.4 - 3.2
1.8 - 2.4
1.3 - 1.8
1.0 - 1.3
0.75 - 1.0
0.56 - 0.75
0.42 - 0.56
0.32 - 0.42
0.24 - 0.32
0.18 - 0.24
0.13 - 0.18
0.10 - 0.13
< 0.10
Marine
Geospatial
Ecology
Lab

Discussion

The models that used climatological predictors consistently explained more deviance than the models that used contemporaneous predictors. On this basis, we selected the climatological model that was fitted to all of the segments as our best estimate of Risso's dolphin distribution and abundance. Consistent with prior habitat analysis (Baumgartner 1997), the model predicted highest density along the continental slope; depth and slope were the second and third most important predictors in the model, by F score.

Because the survey effort used as input to this model was biased toward spring and summer and was spatiotemporally patchy (see maps in the Temporal Variability section above), we were not confident that our models could produce realistic predictions at a monthly temporal resolution. This problem affected all species that we modeled in the Gulf of Mexico, and we recommend that year-round average predictions be used for all Gulf of Mexico species.

Our model predicted a total abundance that was about 28% higher than NOAA's most recent abundance estimate, although our estimate was within the confidence limits of NOAA's estimate. Besides a difference in the data used to fit the two models, we attribute the difference in the abundance estimates to a difference in the g(0) parameter: NOAA's estimate assumed that g(0)=1 while we did not. Unlike some other odontocetes that occur in the Gulf of Mexico, Risso's dolphin occurs mainly in small groups: approximately 40% of the aerial sightings were of groups of 1-5 individuals and 90% of the shipboard sightings were of groups of 1-20 individuals. To correct for perception bias, we applied g(0)=0.43 and g(0)=0.856 to these sightings, respectively. This correction increased our estimate proportionally from what it would have been had we assumed that g(0)=1 as NOAA did.

References

Barlow J, Forney KA (2007) Abundance and density of cetaceans in the California Current ecosystem. Fish. Bull. 105: 509-526.

Baumgartner MF (1997) The Distribution of Risso's Dolphin (grampus Griseus) with Respect to the Physiography of the Northern Gulf of Mexico. Marine Mammal Science 13: 614-638.

Carretta JV, Lowry MS, Stinchcomb CE, Lynn MS, Cosgrove RE (2000) Distribution and abundance of marine mammals at San Clemente Island and surrounding offshore waters: results from aerial and ground surveys in 1998 and 1999. Administrative Report LJ-00-02, available from Southwest Fisheries Science Center, P.O. Box 271, La Jolla, CA USA 92038. 44 p.

Hansen LJ, Mullin KD, Roden CL (1995) Estimates of cetacean abundance in the northern Gulf of Mexico from vessel surveys. Southeast Fisheries Science Center, Miami Laboratory, Contribution No. MIA-94/95-25, 9 pp.

Hiby L (1999) The objective identification of duplicate sightings in aerial survey for porpoise. In: Marine Mammal Survey and Assessment Methods (Garner GW, Amstrup SC, Laake JL, Manly BFJ, McDonald LL, Robertson DG, eds.). Balkema, Rotterdam, pp. 179-189.

Jefferson TA, Weir CR, Anderson RC, Ballance LT, Kenney RD, et al. (2014) Global distribution of Risso's dolphin Grampus griseus: a review and critical evaluation. Mammal Review 44: 56-68.

Mullin KD (2007) Abundance of cetaceans in the oceanic Gulf of Mexico based on 2003-2004 ship surveys. 26 pp.

Mullin KD, Fulling GL (2004) Abundance of cetaceans in the oceanic northern Gulf of Mexico. Mar. Mamm. Sci. 20(4): 787-807.

Palka DL (2006) Summer Abundance Estimates of Cetaceans in US North Atlantic Navy Operating Areas. US Dept Commer, Northeast Fish Sci Cent Ref Doc. 06-03: 41 p.

Waring GT, Josephson E, Maze-Foley K, Rosel PE, eds. (2013) U.S. Atlantic and Gulf of Mexico Marine Mammal Stock Assessments – 2012. NOAA Tech Memo NMFS NE 223; 419 p.